Electronic Supplementary Material (ESI) for Green Chemistry.

Supporting information

Blossoms of the plant genus *Hypericum* as versatile photoredox catalyst

J. Wang,[a] K. Schwedtmann,[a] K. Liu,[a] S. Schulz,[a], J. Haberstroh,[a] G. Schaper,[a] A. Wenke,[b] J. Naumann,[b] T. Wenke,[b] S. Wanke,[b] J. J. Weigand[a*]

[a]Faculty of Chemistry and Food Chemistry, Technische Universität Dresden, Dresden, Germany
jan.weigand@tu-dresden.de
[b]Faculty of Biology, Technische Universität Dresden, Dresden, Germany

Contents

1. General information

Protohypericin and hypericin were synthesized according to a reported procedure[1]. Protopseudohypericin and pseudohypericin external standards were bought from Wuhan Chem Faces Biochemical Co., Ltd. and Carl Roth GmbH respectively. Chemicals used in the glovebox including commercially available aryl halides, trapping reagents and self-synthesized compounds were dried and degassed using Schlenk techniques. Dry, oxygen-free DMSO and CH_3CN were refluxed and distilled over CaH_2 under reduced pressure or Argon protection and preserved in a Schlenk flask filled with activated 3 Å molecular sieve. Manipulations to prepare the reactions were performed in a Glovebox MB Unilab using an atmosphere of nitrogen.

^{1}HNMR and ^{13}C NMR spectra were measured on a Bruker AVANCE III HD Nanobay 400 MHz UltraShield (^{1}H (400.13 MHz), ^{13}C (100.61 MHz), ^{31}P (161.98 MHz)) or on a Bruker AVANCE III HDX, 500 MHz Ascend (^{1}H 500.13 MHz), ^{13}C (125.75 MHz), ^{31}P (202.45 MHz)) in $CDCl_3$ solution or DMSO-d_6 with internal solvent signal reference ($CDCl_3$: 7.26 and 77.16 ppm or DMSO-d_6: 2.50 and 39.52 ppm; $CDCl_3$ contains 0.03 % (v/v) TMS). All ^{13}CNMR spectra were exclusively recorded with composite pulse decoupling. Multiplicities are indicated as s (singlet), d (doublet), t (triplet), q (quartet), quint (quintet), sept (septet), m (multiplet)); chemical shifts (δ) are reported in ppm; coupling constants (J) are given in Hertz (Hz).

Ultra-performance liquid chromatography coupled to UV-vis (UPLC-UV-vis) and tandem quadrupole mass spectrometry (UPLC-MS) analysis were conducted in Waters Acquity UPLC system using a C18 column (length: 50 mm; inner diameter: 2.1 mm; Particle size: 1.7 μm) with proper eluent. UPLC-UV-vis was performed on photodiode array (PDA) detector while UPLC-MS was equipped with tandem quadrupole (TQ) mass detector. The identification and quantification of substances were based on external standard method.

Photoirradiation experiments were conducted with blue LEDs (OSRAM Oslon SSL 80 LBCP7P-GYHY (blue, λ_{max} = 470 nm, I_{max} = 1000 mA, 1.12 W)), green LEDs (OSRAM Oslon SSL 80 LTCP7P-KXKZ (green, λ_{max} = 530 nm, I_{max} = 1000 mA, 1.12 W)) or yellow LEDs (OSRAM Oslon SSL 80 LBCP7P-JRJT (yellow, λ_{max} = 590 nm, I_{max} = 1000 mA, 0.77 W)).

All reactions were monitored by thin-layer chromatography using Macherey-Nagel ALUGRAM silica gel G/UV_{254} TLC plate and visualization was accomplished with UV light 254 nm and 366 nm sources or by UPLC. Standard flash chromatography was performed using silica gel (particle size 40-63 μm).

UV-vis spectra were measured on Perkin-Elmer Lambda 25 UV-vis Spectrometer and fluorescence spectra were recorded on a Perkin-Elmer Fluorescence Spectrometer LS 55 using a 10 mm fluorescence quartz cell.

2. General procedures

2.1 Preparation of plant materials

Ten *Hypericum* species collected from wild populations in Greece, Austria and Germany from May 2018 to May 2019 were investigated. Five plants of each population were pressed and voucher specimens were deposited at the herbarium Dresden (DRE), and one either at the herbarium of Thessaloniki (TAU) or Athens (ATHU). The herbarium voucher information is shown in Table S1. 10 plants of each population were pre-dried with a fan heater for approximately 4-6 h under exclusion of light followed by drying at 40 °C for 24 h in a drying chamber.

Table S1. *Hypericum* species collection information.

Entry	*Hypericum* species	Collection time	Collection location	Voucher number
1	*H. cerastioides*	May-2018	Ioáninna, Greece	DR 056534 - DR 056538
2	*H. empetrifolium*	May-2018	Fokídos, Greece	DR 056526 - DR 056528, DR 056562, DR 056563
3	*H. hirsutum*	May-2018	Oberösterreich, Austria	DR 056501 - DR 056505
4	*H. olympicum*	May-2018	Tríkala, Greece	DR 056555 - DR 056559
5	*H. maculatum*	May-2018	Sachsen, Germany	DR 056516 - DR 056520
6	*H. perfoliatum*	May-2018	Thesprotía, Greece	DR 056529 - DR 056533
7	*H. perforatum*	May-2019	Ális, Greece	DR 057535 - DR 057540
8	*H. vesiculosum*	May-2019	Messinía, Greece	DR 057530 - DR 057534
9	*H. spruneri*	May-2018	Tríkala, Greece	DR 056550 - DR 056554
10	*H. rochelii*	May-2018	Aitolía kai, Greece	DR 056564 - DR 056568

The blossoms of the plant materials were picked up and ground to a fine powder using an electric grinder, followed by screening through a sieve with pore size of 315 μm. 50 mg of the plant powder was weighed in a two-necked flask equipped with a condenser. Then the system was evacuated and refilled with Argon for three times. After adding 25.0 mL of extraction agent (MeOH:H_2O=9:1, v:v), the mixture was heated to 60 ^oC for 2 h under exclusion of light. The mixture was allowed to cool down to room temperature and filtered through a 0.22 μm syringe filter to obtain samples for UPLC-MS analysis.

2.2 General procedure for the quantification of hypericin homologues in plant materials

UPLC condition: A linear gradient of acetonitrile/methanol/triethylammonium acetate buffer (100 mM in H_2O, pH = 7) from 30:39:31 to 20:60:20 over 15 min was used as mobile phase at a flow rate of 0.3 mL/min. PDA detector was set at 588 nm and negative electrospray ionization (ESI^-) model at a cone voltage of 92 V was used in TQ detector.

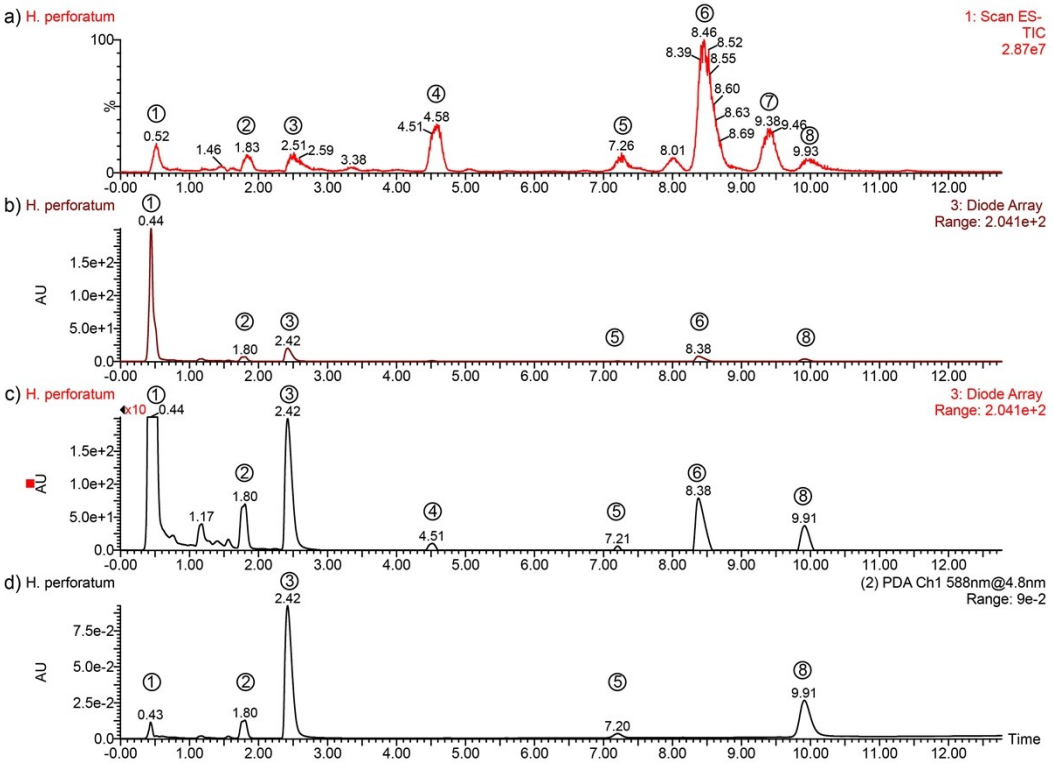

Figure S1. Typical UPLC-UV/MS trace of *Hypericum perforatum* a) detected by the TQ detector in the ESI^- mode; b) detected by PDA detector at 3D channel in range of 200 nm to 800 nm; c) enlarged trace by tenfold detected by PDA detector at 3D channel; d) detected by PDA detector at 2D channel at wavelength of 588 nm.

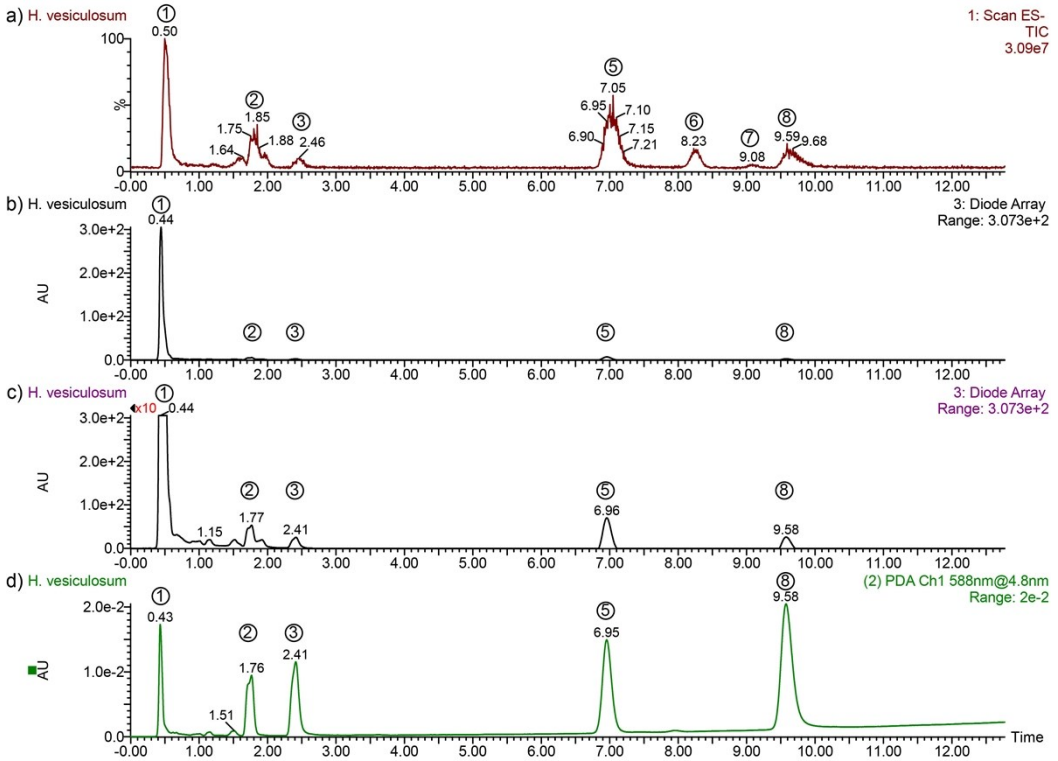

Figure S2. Typical UPLC-MS trace of *Hypericum vesiculosum.* a) detected by the TQ detector in the ESI⁻ mode; b) detected by PDA detector at 3D channel in range of 200 nm to 800 nm; c) enlarged trace by tenfold detected by PDA detector at 3D channel; d) detected by PDA detector at 2D channel at wavelength of 588 nm.

Table S2. Assignment of UPLC trace peaks and the corresponding compounds.

Number in UPLC trace	Compounds	Mass spectrum peaks
1	Hyperoside, Rutin, Quercitrin	447, 463, 609
2	Protopseudohypericin	521
3	Pseudohypericin	519
4	Hyperfirin	467
5	Protohypericin	505
6	Hyperforin	535
7	Adhyperforin	549
8	Hypericin	503

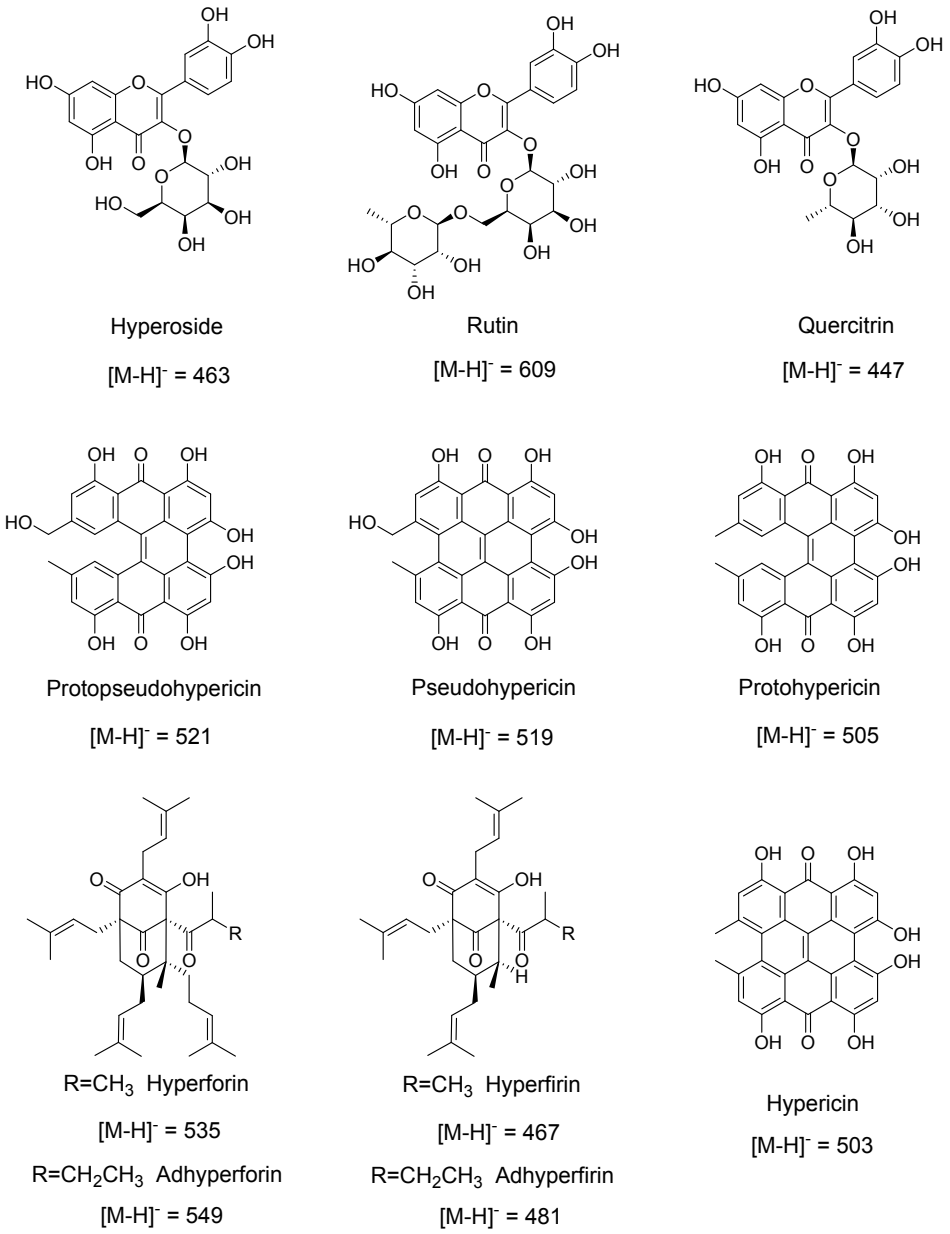

Figure S3. Structures of compounds extracted from *Hypericum* plants.

A series of standard solutions of all hypericin homologues (protopseudohypericin, pseudohypericin, protohypericin and hypericin) were prepared in the range of 0.002 mg/mL to 0.02 mg/mL. Each time, 5.0 μL of sample solution was injected. A linear plot was obtained by plotting the peak areas versus the corresponding concentrations of the standard solution. The amount of specific hypericin homologues can be determined according to the following equation (Eq 1):

$$\%w/w = \frac{w_{HYP}}{W} \times 100\% = \frac{\frac{A_t}{k_t} \times v_t}{W} \times 100\% = \frac{A_t \times v_t}{W \times k_t} \times 100\ \% \qquad \text{Eq 1}$$

where %w/w is the weight fraction of the corresponding hypericin homologue, W is the weight of the plant sample, A_s is the integral area of the corresponding hypericin homologue, k_t is the slope of the linear plot of the corresponding hypericin homologue and v_t is the volume of

extraction agent for the plant sample.

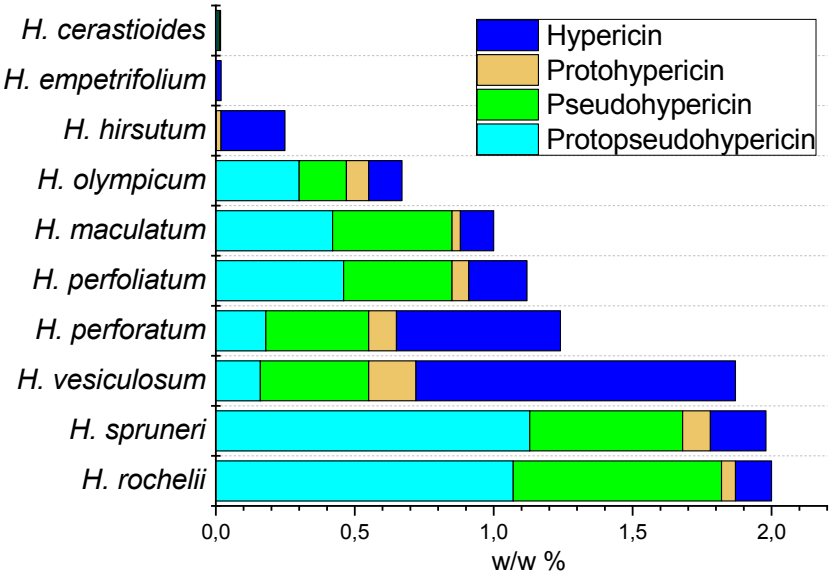

Figure S4. Comparison of hypericin homologues in different *Hypericum* species.

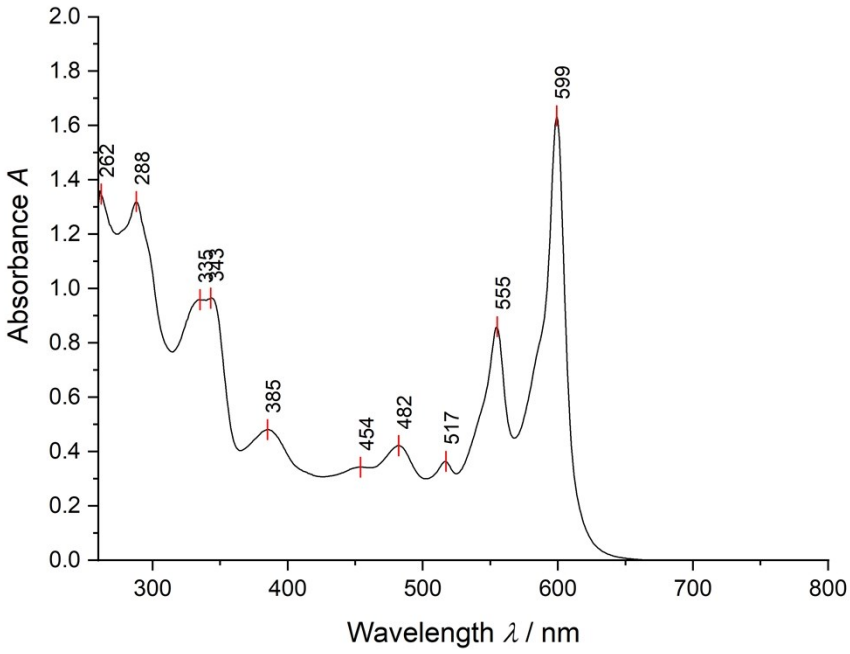

Figure S5. UV-vis spectrum of hypericin (c = 0.05 mM, d = 1 cm) in DMSO.

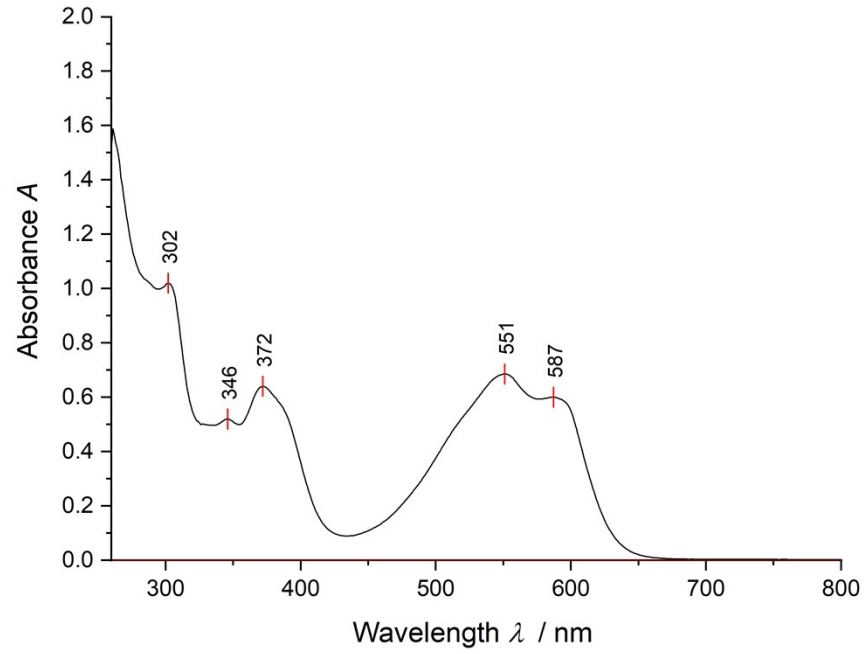

Figure S6. UV-vis spectrum of protohypericin (c = 0.05 mM, d = 1 cm) in DMSO.

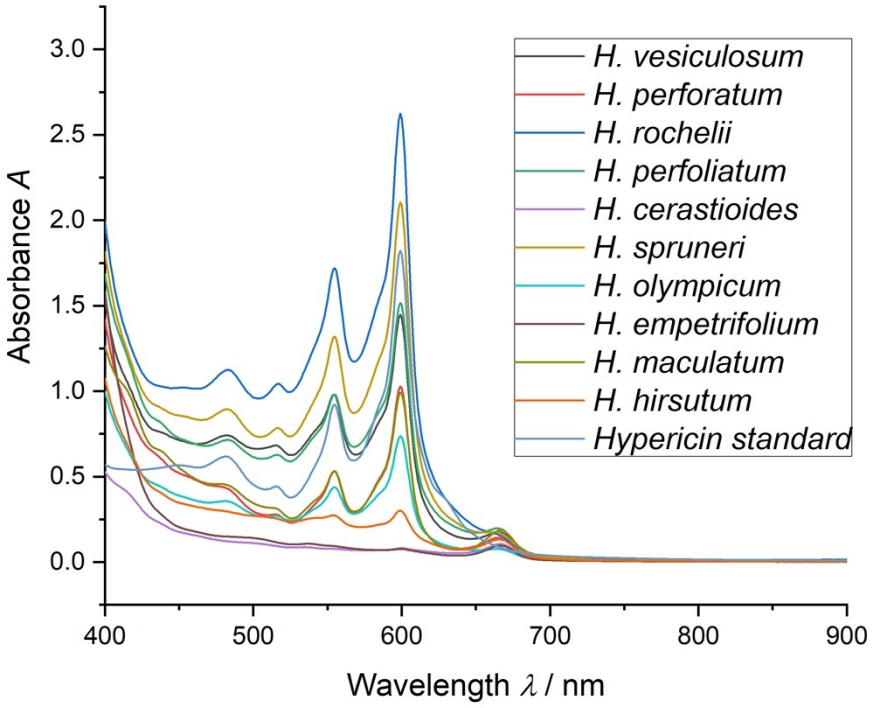

Figure S7. UV-vis spectrum of different *Hypericum* species plant extraction (3.0 mg plant materials extracted by 1.5 mL DMSO) and hypericin standard (d = 1 cm) in DMSO.

2.3 General procedure for the photoreductive coupling reactions of aryl halides using *Hypericum vesiculosum* as catalyst

The blossoms of the dried plant material were ground to a fine powder using an electric grinder followed by screening through a sieve with a pore size of 315 μm. The obtained fine powder was kept under exclusion of light at ambient temperature.

In a 10 ml Schlenk flask 100 mg of the blossom powder were suspended in 1.0 ml DMSO and the respective aryl halide (0.2 mmol, 1 equiv.), the trapping reagent (4.0 mmol, 20 equiv.) and DIPEA (0.2 mmol, 1.0 equiv.) were added subsequently. After irradiated by blue LED (470 nm) at 25 ^{o}C for 24 h, the resulting mixture was extracted by dichloromethane (3 × 5 mL). The combined organic layers were washed with H_2O (2 × 10 mL), dried over Na_2SO_4, filtered and concentrated under reduced pressure. The crude material was applied to a silica gel column for further purification using an ethyl acetate/isohexane eluent.

2.4 General procedure for the photoreductive coupling reactions of aryl halides using Hypericin as catalyst

In a glovebox, protohypericin (0.004 mmol, 0.01 equiv, 2.0 mol %) was weighed in a 10 ml Schlenk flask and dissolved in 1.0 ml of dry DMSO. The protohypericin solution was then sealed in Schlenk flask and irradiated by a blue LED for three hours until full conversion of protohypericin to hypericin was achieved. Subsequently aryl halides (0.2 mmol, 1.0 equiv), trapping reagent (4.0 mmol, 20 equiv) and DIPEA (0.2 mmol, 1.0 equiv) were added. Afterwards, the resulting reaction mixture was irradiated by blue LED at 25 ^{o}C. The resulting mixture was extracted by dichloromethane (3 × 5 mL). The combined organic layers were washed with H_2O (2 × 10 mL), dried over Na_2SO_4, filtered and concentrated under reduced pressure. The crude material was applied to a silica gel column for further purification using the eluent of ethyl acetate/isohexane.

2.5 General procedure for the quantification of the photoreductive coupling reactions

The standard product (2-(1-methyl-1H-pyrrol-2-yl) benzonitrile) for the benchmark reaction was synthesized by the procedure mentioned as above. The product was purified by silica gel chromatographic column and recrystallized from isohexane. The structure and purity of the product was confirmed by NMR, UPLC and X-ray diffraction analysis.

Solutions of the standard product with concentrations from 0.01 mg/mL to 0.1 mg/mL were prepared and the standard calibration curve of concentrations and integral areas was established by UPLC analysis by an eluent of a combination of KH_2PO_4/H_3PO_4 buffer and MeCN.

Using this standard calibration curve, the product yields from different reaction conditions were calculated based on the detected product peak areas from the diluted (400 times) reaction mixture.

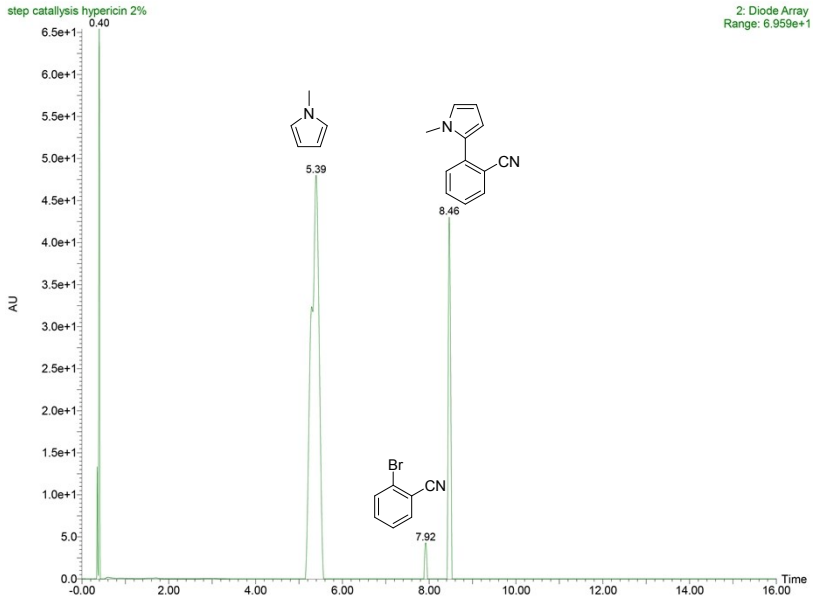

Figure S8. Typical UPLC trace of the benchmark reaction detected by PDA detector at 3D channel.

2.6 Condition optimization for the photoreduction reactions

Table S3. Condition optimization of photoreductive coupling reactions of aryl halides using hypericin as catalyst[a]

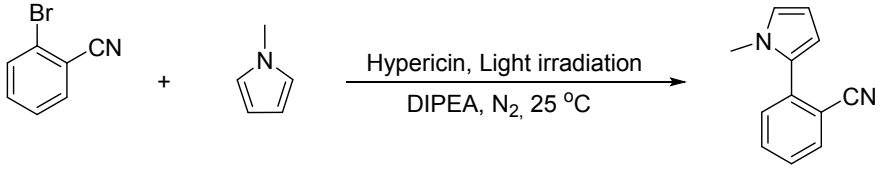

Entry	Catalyst (mol %)	Donor (equiv)	Condition	Yield[b] [%]
1	Hypericin (10)	DIPEA (1.0)	590 nm, 24 h	2 %
2	Hypericin (10)	DIPEA (1.0)	530 nm, 24 h	11 %
3	Hypericin (10)	DIPEA (1.0)	455 nm, 24 h	63 %
4	Hypericin (5)	DIPEA (1.0)	455 nm, 24 h	69 %
5	Hypericin (2)	DIPEA (1.0)	455 nm, 24 h	73 %
6	Hypericin (1)	DIPEA (1.0)	455 nm, 24 h	51 %
7	Hypericin (2)	DIPEA (1.0)	455 nm, 36 h	78 %
8	**Hypericin (2)**	**DIPEA (1.0)**	**455 nm, 48 h**	**85 %**
9	Hypericin (2)	DIPEA (1.5)	455 nm, 24 h	54 %
10	Hypericin (2)	DIPEA (0.8)	455 nm, 24 h	42 %
11	Hypericin (2)	-	455 nm, 24 h	3 %
12	-	DIPEA (1.0)	455 nm, 24 h	0 %
13	Hypericin (2)	DIPEA (1.0)	Dark, 24 h	0 %

[a] Reactions were performed using 0.1 mmol 2-bromobenzonitrile, 2.0 mmol N-methylpyrrole, 2μmol hypericin and 0.1 mmol DIPEA in 1.0 mL DMSO under nitrogen with light irradiation. [c] Yield calculated from UPLC analysis by the external standard method.

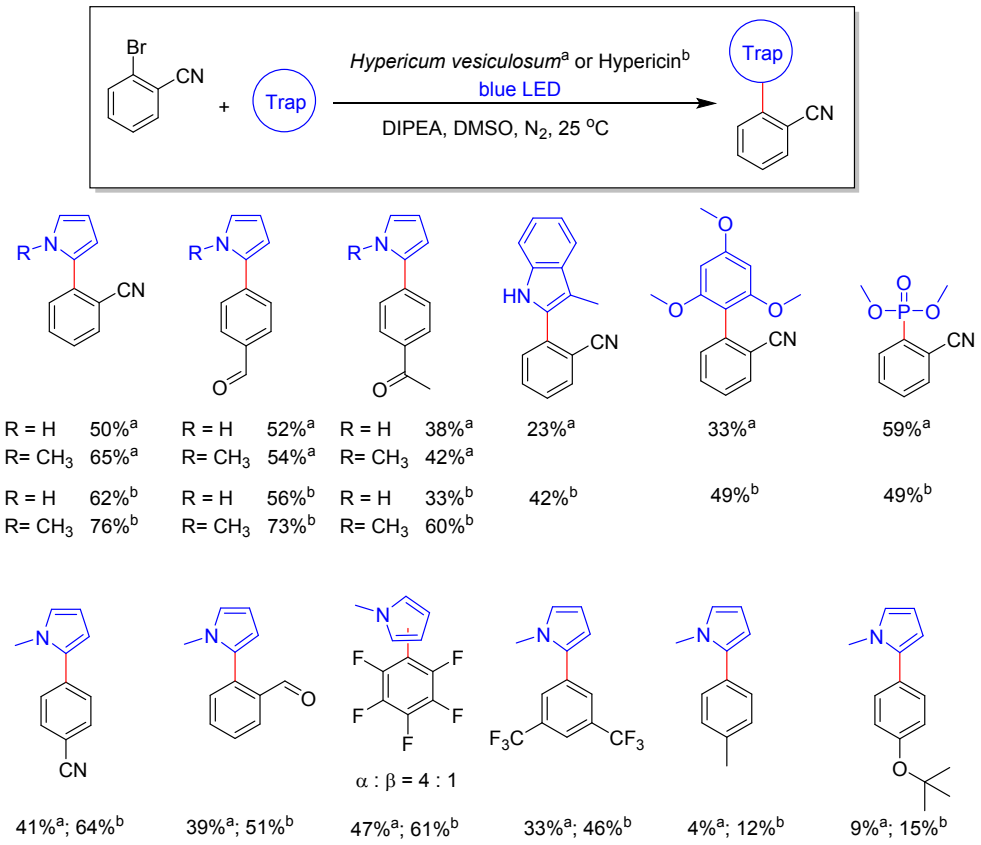

Figure S9. Photoreduction reactions using blossoms of *Hypericum vesiculosum*[a] or hypericin[b] as catalyst. Reactions were performed according to the general procedures.

2.7 General procedure for the photooxidative coupling reactions of *N*-aryl-tetrahydroisoquinoline using *Hypericum vesiculosum* as catalyst

In a reaction tube 50 mg of the blossom powder, *N*-aryl-tetrahydroisoquinoline (0.2 mmol, 1.0 equiv.) and the electrophile (10.0 mmol, 50 equiv.) were added. The mixture was suspended in 2.0 ml MeOH and irradiated with green light at ambient atmosphere. The reactions were monitored by TLC until the full conversion of the substrate was observed. The reaction mixture was subsequently dried *in vacuo* and the crude mixture was applied to a silica gel column for purification with the eluent mixture of ethyl acetate/ isohexane.

2.8 General procedure for the photooxidative coupling reactions of *N*-aryl-tetrahydroisoquinoline using Hypericin as catalyst

In a reaction tube protohypericin (0.002 mmol, 1 mmol%) was dissolved in 2.0 ml DMF and irradiated with blue light. Afterwards *N*-aryl-tetrahydroisoquinoline (0.2 mmol, 1.0 equiv.) and the electrophile (10.0 mmol, 50 equiv.) were added and the reaction mixture was irradiated with green light at ambient atmosphere. The reactions were monitored by TLC until the full conversion of the substrate was observed. The reaction mixture was subsequently dried *in vacuo* and the crude mixture was applied to a silica gel column for purification with the eluent mixture of ethyl acetate/ isohexane.

2.9 Condition optimization for the photooxidation reactions

Table S4. Condition optimization of photooxidation coupling reactions using *Hypericum* plant as catalyst[a]

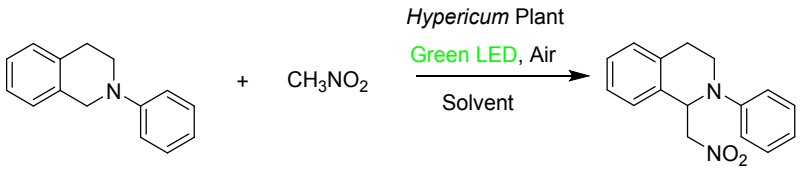

Entry	Hypericum Plant (mg)	Solvents	Nitromethane (eqv.)	Time (h)	Yield[b] (%)
1	**50**	**MeOH**	**50**	**8**	**79**
2	50	EtOH	50	8	63
3	50	MeCN	50	8	66
4	50	Acetone	50	8	68
5	50	DMSO	50	8	73
6	50	DMF	50	8	63
7	100	MeOH	50	8	73
8	25	MeOH	50	8	34
9	50	MeOH	25	8	67
10	50	MeOH	100	8	52

[a] Reactions were performed using 0.2 mmol N-aryl-tetra-hydroisoquinolines, 10.0 mmol nitromethane and specific amount of *Hypericum* plant under ambient atmosphere with a Green LED (530 nm). [b] Isolated yields.

Table S5. Condition optimization of photooxidation coupling reactions using hypericin as catalyst[a]

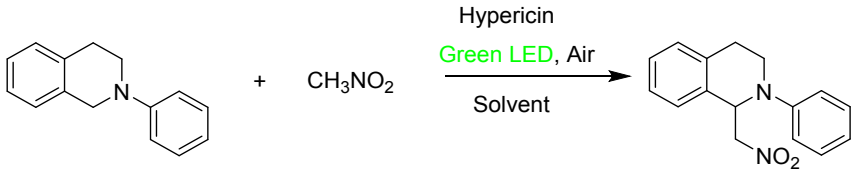

Entry	Hypericin (mmol%)	Solvents	Nitromethane (eqv.)	Time (h)	Yield[b] (%)
1	1	MeOH	50	8	46
2	1	EtOH	50	8	78
3	1	MeCN	50	8	72
4	1	Acetone	50	4	82
5	1	DMSO	50	6	72
6	**1**	**DMF**	**50**	**4**	**92**
7	0.5	DMF	50	4	87
8	2	DMF	50	4	90
9	1	DMF	25	4	78
10	1	DMF	10	4	71
11[c]	1	DMF	50	4	43
12[d]	1	DMF	50	4	Trace[e]
13	-	MeOH	50	3	Trace[e]
14[f]	1	MeOH	50	3	Trace[e]

[a] Reactions were performed using 0.2 mmol *N*-aryl-tetra-hydroisoquinolines, 10.0 mmol nitromethane and specific amount of hypericin under ambient atmosphere with a green LED (530 nm). [b] Isolated yields without further specification. [c] TEMPO (0.2 mmol, 1.0 equiv.) was added as radical trap. [d] Reaction was performed in nitrogen atmosphere. [e] Conversion determined by NMR using internal standard method. [f] Reaction was performed in dark.

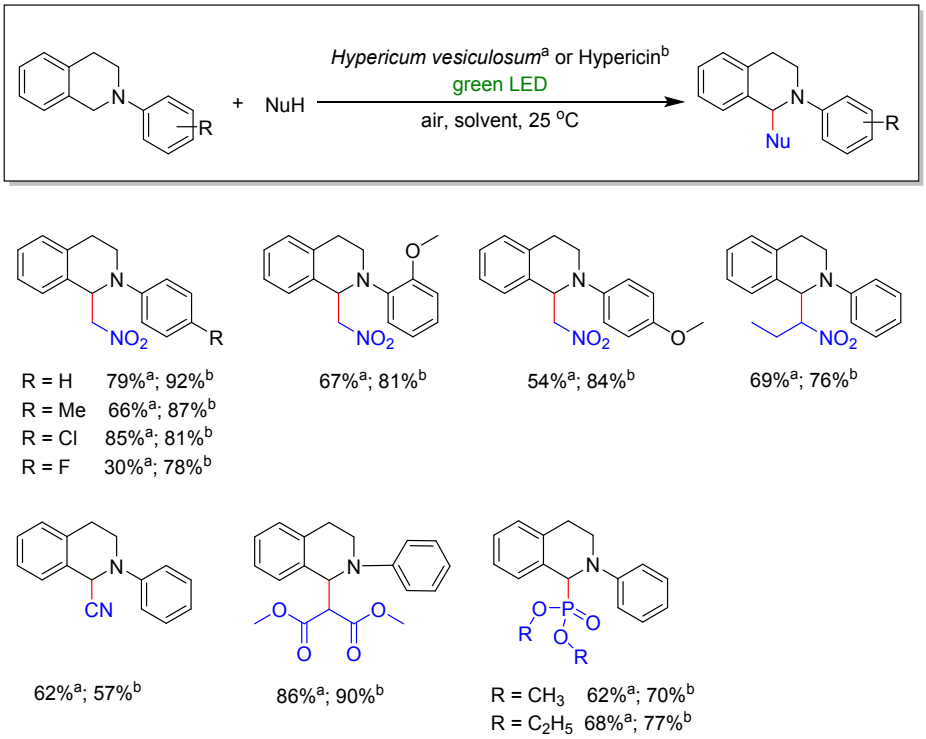

Figure S10. *Hypericum vesiculosum* plant or hypericin as photoredox catalyst in photooxidative coupling reactions of *N*-aryl-tetra-hydroisoquinolines with nitromethane and dialkylphosphites ($(OR)_2P(O)H$) under green light (530 nm) irradiation. Reactions were performed according to the general procedures.

2.10 Stern-Volmer quenching experiments

Hypericin DMSO solution (0.01 mM) was mixed with calculated amount of DIPEA. Then the mixture was diluted to 5.0 mL and used for UV-vis and fluorescence measurement.

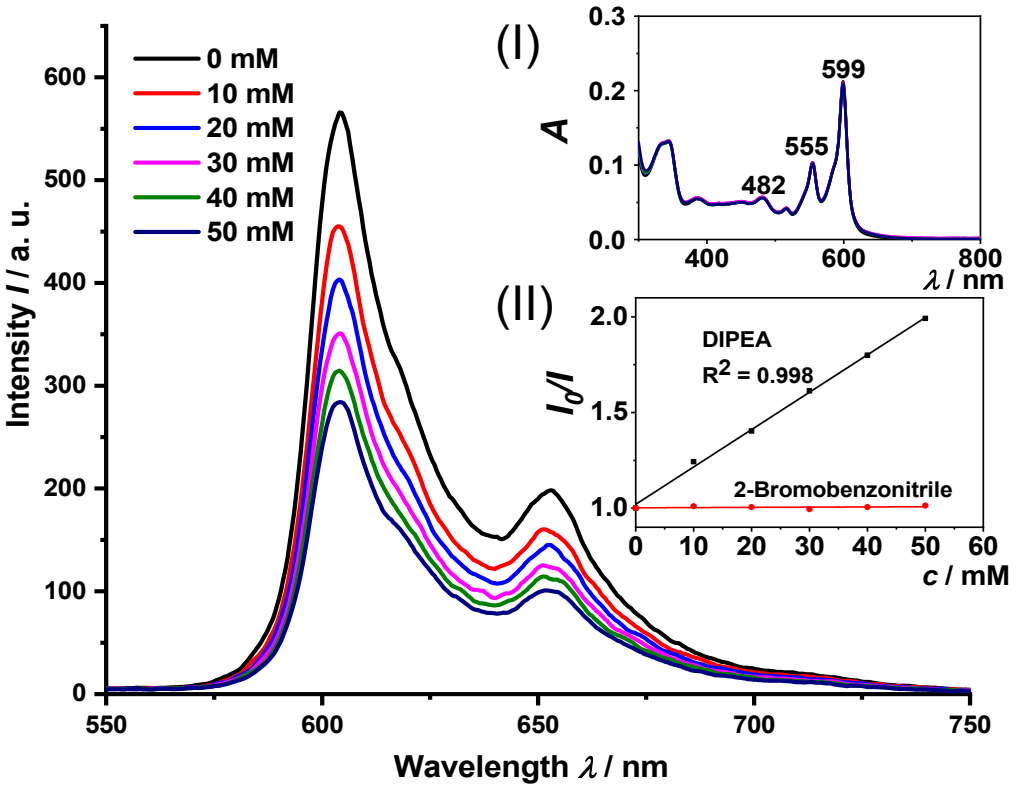

Figure S11. Changes in fluorescence spectra (λ_{Ex} = 470 nm) of HypH DMSO solution upon gradual addition of DIPEA. Insets: (I) the changes in UV-vis spectra; (II) Stern-Volmer plots for the quenching of Hyp^- in presence of DIPEA and 2-Bromobenzontrile.

2.11 General electrochemical procedures

All electrochemical (*EC*) and *in situ* UV-vis spectroelectrochemical (*in situ SEC*) measurements were performed in a Glovebox Pure Lab HE GP-1 SR (Innovative Technology, USA) in an atmosphere of purified nitrogen (<0.1ppm O_2; <0.1ppm H_2O). The glovebox was equipped with military grade BNC feedthroughs in a custom-made gas tight flange for low noise electrical connection of electrochemical and spectroelectrochemical cells inside. UV-vis-NIR spectroscopy inside the glovebox was performed *via* another homemade, gas tight flange containing four light tight chambers with optical grade fused silica windows and four 74-UV (Ocean Optics Inc., USA) collimating lens with SMA 905 connectors for optical fibers. EC and SEC cells were connected to a PGSTAT302 (Metrohm Autolab, Utrecht, The Netherlands) E = ±10 V, U = ±35 V with an auxiliary voltage monitor (BK Precision 2831E, Yorba Linda, CA USA). NOVA Software (Metrohm Autolab) Version 1.11.2 was used to control the potentiostat, magnetic stirring and to trigger the spectrometer. UV-vis spectra recorded by OceanView software (Version 1.4.1, Ocean Optics) were triggered by a DG1032Z arbitrary waveform function generator (Rigol, Beijing, China) controlled by the Nova Software (1.10.4, Fa Metrohm Autolab) by the DAC164 analog/digital converter. Data analysis of the spectral and electrochemical data was performed using OriginPro 2019 (OriginLab Cooperation, Northampton, MA, USA).

Solvent preparation / supporting electrolyte preparation

DMSO (Fisher Scientific, >99.9%) and CH_3CN were dried by heating with CaH_2 to reflux conditions for at least 6 h and distillation under Argon or reduced pressure (DMSO) onto vacuum activated molecular sieves (CH_3CN: 3 Å ; DMSO: 4 Å, $1 \cdot 10^{-3}$ mbar, 350 °C, 12 h). Additionally all solvents were stored over vacuum activated molecular sieves for at least 14 days. [^{n}Bu$_4$N][BF_4] and [^{n}Bu$_4$N][PF_6] were dried at least 5 times by dissolving in CH_2Cl_2, evaporating the solvent to high vacuum at 80 °C and finally drying in high vacuum ($1 \cdot 10^{-3}$ mbar) for 2 days at 140 °C. Prior to each measurement the solvent is passed through a Pasteur pipette with an activated ($1 \cdot 10^{-3}$ mbar, 350 °C, 24 h) aluminum oxide bed (D = 5 mm; L = 70 mm) in the glove box before the supporting electrolyte is added. DMSO prepared according to this procedure is termed “pre-dried DMSO” since the residual water levels still exceeded the range of >25 ppm. The dried CH_3CN was shown to be within this range[2]. As a reference, “non-dried DMSO” was prepared by degassing DMSO (new bottle Fisher Scientific, >99.9%, as received) with three cycles of the freeze-pump-thaw method. It was then used like the pre-dried DMSO.

Substrate preparation

Hypercin solutions in CH_3CN and DMSO (pre-dried and non-dried) for electrochemical investigation by disc electrode voltammetry and spectroelectrochemical measurements were prepared by irradiating a solution of proto hypericin in double-concentrated (based on the desired final concentration) solutions in a small standard schlenk tube under stirring using a Toolcraft FCL/T5/22 W Daylight lamp for at least 12 h. After this procedure supporting electrolyte was added to a concentration of 0.1 M. After a background current measurement with 5 mL 0.1 M supporting electrolyte solution, 5 mL of hypericin in 0.1 M supporting electrolyte were added to the cell to archive the measurement concentration. For spectroelectrochemical investigation the final concentration was adjusted by diluting the previously irradiated hypericin solution by adding supporting electrolyte solution in the cuvette cell.

2.12 Voltammetry data of Hypericin in DMSO and CH_3CN

Variable scan rate CV data

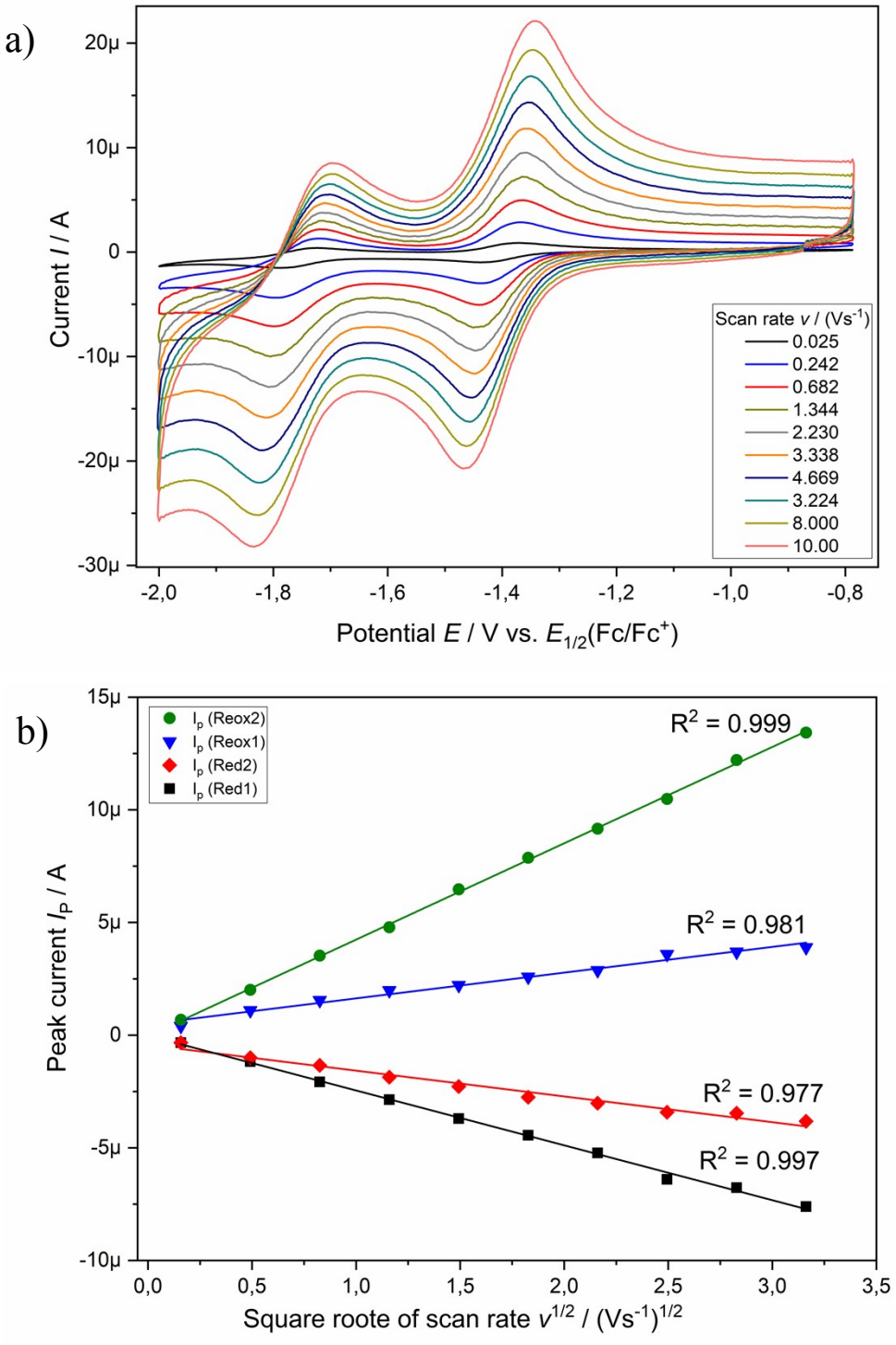

Figure S12. a) CV of hypericin (1.0 mM) in DMSO / 0.1 M [^{n}Bu$_4$N][BF$_4$] at 1.6 mm platinum disc electrodes with different scan rates. b) Randles-Ševčík plot for confirmation of the reversibility of the electrochemical processes based on the peak currents from the first and second reduction peaks I_P(Red1; Red2) and corresponding reoxidation peaks I_P(Reox1; Reox2).

According to the Randles-Ševčík equation (Eq. 1)[3], a proof of the reversibility of the two one-electron reduction processes of Hyp^- from HypH in DMSO is given by measuring CV data at different scan rates between 25 mV/s and 10 V/s in square-root steps (Figure S12 a)). The CV curves show very low dependence to independence of the peak potentials to the scan rate. Additionally, peak current measurements are plotted to the square-root of the scan rate, (Figure S12 b)) showing a peak current dependency to $v^{1/2}$ according to the linearized form of the Randles-Ševčík equation (Eq. 2). All peak currents indicate a linear behavior to the square-root of the scan rate with a very good linear correlation proving two reversible electrochemical reduction processes ($Hyp^- / Hyp^{\bullet 2-}$ and $Hyp^{\bullet 2-} / Hyp^{3-}$) of Hyp^- in DMSO.

$$Eq.1\ I_P = 2.69 \cdot 10^5 \cdot n^{3/2} \cdot \sqrt{D} \cdot C_0 \cdot \sqrt{v}$$

$$Eq.2\ I_P = m \cdot \sqrt{v} + b$$

CV data of HypH with different water contents of DMSO

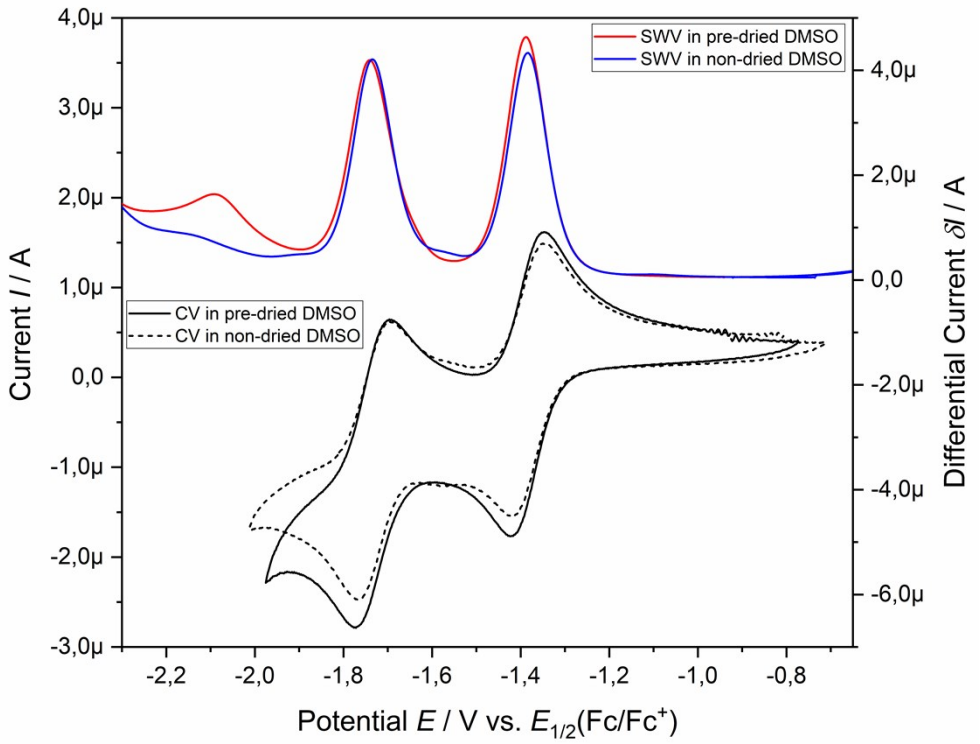

Figure S13. SWVs (blue and red line) and CVs (black lines) of hypericin (1.0 mM) in 0.1 M [^{n}Bu$_4$N][BF$_4$] electrolyte solution at a 1.6 mm platinum disc electrodes measured in non-dried DMSO (Fisher Scientific, > 99.9%, degassed) and pre-dried DMSO (see above) with a scan rate of v = 0.1 V/s.

Hypericin in its non-deprotonated form HypH was investigated by cyclic voltammetry in DMSO by Redepenning et. al[4]. The two reversible one-electron reduction processes were assigned to the direct reduction of HypH (HypH / $HypH^{\bullet -}$ and $HypH^{\bullet -} / HypH^{2-}$), but have since been altered and reassigned to the reduction processes ($Hyp^- / Hyp^{\bullet 2-}$ and $Hyp^{\bullet 2-} / Hyp^{3-}$) of deprotonated Hyp^- according to the newer literature[5]. Gerson et al. reattributed the observation

of Redepenning et al. from redox processes of HypH to Hyp^- because of their use of "non-dried DMSO" and supporting electrolyte that had been used as received. The ion-pair formation of HypH to [Hyp]H by residual water in DMSO has been investigated in this work by performing CV and SWV experiments of HypH generated in differently prepared DMSO from protohypericin by irradiation with visible light. For this, DMSO was a) used as received, but degassed ("non-dried DMSO", see 2.11 Solvent preparation) and b) used after drying with standard laboratory drying procedures ("pre-dried DMSO" see 2.11 Solvent preparation).

In the CV and SWV comparison (Figure S13) both cases show two one-electron reduction processes ($Hyp^- / Hyp^{\bullet 2-}$ and $Hyp^{\bullet 2-} / Hyp^{3-}$). Only the third reduction process is less prone in the DMSO with a higher residual water content maybe because of the reactive reduction product ($Hyp^{\bullet 3-}$) reacting with water. Since the photoredoxcatalysis reactions were also performed in "pre-dried DMSO" it is assumed that even in DMSO with a lower residual water content, HypH reacts to form Hyp^- as an active species.

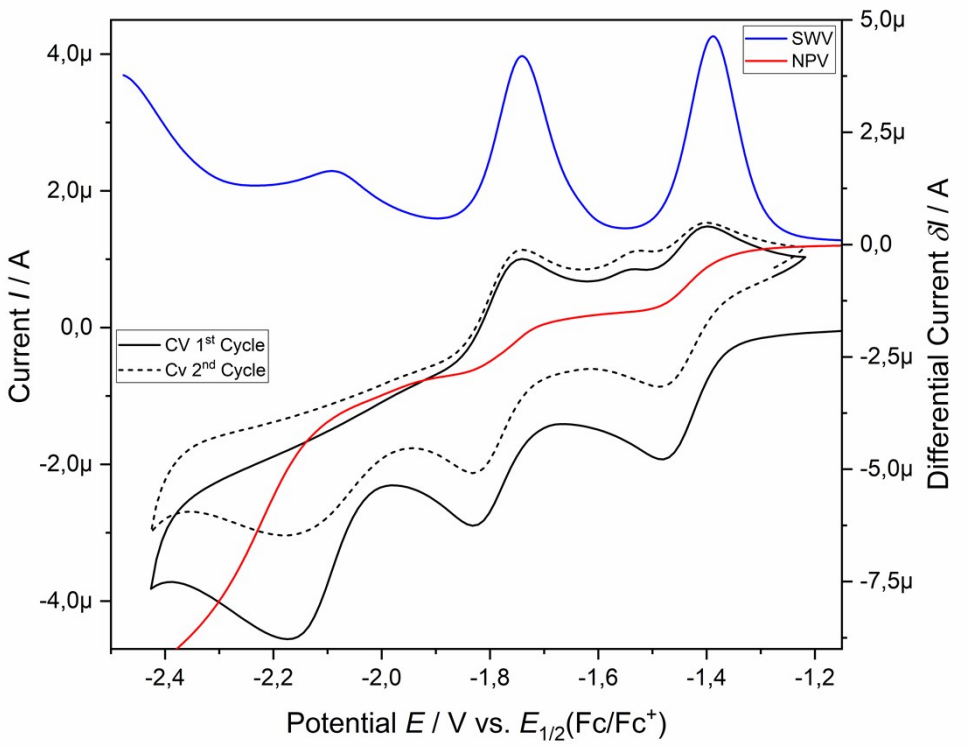

Figure S14. SWVs (blue line), CVs (black lines) and NPV (red line) of hypericin (1.0 mM) in 0.1 M [^{n}Bu$_4$N][BF$_4$] electrolyte solution at a 1.6 mm platinum disc electrodes measured in pre-dried DMSO (see above) with a scan rate of v = 0.1 V/s.

The accessible potential window in "pre-dried DMSO" allowed an observation of the third one-electron reduction process of Hyp^{3-} to $Hyp^{\bullet 4-}$. Since the third reduction takes place at the reduction limit of DMSO a chemical follow-up reaction takes place resulting in a non-reversible peak form. From the SWV a redox potential at $E_{1/2}$ = -2.094 V is observed. Normal-pulse voltammetry of the full potential window reveals the same number of electrons for all three reduction processes by a comparable plateau height.

CV data of HypH in CH_3CN

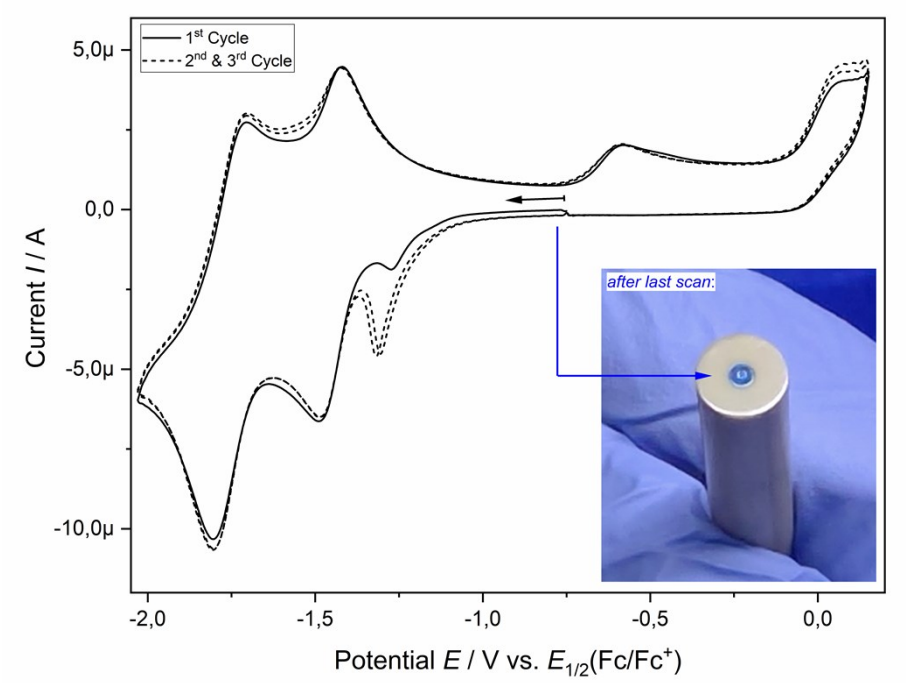

Figure S15. CV of hypericin (1.98 mM) in 0.1 M [^{n}Bu$_4$N][PF_6] electrolyte solution at a 1.6 mm platinum disc electrodes measured in CH_3CN (see above) with a scan rate of v = 0.1 V/s. Insert: Coated electrode surface past the 3rd cycle after rinsing with CH_3CN.

CV investigations of HypH in CH_3CN have not been reported yet due to the low solubility of HypH. We circumvented this issue by irradiating solutions of better soluble protohypericin in carefully dried CH_3CN to form HypH (1.98 mM). Gerson et al.[5] reported CV data of HypNa in CH_3CN at Pt disc electrodes and determined the redox potentials of the first two one-electron reductions processes:

$E_{1/2}(Hyp^{\bullet 2-} / Hyp^-)$ = -1.45 V vs. $E_{1/2}(Cp_2Fe/Cp_2Fe^+)$

$E_{1/2}(Hyp^{3-} / Hyp^{\bullet 2-})$ = -1.77 V vs. $E_{1/2}(Cp_2Fe/Cp_2Fe^+)$

Based on the first CV data of HypH in the same solvent as HypNa both one-electron reduction potentials $E_{1/2}(Hyp^{\bullet 2-} / Hyp^-)$ = -1.457 V and $E_{1/2}(Hyp^{3-} / Hyp^{\bullet 2-})$ = -1.749 V match, indicating the presence of Hyp^-. In accordance with the presence of Hyp^- the first non-reversible peak (E_p = - 1.303 V; "$E_{1/2}$" = -1.316 V, based on the 1st derivative of the CV) is attributed to the proton reduction: HypH + e^- → Hyp^- + ½ H•. This process appears distinctly in the first scan and decreases with the number of cycles due to the reversible reduction reactions forming Hyp^- by reoxidation. Extending the oxidation limit to the first oxidation reaction results in a visible deposition of a blue colored film on the electrode surface (Figure S15 b).

2.13 *In situ UV-vis SEC* in transmission geometry:

In situ UV-vis MPCA

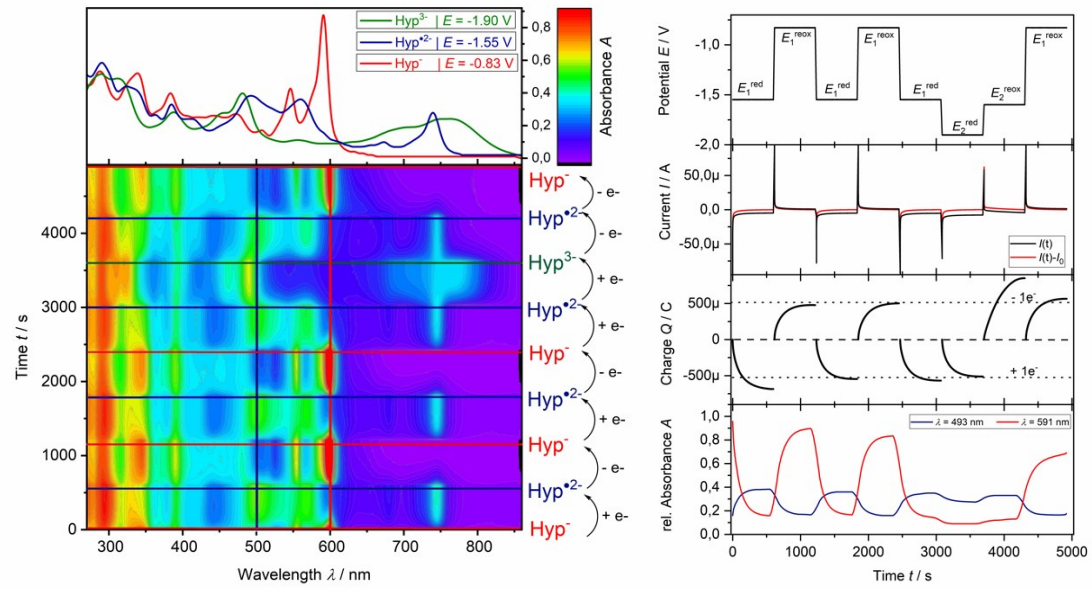

Figure S16. *In situ* UV-vis multi pulse chronoamperometry (MPCA) of HypH (0.5 mM) in DMSO / 0.1 M [^{n}Bu$_4$N][BF$_4$] at a platinum mesh electrode in a double compartment cuvette cell (d = 0.5 mm); right: 2D-Plot of in situ UV-vis spectra during the MPCA measurement; left top to bottom: potential profile, chonoamperogramm, chronocoulogramm, chronoabsorptiometry.

Repetitive chronoamperometric switching between Hyp$^-$ (Figure S16, left, red line) and Hyp$^{\bullet 2-}$ (blue line) and further Hyp^{3-} (green line) revealed two one-electron processes (Figure S16, right, chronocoulogram). Furthermore, this measurement show an exhaustive conversion between all redox stats of Hyp$^-$ proceeding over stable intermediates back to Hyp$^-$.

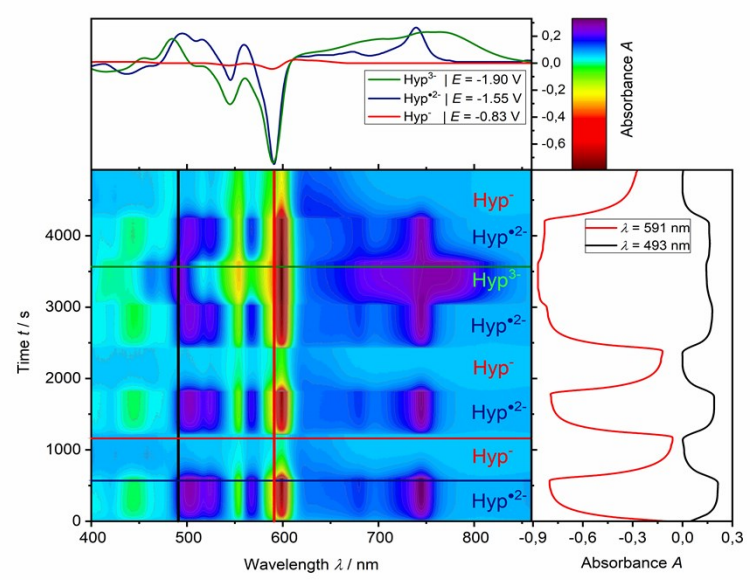

Figure S17. *In situ* UV-vis Multipulse chrono amperometry (*in situ* UV-vis-MPCA) of hypericin (0.50 mM) in 0.1 M [^{n}Bu$_4$N][BF$_4$] / DMSO electrolyte solution at a platinum mesh electrode in a double compartment cuvette cell (d = 0.5 mm). Top: Relative (reference: hypericin in 0.1 M [^{n}Bu$_4$N][BF$_4$] / DMSO) UV-vis spectra after a step time of t = 600 s showing Hyp$^-$ (E > -0.83 V, red line), Hyp$^{\bullet 2-}$ (-1.55 V < E < -0.83 V, blue line) and Hyp^{3-} (E < -1.90 V, green line).

Figure S17 depicts the relative UV-vis absorbance (reference: 0.5 mM HypH in 0.1 M [^{n}Bu$_4$N][BF$_4$] / DMSO electrolyte) during the chronoamperometric measurement with *in situ* UV-vis spectroscopy. The relative UV-vis spectra at potentials where Hyp$^-$ (E = -1.55 V, Figure S17, red line, top) is fully converted to Hyp$^{\bullet 2-}$ (blue line) and Hyp$^{\bullet 2-}$ to Hyp^{3-} (green line) are observed after an equilibration time of 10 min for each multiple chronoamperometry pulse. During the multiple pulses a fully reversible conversion between the different redox states Hyp$^-$ / Hyp$^{\bullet 2-}$ / Hyp^{3-} is observed from the *in situ* UV-vis MPCA measurement.

***In situ* UV-vis CV**

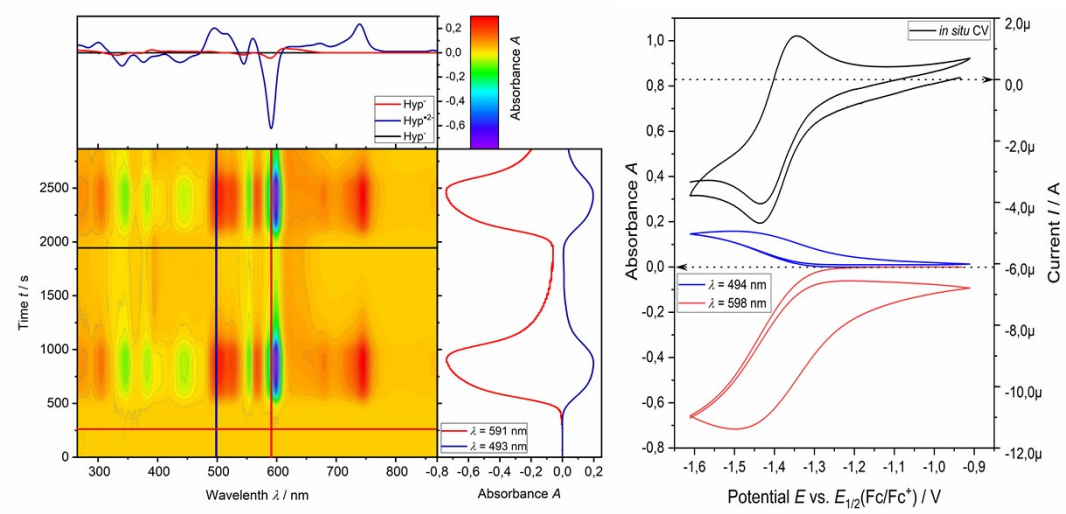

Figure S18. *In situ* UV-vis CV measurement (v = 0.9 mV/s) of hypericin (0.50 mM) in DMSO / 0.1 M [^{n}Bu$_4$N][BF$_4$] at a platinum mesh electrode in a double compartment cuvette cell (d = 0.5 mm); left: 2D-Plot of relative UV-vis spectra during the CV measurement (2 cycles); upper right: *In situ* cyclic voltammogram; lower right & middle upright: Relative absorbance of Hyp$^-$ (λ = 598 nm, red) and Hyp$^{\bullet 2-}$ (λ = 494 nm, blue) during the CV measurement.

In situ UV-vis CV measurement of hypericin as relative absorbance (reference: 0.50 mM HypH in 0.1 M [^{n}Bu$_4$N][BF$_4$] / DMSO electrolyte) shows the fully spectroscopically reversible process in addition to the electrochemically reversible *in situ* cyclic voltammogram (Figure S18, top right, black curve) by a flat base line after the first CV cycle in the *in situ* UV-vis spectrum (top left, black curve). Absorption-based *in situ* CV data for the characteristic bands of Hyp- (red curve, right, bottom) and Hyp$^{\bullet 2-}$ (blue curve) prove an exhaustive switching between Hyp- and Hyp$^{\bullet 2-}$ during the cycle around the first half wave potential (E = -1.390 V).

2.14 *In situ* irradiation UV-vis-NIR spectroscopy set-up

A custom made set-up based on an OSRAM LED Oslon SSL 80 LBCP7P-GYHY (blue, λ_{max} = 470 nm, I_{max} = 1000 mA, 1.12 W) that is mounted to a heat-sink next to the cuvette compartment of a peltier cooled cuvette holder qpod 2e (Quantum Northwest, USA) at 20 °C. Recooling is performed by an ethanol cooling loop at 0 °C from a standard laboratory cryostat (outside the glove box). Aperture at the 10 mm fluorescence (silica glass) cuvette for the irradiation path was 8 × 10 mm and 4 × 10 mm for the UV-vis-NIR spectroscopy pathway. The collimation lenses were connected to the same UV-vis-NIR diode array spectrometer Maya 2000PRO as used for spectroelectrochemical measurements with the DH-2000-BAL light source (*vide supra*). Triggering of the spectra acquisition was achieved with a PGSTAT302 potentiostat powering the LED (WE +, CE/RE-) with a chronopotentiometric pulse (I = 750 mA = const, t = 10 s) followed by a pulse to gate trigger a Rigol DG1032Z arbitrary waveform function generator generating an edge trigger to acquire and average 15 CCD read outs ($t_{integration}$ = 35 ms) to a spectrum. This cycle is continuously repeated during the measurement time.

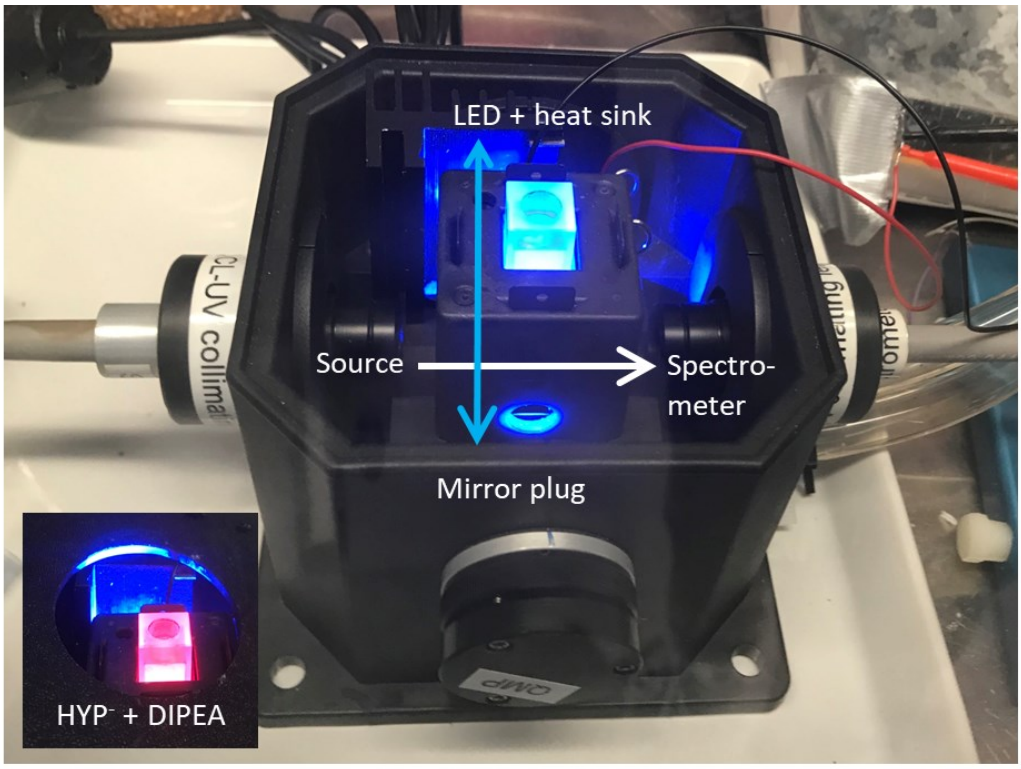

Figure S19. Experimental set-up for high intensity *in situ* irradiation UV-vis-NIR spectroscopy in 90° geometry. Peltier controlled cuvette compartment in a nitrogen-filled glove box system. Insert: Fluorescence of a hypericin solution (0.016 mM)) after addition of 50 equiv. DIPEA in DMSO.

3 NMR characterization

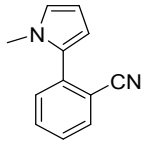

2-(1-methyl-1H-pyrrol-2-yl)benzonitrile: Colorless solid. ^{1}H NMR ($CDCl_3$, 300 K, in ppm): δ 7.74 (ddd, *J* = 7.7, 1.4, 0.6 Hz, 1H), 7.64-7.58 (m,1H), 7.45-7.38 (m, 2H), 6.79 (dd, *J* = 2.6, 1.8 Hz, 1H), 6.41 (dd, *J* = 3.7, 1.8 Hz, 1H), 6.25 (dd, *J* = 3.7, 2.7 Hz, 1H), 3.61 (s, 3H). ^{13}C{^{1}H} NMR ($CDCl_3$, 300 K, in ppm): δ 137.1, 133.7, 132.5, 131.0, 130.1, 127.5, 124.9, 118.7, 113.0, 111.6, 108.5, 35.0.

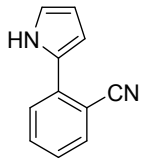

2-(1H-pyrrol-2-yl)benzonitrile: Colorless oil. ^{1}H NMR ($CDCl_3$, 300 K, in ppm): δ 9.20 (s, 1H), 7.67-7.61 (m, 2H), 7.57-7.53 (m, 1H), 7.27-7.22 (m, 1H), 6.99-6.95 (m, 1H), 6.85-6.80 (m, 1H), 6.37-6.32 (m, 1H). ^{13}C{^{1}H} NMR ($CDCl_3$, 300 K, in ppm): δ 135.9, 134.2, 133.3, 128.3, 126.8, 126.0, 121.0, 120.3, 110.5, 110.5, 106.1.

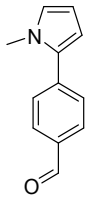

4-(1-methyl-1H-pyrrol-2-yl)benzaldehyde: Colorless solid. ^{1}H NMR ($CDCl_3$, 300 K, in ppm): δ 10.02 (s, 1H), 7.92-7.88 (m, 2H), 7.60-7.55 (m, 2H), 6.81-6.76 (m, 1H), 6.39 (dd, *J* = 3.6, 1.6 Hz, 1H), 6.26-6.21 (m, 1H), 3.74 (s, 3H). ^{13}C {^{1}H}NMR ($CDCl_3$, 300 K, in ppm): δ 191.8, 139.4, 134.4, 133.4, 130.1, 128.4, 125.9, 110.9, 108.7, 35.7.

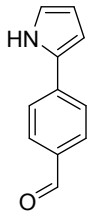

4-(1H-pyrrol-2-yl)benzaldehyde: Colorless solid. ^{1}H NMR ($CDCl_3$, 300 K, in ppm): δ 9.95 (s, 1H), 8.82 (s, 1H), 7.90-7.81 (m, 2H), 7.65-7.57 (m, 2H), 6.98-6.91 (m, 1H), 6.75-6.70 (m, 1H), 6.38-6.38 (m, 1H). ^{13}C{^{1}H} NMR ($CDCl_3$, 300 K, in ppm): δ 191.7, 138.4, 133.9, 130.8, 123.7, 121.1, 111.1, 108.9.

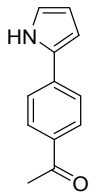

1-(4-(1H-pyrrol-2-yl)phenyl)ethan-1-one: Light yellow oil. ^{1}H NMR ($CDCl_3$, 300 K, in ppm): δ 8.63 (s, 1H), 7.97-7.94 (m, 2H), 7.56-7.53 (m, 2H), 6.96-6.93 (m, 1H), 6.70-6.66 (m, 1H), 6.36-6.32 (m, 1H), 2.60 (s, 3H). ^{13}C{^{1}H} NMR ($CDCl_3$, 300 K, in ppm): δ 197.5, 137.1, 134.6, 131.0, 129.4, 123.4, 120.6, 110.9, 108.3, 26.6.

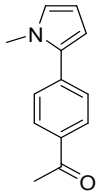

1-(4-(1-methyl-1H-pyrrol-2-yl)phenyl)ethan-1-one: Colorless solid. ^{1}H NMR ($CDCl_3$, 300 K, in ppm): δ 8.02-7.96 (m, 2H), 7.53-7.48 (m, 2H), 6.79-6.75 (m, 1H), 6.37-6.34 (m, 1H), 6.25-6.21 (m, 1H), 3.72 (s, 3H), 2.62 (s, 3H). ^{13}CNMR (125 MHz, $CDCl_3$): δ 197.7, 138.0, 135.1, 133.5, 128.7, 128.1, 125.4, 110.4, 108.5, 35.6, 26.7.

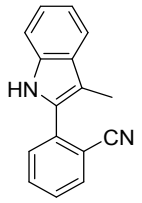

2-(3-methyl-1H-indol-2-yl)benzonitrile: Colorless solid. ^{1}H NMR ($CDCl_3$, 300 K, in ppm): δ 8.24 (s, 1H), 7.80 (dd, *J* = 7.8, 0.9 Hz, 1H), 7.70-7.66 (m, 1H), 7.66-7.61 (m, 2H), 7.49-7.45 (m, 1H), 7.41-7.39 (m, 1H), 7.29-7.25 (m, 1H), 7.20-7.16 (m, 1H), 2.41 (s, 3H). ^{13}C{^{1}H} NMR ($CDCl_3$, 300 K, in ppm): δ 136.9, 136.4, 134.0, 132.8, 131.0, 130.3, 129.3, 128.1, 123.5, 120.0, 119.6, 118.7, 112.4, 112.1, 111.2, 10.1.

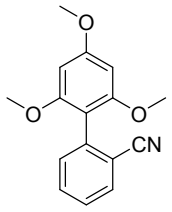

2',4',6'-trimethoxy-[1,1'-biphenyl]-2-carbonitrile: Colorless solid. ^{1}H NMR ($CDCl_3$, 300 K, in ppm): δ 7.72-7.68 (m, 1H), 7.60-7.56 (m, 1H), 7.42-7.34 (m, 2H), 6.24 (s, 2H), 3.87 (s, 3H), 3.75 (s, 3H). ^{13}C{^{1}H} NMR ($CDCl_3$, 300 K, in ppm): δ 162.0, 158.4, 138.9, 132.7, 132.5, 132.0, 127.0, 119.0, 114.9, 108.7, 91.0, 55.9, 55.5.

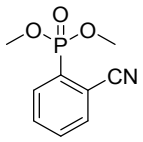

Dimethyl (2-cyanophenyl)phosphonate: Colorless solid. ^{1}H NMR ($CDCl_3$, 300 K, in ppm): δ 8.13-8.06 (m, 1H), 7.83-7.78 (m, 1H), 7.73-7.62 (m, 1H), 3.87 (d, J = 11.3 Hz, 6H). ^{13}CNMR (100 MHz, $CDCl_3$): δ 134.8 (d, J = 8.5 Hz), 134.6 (d, J = 11.2 Hz), 132.8 (d, J = 2.6 Hz), 132.4 (d, J = 14.2 Hz), 131.3 (d, J = 189.2 Hz), 117.2 (d, J = 5.8 Hz), 114.8 (d, J = 5.0 Hz), 53.6 (d, J = 6.0 Hz). ^{31}P NMR ($CDCl_3$, 300 K, in ppm): δ 15.5.

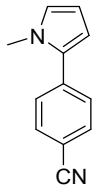

4-(1-methyl-1H-pyrrol-2-yl)benzonitrile: white solid. ^{1}H NMR ($CDCl_3$, 300 K, in ppm): δ = 7.70-7.64 (m, 2H), 7.52-7.48 (m, 2H), 6.81-6.76 (m, 1H), 6.35 (dd, J = 3.7, 1.7 Hz, 1H), 6.23 (dd, J = 3.7, 2.7 Hz, 1H), 3.72 (s, 3H). ^{13}C{^{1}H} NMR ($CDCl_3$, 300 K, in ppm): δ = 137.8, 132.8, 132.4, 128.4, 126.0, 119.2, 110.9, 109.8, 108.7, 35.6.

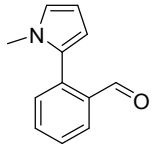

2-(1-methyl-1H-pyrrol-2-yl)benzaldehyde: colorless oil. ^{1}H NMR ($CDCl_3$, 300 K, in ppm): δ = 9.93 (s, 1H), 8.01 (d, J = 7.8 Hz, 1H), 7.63 (t, J = 7.5 Hz, 1H), 7.49 (t, J = 7.6 Hz, 1H), 7.43 (d, J = 7.7 Hz, 1H), 6.82-6.78 (m, 1H), 6.28-6.23 (m, 1H), 6.22-6.17 (m, 1H), 3.52 (s, 1H). ^{13}C{^{1}H} NMR ($CDCl_3$, 300 K, in ppm): δ = 192.7, 136.7, 135.4, 133.5, 131.7, 129.1, 128.1, 127.6, 124.2, 112.9, 108.2, 34.7.

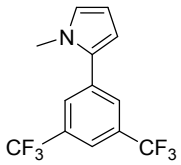

2-(3,5-bis(trifluoromethyl)phenyl)-1-methyl-1H-pyrrole: colorless oil. ^{1}H NMR ($CDCl_3$, 300 K, in ppm): δ = 7.84 (s, 2H), 7.79 (s, 1H), 6.82-6.78 (m, 1H), 6.37 (dd, J = 3.6, 1.7 Hz, 1H), 6.27-6.23 (m, 1H), 3.71 (s, 1H). ^{13}C{^{1}H} NMR ($CDCl_3$, 300 K, in ppm): δ = 135.4, 132.0 (q, J = 33.3 Hz), 131.6, 128.2-128.0 (m), 125.8, 123.5 (q, J = 272.7 Hz), 120.2-120.0 (m), 110.9, 108.8, 35.3. ^{19}F NMR ($CDCl_3$, 300 K, in ppm): δ = -63.0.

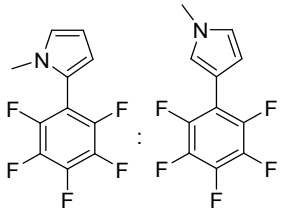

α : β = 10 : 3

1-methyl-2/3-(perfluorophenyl)-1H-pyrrole: white solid (Ratio: α : β = 10 : 3). ^{1}H NMR ($CDCl_3$, 300 K, in ppm): δ = 7.14-7.10 (m, 0.3H, β), 6.88-6.83 (m, 1H, α), 6.73-6.69 (m, 0.3H, β), 6.61-6.58 (m, 0.3H, β), 6.34-6.31 (m, 1H, α), 6.30-6.27 (m, 1H, α), 3.74 (s, 0.9H, β), 3.55 (s, 3H, α). ^{13}C{^{1}H} NMR ($CDCl_3$, 300 K, in ppm): δ = 144.9 (dm, $^{1}J_{CF}$ = 247.0 Hz, α), 144.1 (dm, $^{1}J_{CF}$ = 251.0 Hz, β), 140.9 (dm, $^{1}J_{CF}$ = 254.5 Hz, α), 137.8 (dm, $^{1}J_{CF}$ = 251.0 Hz, α), 139.4-139.2, 137.4-137.1 (m, β), 125.2 (α), 123.4 (t, J_{CF} = 7.1 Hz, β), 122.5 (β), 116.8 (β), 113.0 (α), 111.4 (td, J_{CF} = 15.5, 4.1 Hz, β), 109.7 (t, J_{CF} = 5.8 Hz, α), 108.8 (α), 108.6 (td, J_{CF} = 18.3, 3.9 Hz, α), 36.6 (β), 34.6 (t, J_{CF} = 2.7 Hz, α). ^{13}C{^{19}F} NMR ($CDCl_3$, 300 K, in ppm): δ = 144.8 (α), 144.0 (β), 140.9 (α), 138.2 (β), 138.1 (β), 137.9 (α), 125.1 (dm, $^{1}J_{CH}$ = 184.3 Hz, α), 123.6 (dm, $^{1}J_{CH}$ = 118.1 Hz, β), 112.1 (dm, $^{1}J_{CH}$ = 116.8 Hz, β), 117.0-116.7 (m, β), 113.0 (dm, $^{1}J_{CH}$ = 172.4 Hz, α), 111.4 (β), 109.7 (dm, $^{1}J_{CH}$ = 174.3 Hz, β), 108.8 (dm, $^{1}J_{CH}$ = 172.6 Hz, α), 108.6 (α), 36.6 (q, $^{1}J_{CH}$ = 138.9 Hz, β), 34.6 (q, $^{1}J_{CH}$ = 138.9 Hz, α). ^{19}F NMR ($CDCl_3$, 300 K, in ppm): δ = -139.5 (dd, J = 23.7, 8.3 Hz, 2F, α), -142.8 (dd, J = 21.8, 6.7 Hz, 0.3F, β), -154.7 (t, J = 21.0 Hz, 1F, α), -161.2 (t, J = 21.1 Hz, 0.3F, β), -162.1− -162.3 (m, 2F, α), -164.0 (dt, J = 21.5, 6.6 Hz, 0.6F, β).

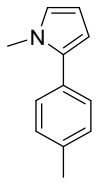

1-methyl-2-(p-tolyl)-1H-pyrrole: colorless oil. ^{1}H NMR ($CDCl_3$, 300 K, in ppm): δ = 7.31-7.29 (m, 2H), 7.22-7.19 (m, 2H), 6.76-6.64 (m, 1H), 6.22-6.16 (m, 1H), 3.65 (s, 3 H), 2.39 (s, 3H). ^{13}C{^{1}H} NMR ($CDCl_3$, 300 K, in ppm): δ = 136.7, 134.8, 130.6, 129.2, 128.8, 123.4, 108.4, 107.8, 35.1, 21.3.

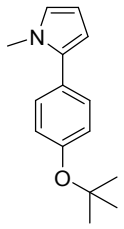

2-(4-(tert-butoxy)phenyl)-1-methyl-1H-pyrrole: colorless oil. ^{1}H NMR ($CDCl_3$, 300 K, in ppm): δ = 7.30-7.27 (m, 2H), 7.03-6.99 (m, 2H), 6.75-6.63 (m, 1H), 6.21-6.15 (m, 2H), 3.65 (s, 3H), 1.38 (s, 9H). ^{13}C{^{1}H} NMR ($CDCl_3$, 300 K, in ppm): δ = 154.6, 134.5, 129.4, 128.5, 124.0, 123.3, 108.3, 107.8, 78.7, 35.1, 29.0.

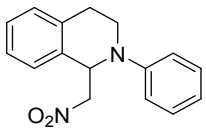

1-(nitromethyl)-2-phenyl-1,2,3,4-tetrahydroisoquinoline: Colorless solid. ^{1}H NMR (DMSO-d_6, 300 K, in ppm): δ = 7.31-7.18 (m, 5 H), 7.14 (d, J = 7.2 Hz, 1 H), 7.00 (d, J = 8.1 Hz, 1 H), 6.87 (t, J = 7.3 Hz, 1H), 5.56 (t, J = 7.1 Hz, 1H), 4.90 (dd, J = 11.9, 7.7 Hz, 1H), 4.58 (dd, J = 11.9, 6.6 Hz, 1H), 3.71-3.60 (m, 2H), 3.13-3.05 (m, 1H), 2.83 (dt, J = 16.3, 5.0 Hz, 1H). ^{13}C{^{1}H} NMR (DMSO-d_6, 300 K, in ppm): δ = 148.5, 135.3, 132.9, 129.5, 129.2, 128.1, 127.0, 126.7, 119.4, 115.1, 78.7, 58.2, 42.0, 26.4.

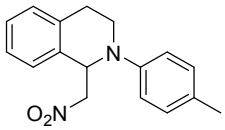

1-(nitromethyl)-2-(p-tolyl)-1,2,3,4-tetrahydroisoquinoline: Colorless solid. ^{1}H NMR ($CDCl_3$, 300 K, in ppm): δ = 7.26-7.11 (m, 4 H), 7.10-7.05 (m, 2 H), 6.92-6.88 (m, 2 H), 5.53-5.47 (m, 1 H), 4.85 (dd, J = 11.9, 8.0 Hz, 1 H), 4.55 (dd, J = 11.9, 6.3 Hz, 1 H), 3.67-3.54 (m, 2 H), 3.10-3.01 (m, 1 H), 2.76 (dt, J = 16.4, 4.6 Hz, 1 H), 2.27 (s, 3 H). ^{13}C{^{1}H} NMR ($CDCl_3$, 300 K, in ppm): δ = 146.4, 135.4, 133.0, 130.1, 129.4, 129.3, 128.1, 127.1, 126.7, 116.1, 78.9, 58.5, 42.5, 26.3, 20.5.

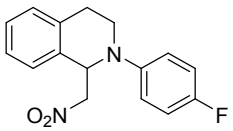

2-(4-fluorophenyl)-1-(nitromethyl)-1,2,3,4-tetrahydroisoquinoline: Pale yellow oil. ^{1}H NMR (DMSO-d_6, 300 K, in ppm): δ = 7.29-7.14 (m, 4H), 7.00-6.90 (m, 4H), 5.45 (dd, J = 8.5, 5.9 Hz, 1H), 4.85 (dd, J = 12.0, 8.6 Hz, 1H), 4.58 (dd, J = 12.0, 5.9 Hz, 1H), 3.67-3.55 (m, 2H), 3.09-2.99 (m, 1H), 2.74 (dt, J = 16.5, 4.2 Hz, 1 H). ^{13}C{^{1}H} NMR (DMSO-d_6, 300 K, in ppm): δ = 157.3 (d, J = 238.9 Hz), 145.4, 135.3, 132.6, 129.6, 128.2, 127.0, 126.9, 118.1 (d, J = 7.2 Hz), 116.0 (d, J = 22.3 Hz), 78.9, 58.8, 43.0, 25.9. ^{19}F NMR ($CDCl_3$, 300 K, in ppm): δ = -124.2.

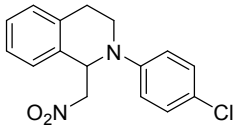

2-(4-chlorophenyl)-1-(nitromethyl)-1,2,3,4-tetrahydroisoquinoline: Colorless oil. ^{1}H NMR ($CDCl_3$, 300 K, in ppm): δ = 7.29-7.17 (m, 5 H), 7.16-7.12 (m, 1 H), 6.93-6.87 (m, 2 H), 5.53-5.46 (m, 1 H), 4.85 (dd, J = 12.0, 8.2 Hz, 1 H), 4.57 (dd, J = 12.0, 6.4 Hz, 1 H), 3.68-3.56 (m, 2 H), 3.12-3.02 (m, 1 H), 2.79 (dt, J = 16.4, 4.8 Hz, 1H). ^{13}C{^{1}H} NMR ($CDCl_3$, 300 K, in ppm): δ = 147.2, 135.2, 132.6, 129.4, 128.4, 127.1, 127.0, 124.6, 116.7, 78.8, 58.3, 42.4, 26.3.

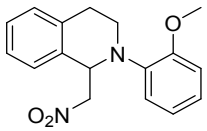

2-(2-methoxyphenyl)-1-(nitromethyl)-1,2,3,4-tetrahydroisoquinoline: Yellow oil. ^{1}H NMR ($CDCl_3$, 300 K, in ppm): δ = 7.27-7.21 (m, 2H), 7.20-7.14 (m, 2H), 7.06-7.02 (m, 2H), 6.95-6.83 (m, 3H), 5.52 (dd, J = 8.2, 5.1 Hz, 1H), 4.84 (dd, J = 12.1, 8.4 Hz, 1H), 4.55 (dd, J = 12.2, 5.1 Hz, 1 H), 3.84 (s, 3H), 3.62 (ddd, J = 13.3, 6.0, 1.8 Hz, 1H), 3.50 (ddd, J = 13.3, 11.3, 4.1 Hz, 1H), 3.04-2.95 (m, 1H), 2.78-2.70 (m, 1H). ^{13}C{^{1}H} NMR ($CDCl_3$, 300 K, in ppm): δ = 153.3, 139.0, 135.5, 133.8, 129.6, 127.7, 126.9, 126.6, 124.3, 122.2, 121.2, 112.7, 79.3, 58.4, 55.9, 43.2, 27.0.

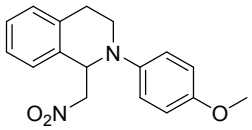

2-(4-methoxyphenyl)-1-(nitromethyl)-1,2,3,4-tetrahydroisoquinoline: Yellow oil. ^{1}H NMR (DMSO-d_6, 300 K, in ppm): δ = 7.25-7.12 (m, 4H), 6.94-6.90 (m, 2H), 6.85-6.72 (m, 2H), 5.39(dd, J = 8.5, 5.9 Hz, 1 H), 74.83 (dd, J = 11.9, 8.6 Hz, 1 H), 4.56 (dd, J = 11.9, 5.8 Hz, 1 H), 3.75 (s, 3H), 3.62-3.52 (m, 2H), 3.06-2.98 (m, 1H), 2.70 (dt, J = 16.5, 4.0 Hz, 1 H). ^{13}C{^{1}H} NMR (DMSO-d_6, 300 K, in ppm): δ = 154.2, 143.2, 135.6, 133.0, 129.6, 128.0, 127.1, 126.8, 119.0, 114.9, 79.1, 59.1, 55.7, 43.3, 26.0.

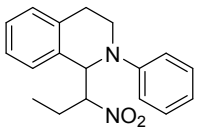

1-(1-nitropropyl)-2-phenyl-1,2,3,4-tetrahydroisoquinoline: light yellow solid (3:2 mixture of diastereoisomers). ^{1}H NMR ($CDCl_3$, 300 K, in ppm): δ = 7.33-7.13 (m, 6H), 7.03-7.94 (m, 2H), 6.86-6.79 (m, 1H), 5.26 (d, J = 9.2 Hz, 0.4H), 5.15 (d, J = 9.5 Hz, 0.6H), 4.93-4.84 (m, 0.6H), 4.75-4.65 (m, 0.4H), 3.92-3.81 (m, 0.6H), 3.72-3.51 (m, 1.4H), 3.15-3.00 (m, 1H), 3.00-2.81 (m, 1H), 2.30-2.05 (m, 1.4H), 1.93-1.75 (m, 0.6H), 1.00-0.92 (m, 3H). ^{13}C{^{1}H} NMR ($CDCl_3$, 300 K, in ppm): δ = 149.2, 149.1, 135.7, 134.8, 134.1, 132.7, 129.5, 129.5, 129.3, 128.8, 128.7, 128.3, 128.3, 127.4, 126.8, 126.0, 119.5, 118.7, 116.0, 114.3, 96.3, 93.2, 62.3, 60.8, 43.7, 42.5, 27.0, 25.9, 25.1, 24.8, 10.8.

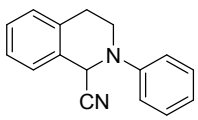

2-phenyl-1,2,3,4-tetrahydroisoquinoline-1-carbonitrile: colorless oil.
^{1}H NMR ($CDCl_3$, 300 K, in ppm): δ = 7.40-7.23 (m, 6H), 7.12-7.08 (m, 2H), 7.05-7.01 (m, 1H), 5.53 (s, 1H), 3.79 (dqd, J = 12.4, 3.0, 1.2 Hz, 1H), 3.50 (ddd, J = 12.4, 10.8, 4.0 Hz, 1H), 3.22-3.13 (m, 1H), 2.98 (dt, J = 16.3, 3.5 Hz, 1H). ^{13}C{^{1}H} NMR ($CDCl_3$, 300 K, in ppm): δ = 148.5, 134.8, 129.7, 129.7, 129.5, 128.9, 127.2, 127.0, 122.0, 117.9, 117.7, 53.4, 44.3, 28.7.

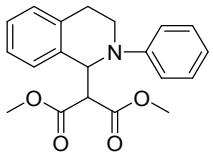

Dimethyl 2-(2-phenyl-1,2,3,4-tetrahydroisoquinolin-1-yl)malonate: brown oil.
^{1}H NMR ($CDCl_3$, 300 K, in ppm): δ = 7.25-7.11 (m, 6H), 7.03-6.97 (m, 2H), 6.81-6.74 (m, 1H), 5.73 (d, J = 9.3 Hz, 1H), 3.97 (d, J = 9.3 Hz, 1H), 3.74-3.61 (m, 5H), 3.56 (s, 3H), 3.13-3.04 (m, 1H), 2.89 (dt, J = 16.5, 5.2 Hz, 1H). ^{13}C{^{1}H} NMR ($CDCl_3$, 300 K, in ppm): δ = 168.4, 167.5, 148.9, 135.8, 134.9, 129.2, 129.1, 127.7, 127.1, 126.1, 118.7, 115.3, 59.2, 58.3, 52.6, 52.6, 42.3, 26.1.

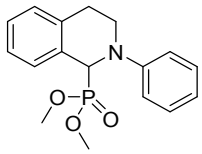

Dimethyl (2-phenyl-1,2,3,4-tetrahydroisoquinolin-1-yl)phosphonate: Brown solid. ^{1}H NMR ($CDCl_3$, 300 K, in ppm): δ = 7.39-7.34 (m, 1H), 7.29-7.23 (m, 2H), 7.21-7.14 (m, 3H), 6.98 (d, J = 8.2 Hz, 1H), 6.81 (t, J = 7.3 Hz, 1H), 5.21 (d, J = 20.0 Hz, 1H), 4.07-3.97 (m, 1H), 3.68-3.61 (m, 7H), 3.12-2.95 (m, 2H). ^{13}C{^{1}H} NMR ($CDCl_3$, 300 K, in ppm): δ = 149.3 (d, J = 6.0 Hz), 136.4 (d, J = 5.7 Hz), 130.4, 129.3, 128.9 (d, J = 2.6 Hz), 128.0 (d, J = 4.5 Hz), 127.6 (d, J = 3.4 Hz), 126.1 (d, J = 2.8 Hz), 118.7, 114.8, 58.8 (d, J = 159.5 Hz), 53.9 (d, J = 7.1 Hz), 53.0 (d, J = 7.7 Hz), 43.6, 26.7. ^{31}P{^{1}H} NMR ($CDCl_3$, 300 K, in ppm): δ = 24.40.

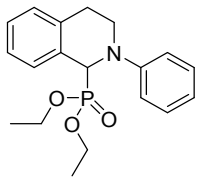

Diethyl (2-phenyl-1,2,3,4-tetrahydroisoquinolin-1-yl)phosphonate: Brown solid. ^{1}H NMR ($CDCl_3$, 300 K, in ppm): δ = 7.41-7.36 (m, 1H), 7.28-7.13 (m, 5H), 6.99 (d, J = 8.3 Hz, 2H), 6.80 (t, J = 7.3 Hz, 1H), 5.19 (d, J = 20.0 Hz, 1H), 4.13-3.85 (m, 5H), 3.68-3.59 (m, 1H), 3.13-2.95 (m, 1H), 1.25 (t, J = 7.1 Hz, 3H), 1.14 (t, J = 7.1 Hz, 1H). ^{13}C{^{1}H} NMR ($CDCl_3$, 300 K, in ppm): δ = 149.5 (J = 5.8 Hz), 136.6 (J = 5.5 Hz), 130.8, 129.3, 128.9 (J = 2.6 Hz), 128.3 (J = 4.6 Hz), 127.6 (J = 3.4 Hz), 126.0 (J = 2.8 Hz), 118.6, 114.9, 63.4 (J = 7.2 Hz), 62.4 (J = 7.7 Hz), 59.0 (J = 159.2 Hz), 43.6, 26.9, 16.6 (J = 5.5 Hz), 16.5 (J = 5.9 Hz). ^{31}P{^{1}H} NMR ($CDCl_3$, 300 K, in ppm): δ = 22.16.

4 References

[1] Aigner, S. & Falk, H. A microwave-assisted synthesis of phenanthroperylene quinones as exemplified with hypericin. *Monatsh*. *Chem*. **139**, 991-993 (2008).

[2] Burfield, D. R. & Smithers R. H. Desiccant efficiency in solvent drying. 3. Dipolar aprotic solvents. *J*. *Org*. *Chem*. **43**, 3966-3968 (1978).

[3] Bard, A. J. & Faulkner, L. R. *Electrochemical Methods*, *John Wiley & Sons Inc., 2 Ed. New York*, 228-232 (2001).

[4] Redepenning, J. & Tao, N. Measurement of Formal Potentials for Hypericin in Dimethylsulfoxide. *Photochem*. *Photobiol*. **58**, 532-535 (1993).

[5] Gerson, F., Gescheidt, G., Häring, P., Mazur, Y., Freeman, D., Spreitzer, H. & Daub, J. Electron-Acceptor Properties of Hypericin and Its Salts: An ESR/ENDOR and Electrochemical Study. *J*. *Am*. *Chem*. *Soc*. **117**, 11861-11866 (1995).

5 NMR spectra of synthesized compounds

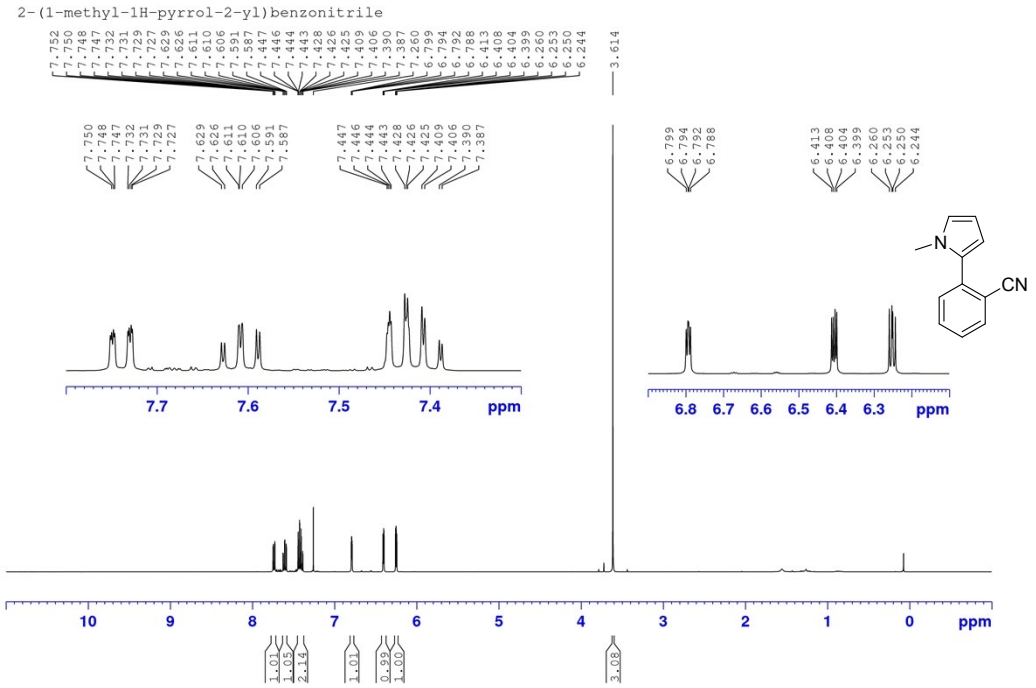

Figure S20. ^{1}H NMR spectrum of 2-(1-methyl-1H-pyrrol-2-yl)benzonitrile ($CDCl_3$, 300 K).

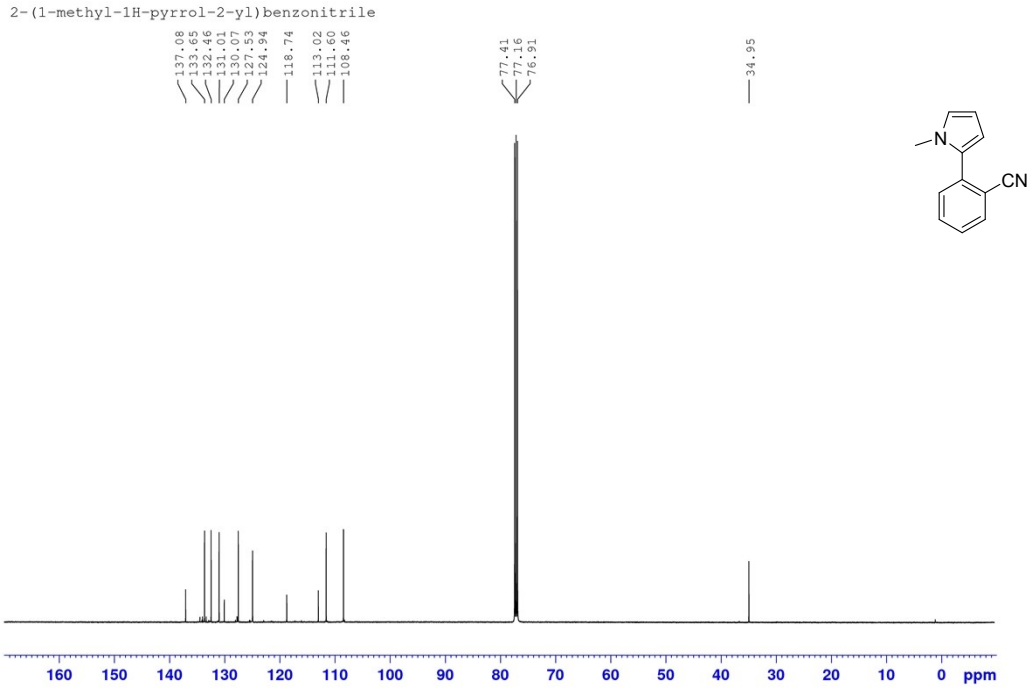

Figure S21. ^{13}C{H} NMR spectrum of 2-(1-methyl-1H-pyrrol-2-yl)benzonitrile ($CDCl_3$, 300 K).

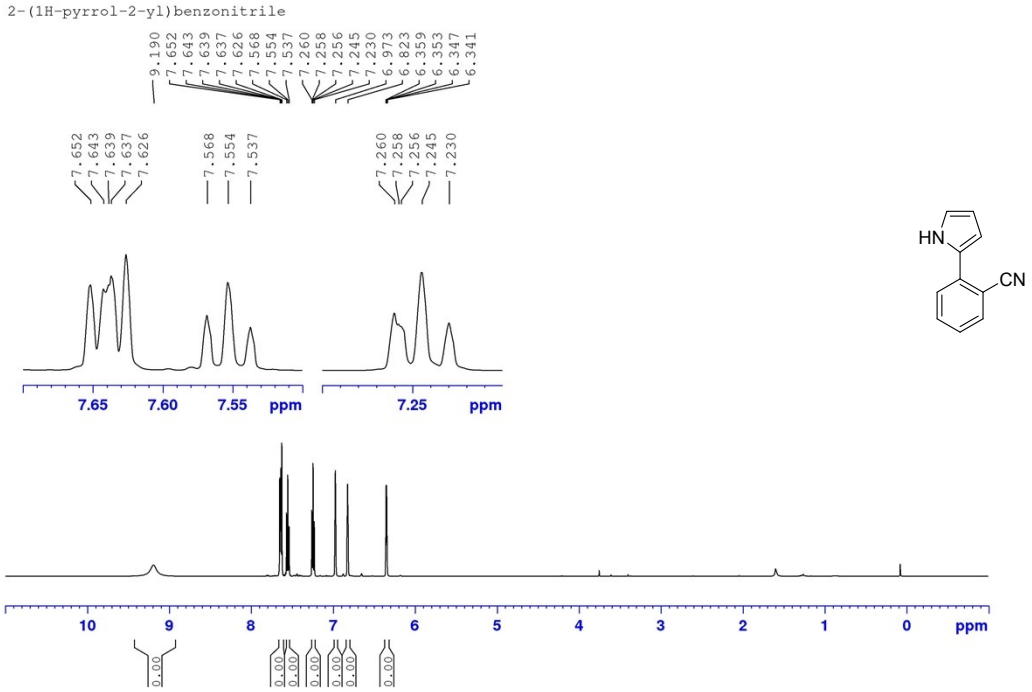

Figure S22. ^{1}H NMR spectrum of 2-(1H-pyrrol-2-yl)benzonitrile ($CDCl_3$, 300 K).

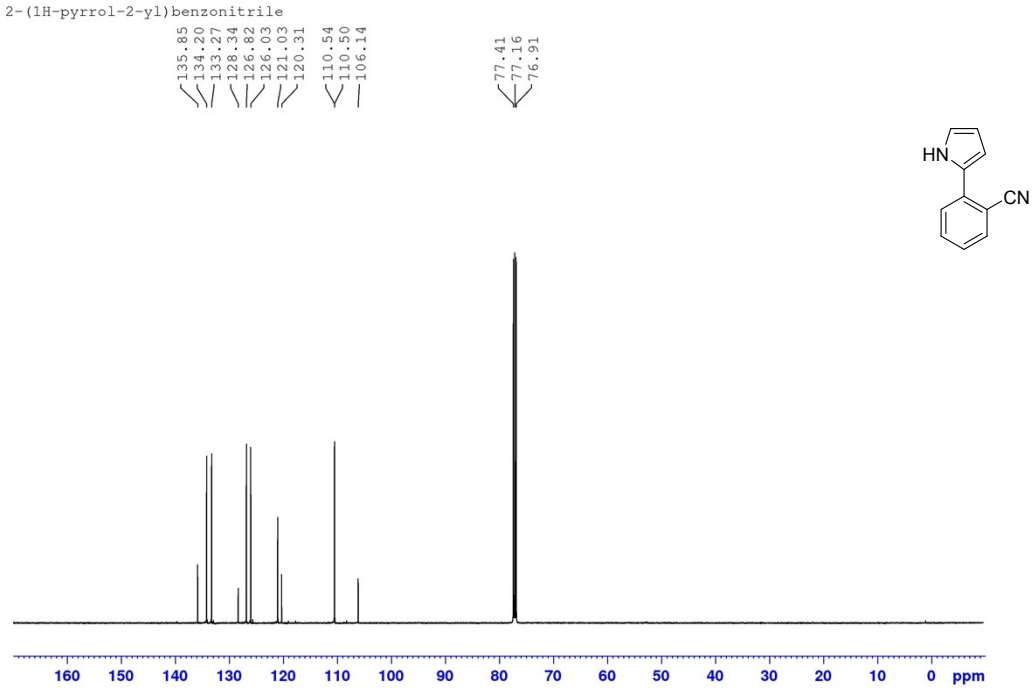

Figure S23. ^{13}C{H} NMR spectrum of 2-(1H-pyrrol-2-yl)benzonitrile ($CDCl_3$, 300 K).

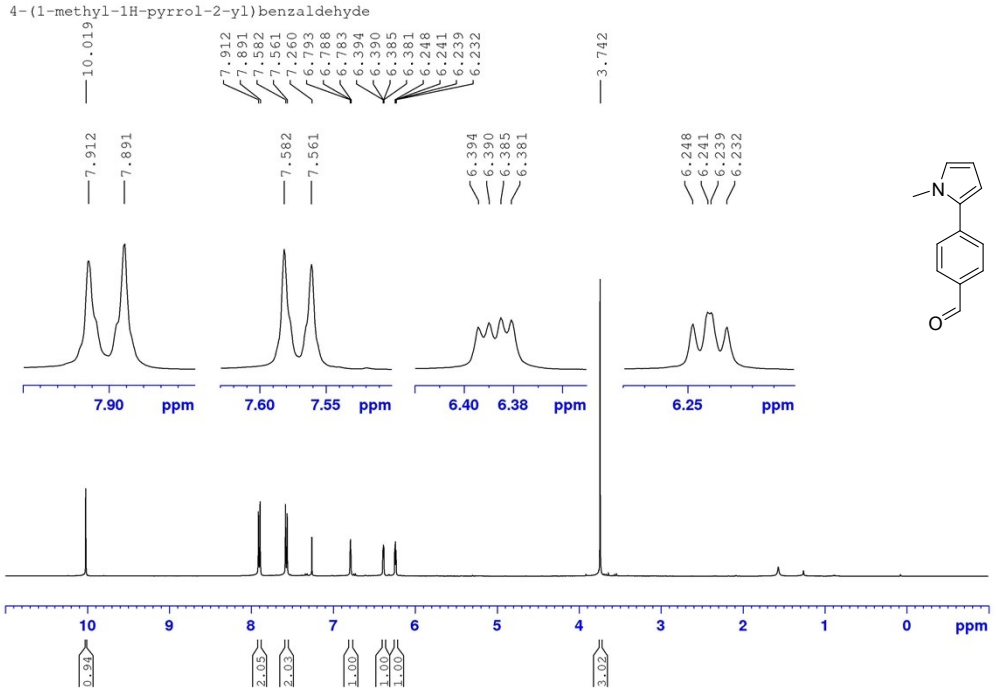

Figure S24. ^{1}H NMR spectrum of 4-(1-methyl-1H-pyrrol-2-yl)benzaldehyde ($CDCl_3$, 300 K).

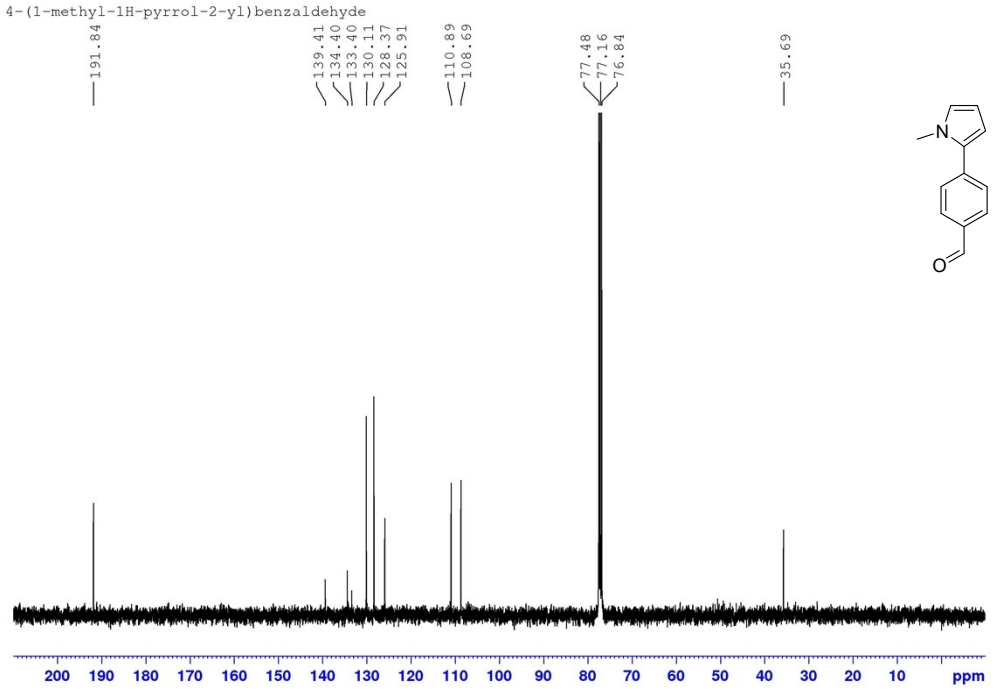

Figure S25. ^{13}C{H} NMR spectrum of 4-(1-methyl-1H-pyrrol-2-yl)benzaldehyde ($CDCl_3$, 300 K).

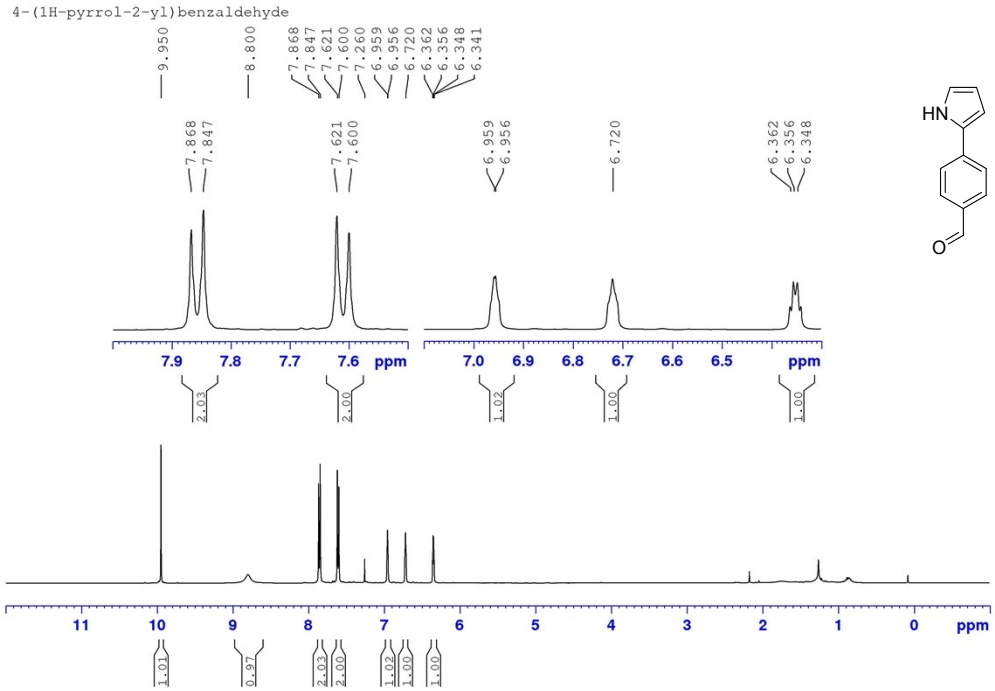

Figure S26. ^{1}H NMR spectrum of 4-(1H-pyrrol-2-yl)benzaldehyde ($CDCl_3$, 300 K); trace amounts of impurities between 0.8 to 2.2 ppm were not removable by column chromatography.

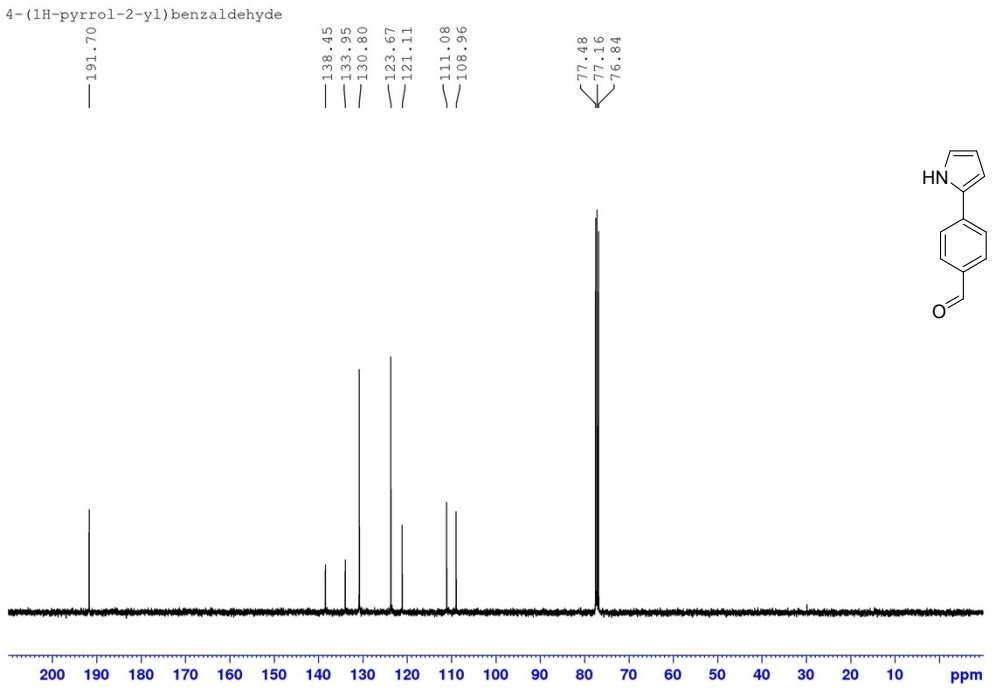

Figure S27. $^{13}C\{H\}$ NMR spectrum of 4-(1H-pyrrol-2-yl)benzaldehyde ($CDCl_3$, 300 K).

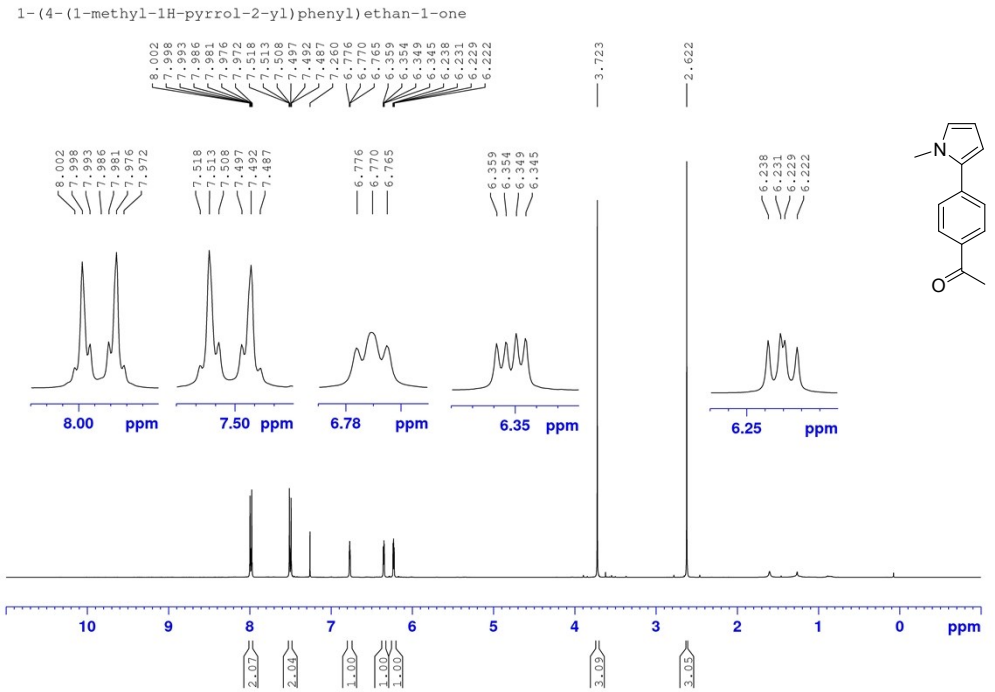

Figure S28. ^{1}H NMR spectrum of 1-(4-(1-methyl-1H-pyrrol-2-yl)phenyl)ethan-1-one ($CDCl_3$, 300 K).

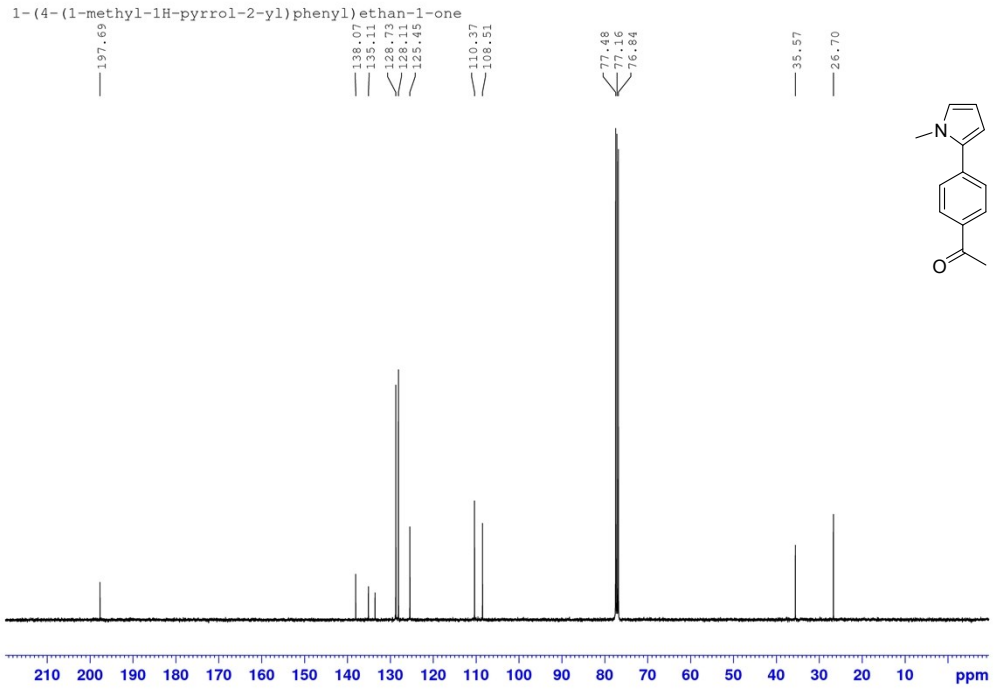

Figure S29. ^{13}C{H} NMR spectrum of 1-(4-(1-methyl-1H-pyrrol-2-yl)phenyl)ethan-1-one ($CDCl_3$,

300 K).

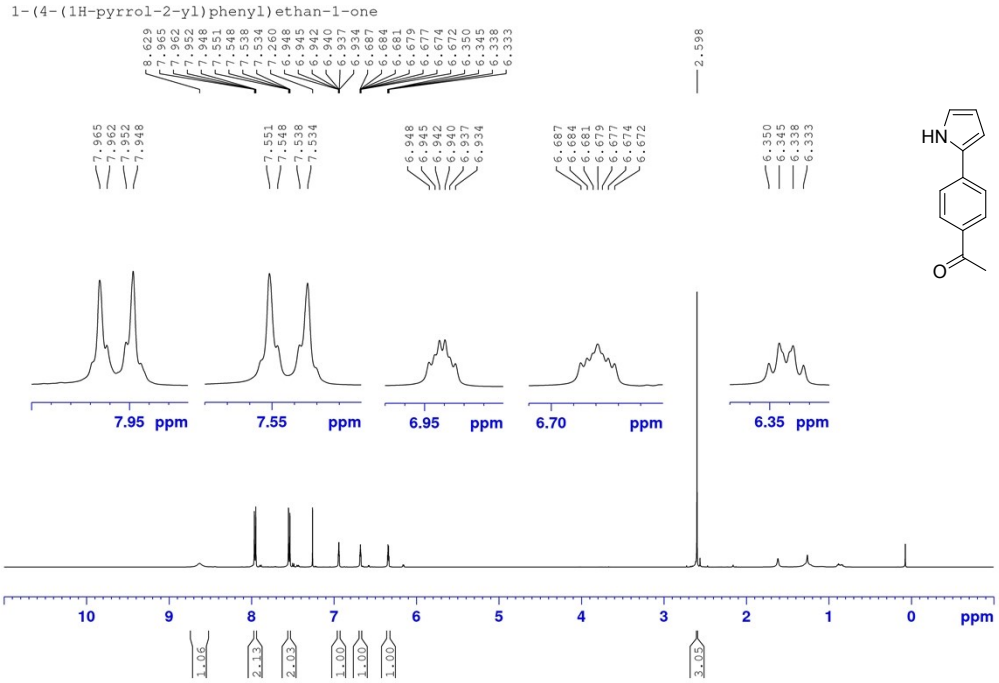

Figure S30. ^{1}H NMR spectrum of 1-(4-(1H-pyrrol-2-yl)phenyl)ethan-1-one ($CDCl_3$, 300 K); trace amounts of impurities between 0.8 to 2.2 ppm were not removable by column chromatography.

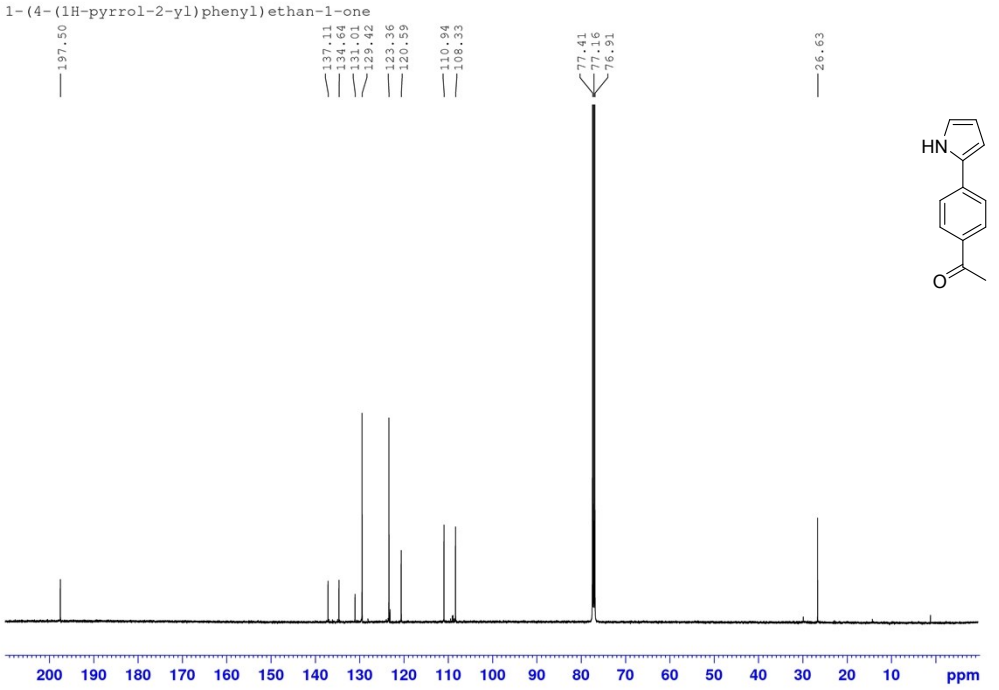

Figure S31. ^{13}C{H} NMR spectrum of 1-(4-(1H-pyrrol-2-yl)phenyl)ethan-1-one ($CDCl_3$, 300 K).

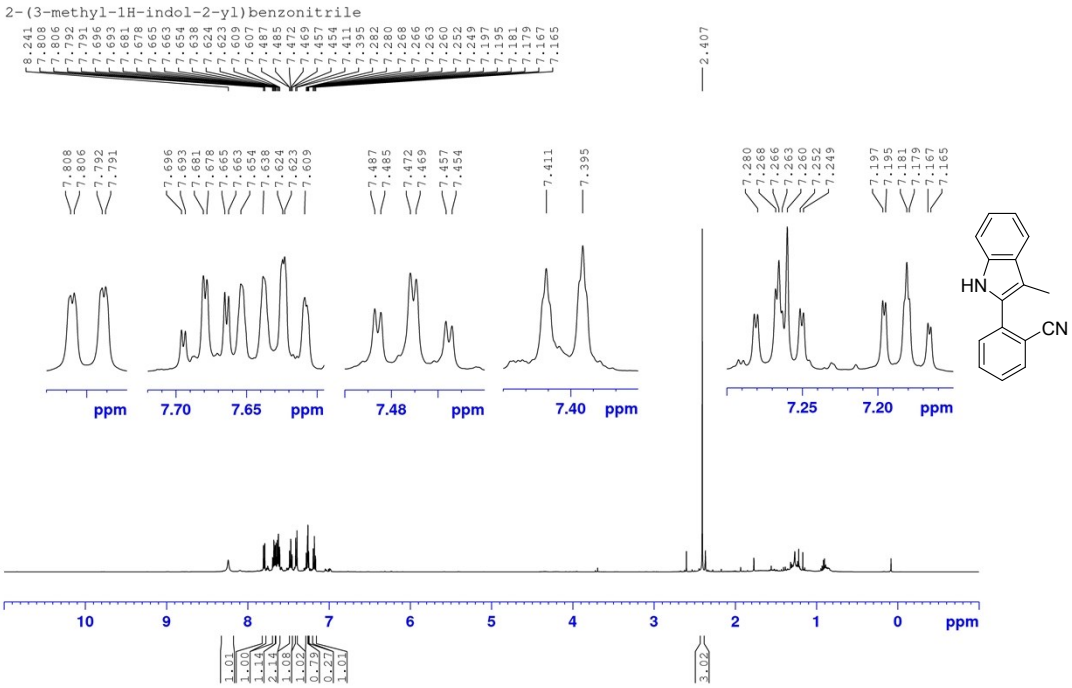

Figure S32. ^{1}H NMR spectrum of 2-(3-methyl-1H-indol-2-yl)benzonitrile ($CDCl_3$, 300 K); trace amounts of impurities between 0.8 to 2.2 ppm were not removable by column chromatography

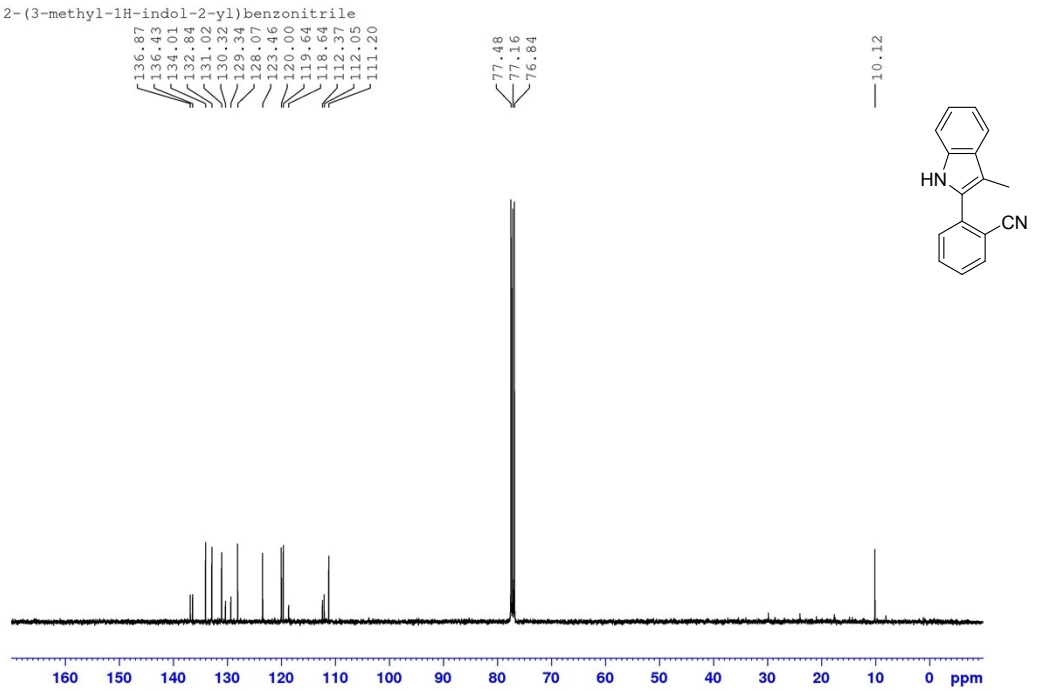

Figure S33. ^{13}C{H} NMR spectrum of 2-(3-methyl-1H-indol-2-yl)benzonitrile ($CDCl_3$, 300 K).

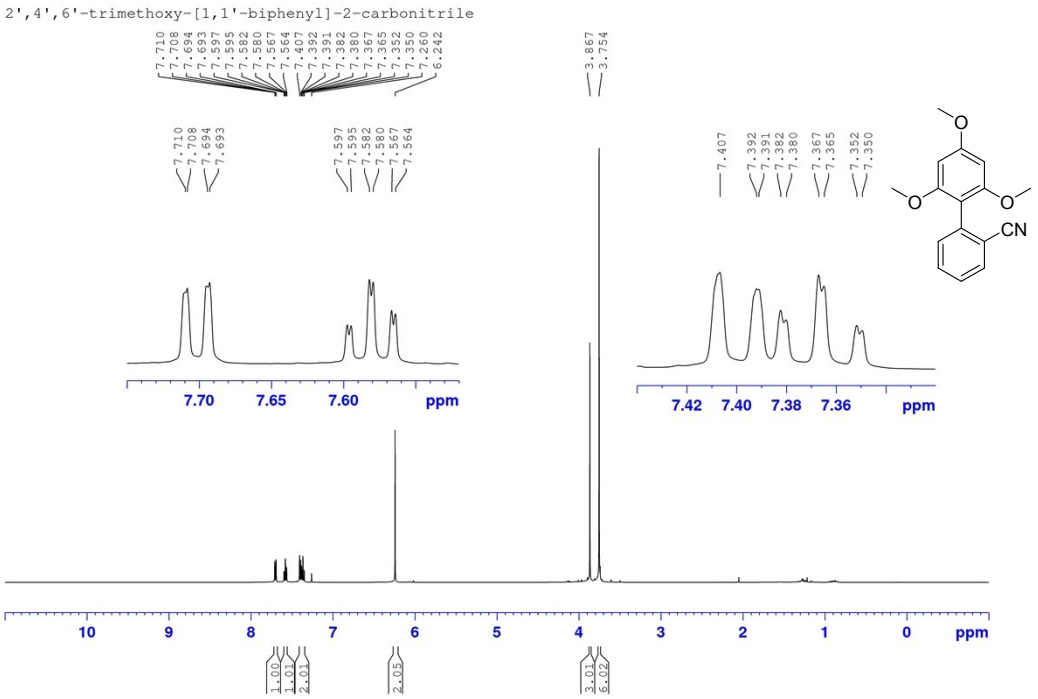

Figure S34. ^{1}H NMR spectrum of 2`,4`,6`-trimethoxy-(1,1`-biphenyl)-2-carbonitrile ($CDCl_3$, 300 K).

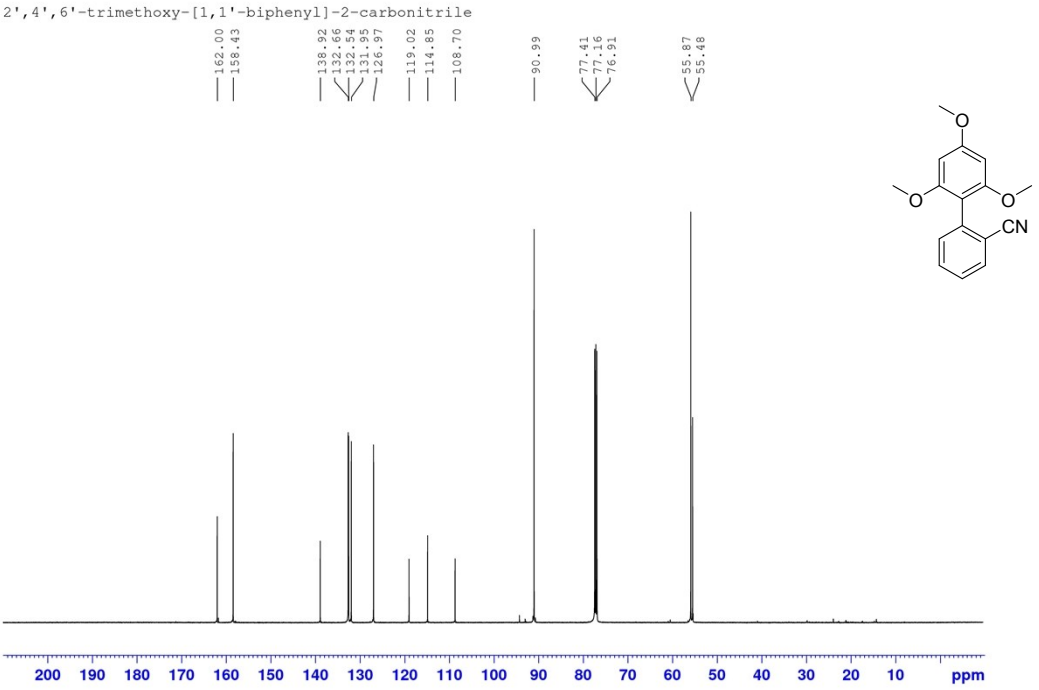

Figure S35. ^{1}H NMR spectrum of 2`,4`,6`-trimethoxy-(1,1`-biphenyl)-2-carbonitrile ($CDCl_3$, 300 K).

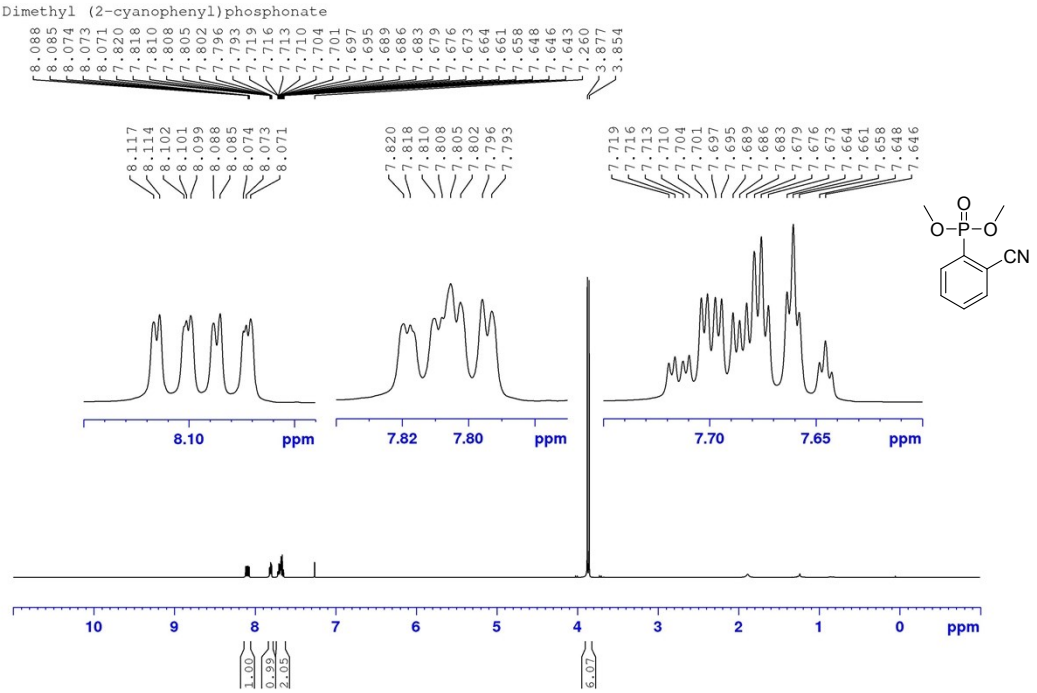

Figure S36. ^{1}H NMR spectrum of dimethyl(2-cyanophenyl)phosphonate ($CDCl_3$, 300 K).

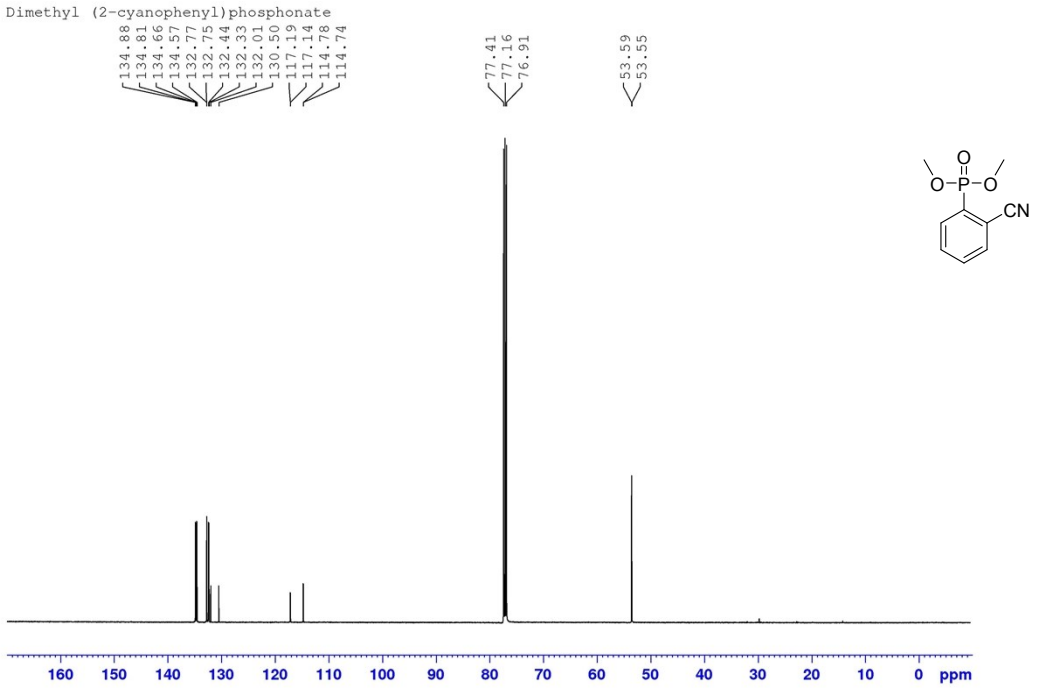

Figure S37. $^{13}C\{H\}$ NMR spectrum of dimethyl(2-cyanophenyl)phosphonate ($CDCl_3$, 300 K).

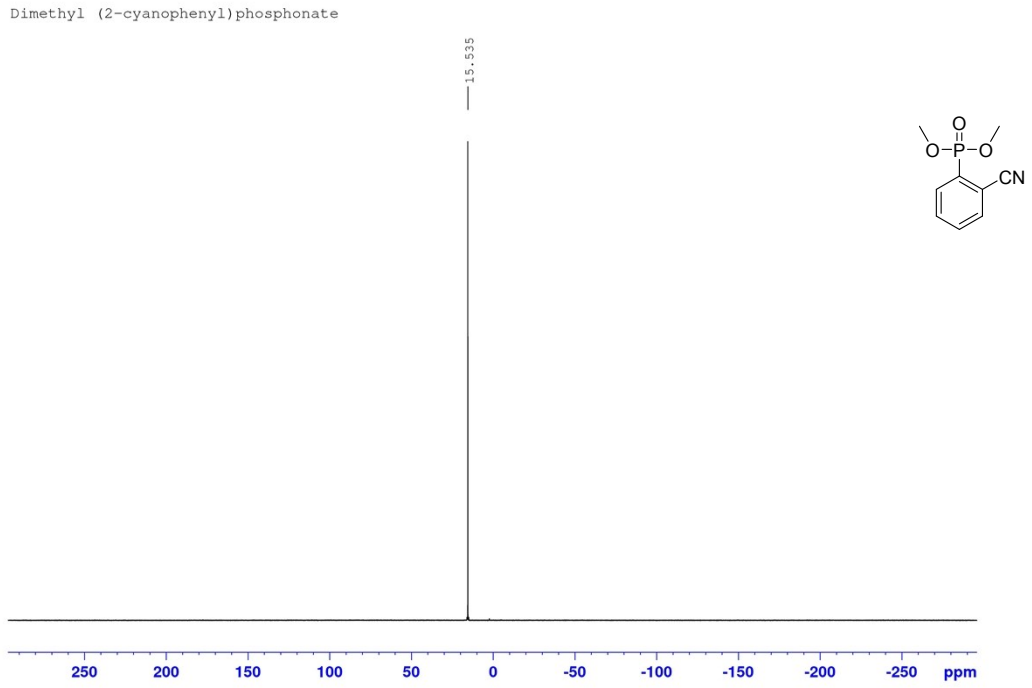

Figure S38. ^{31}P NMR spectrum of dimethyl(2-cyanophenyl)phosphonate ($CDCl_3$, 300 K).

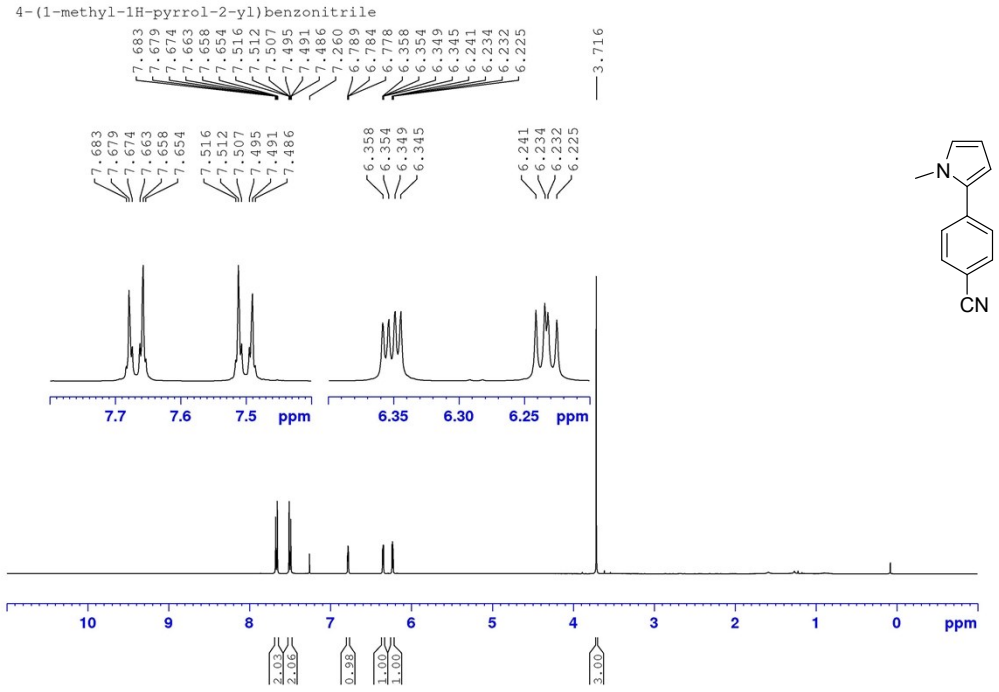

Figure S39. ^{1}H NMR spectrum of 4-(1-methyl-1H-pyrrol-2-yl)benzonitrile ($CDCl_3$, 300 K).

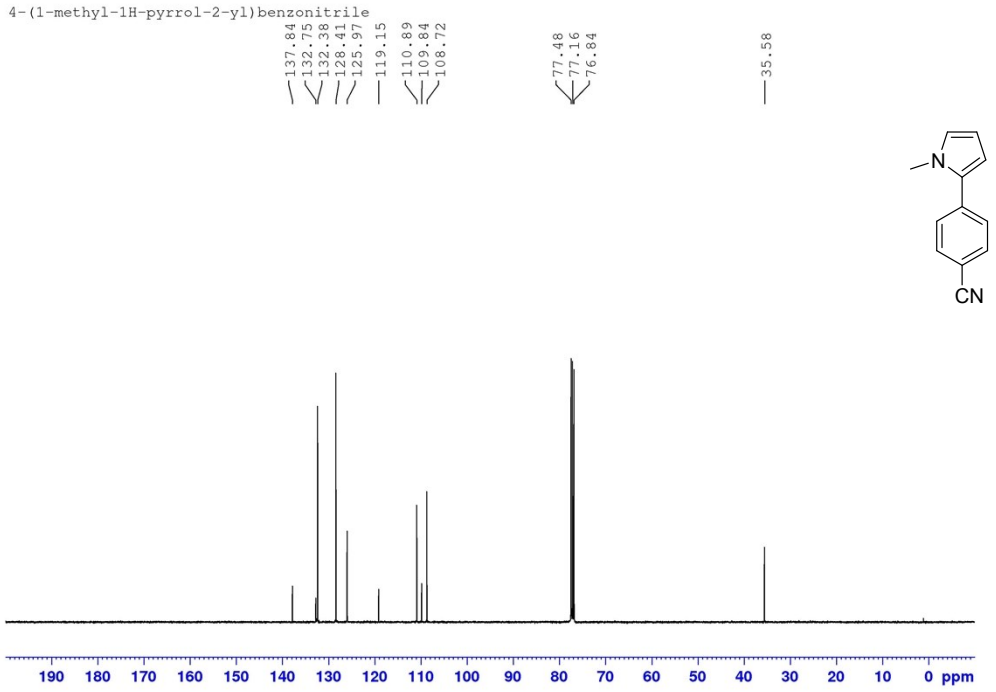

Figure S40. $^{13}C\{H\}$ NMR spectrum of 4-(1-methyl-1H-pyrrol-2-yl)benzonitrile ($CDCl_3$, 300 K).

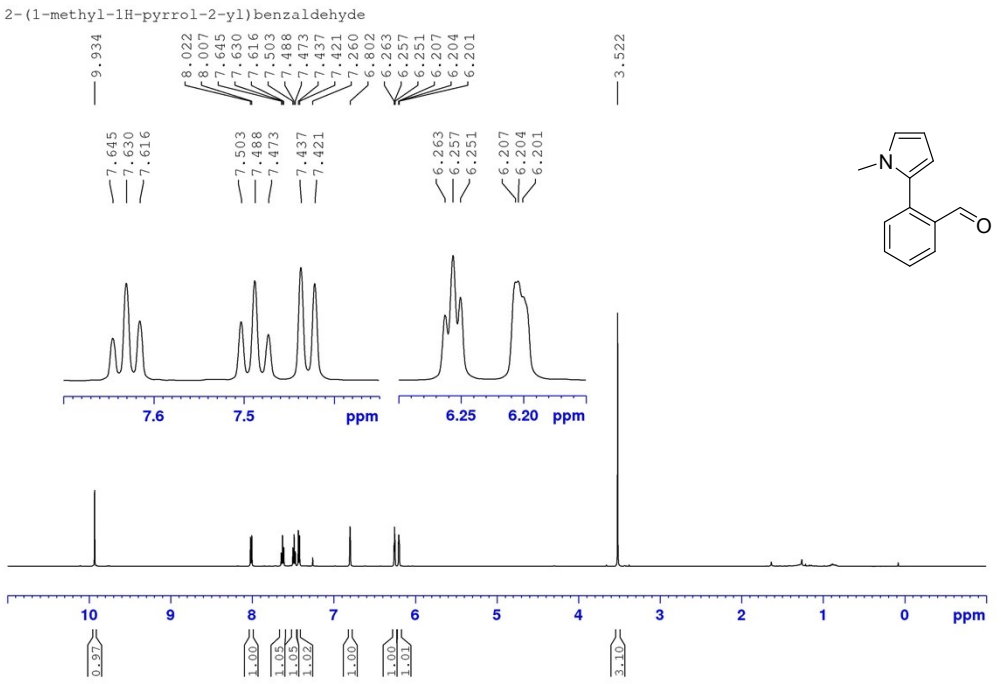

Figure S41. ^{1}H NMR spectrum of 2-(1-methyl-1H-pyrrol-2-yl)benzaldehyde ($CDCl_3$, 300 K).

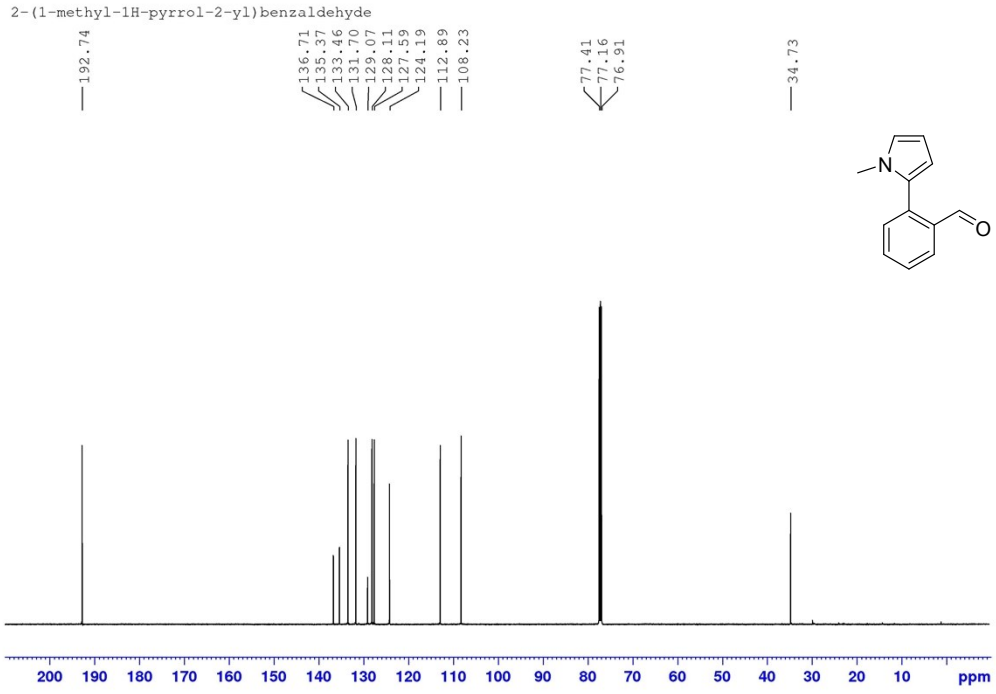

Figure S42. $^{13}C\{H\}$ NMR spectrum of 2-(1-methyl-1H-pyrrol-2-yl)benzaldehyde ($CDCl_3$, 300 K).

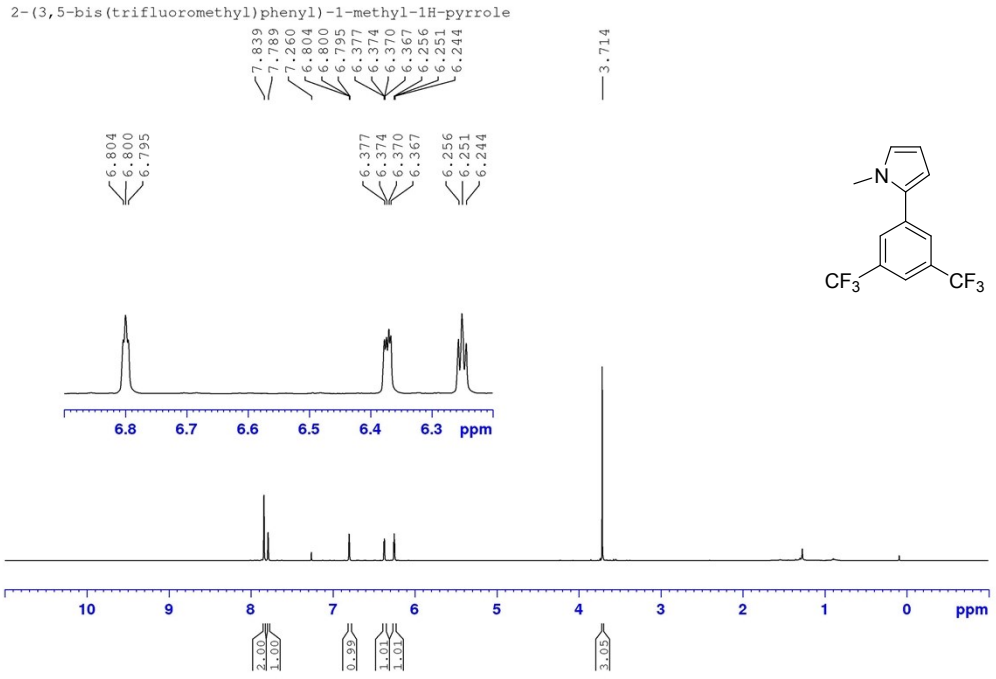

Figure S43. ^{1}H NMR spectrum of 2-(3,5-bis(trifluoromethyl)phenyl)-1-methyl-1H-pyrrole ($CDCl_3$, 300 K).

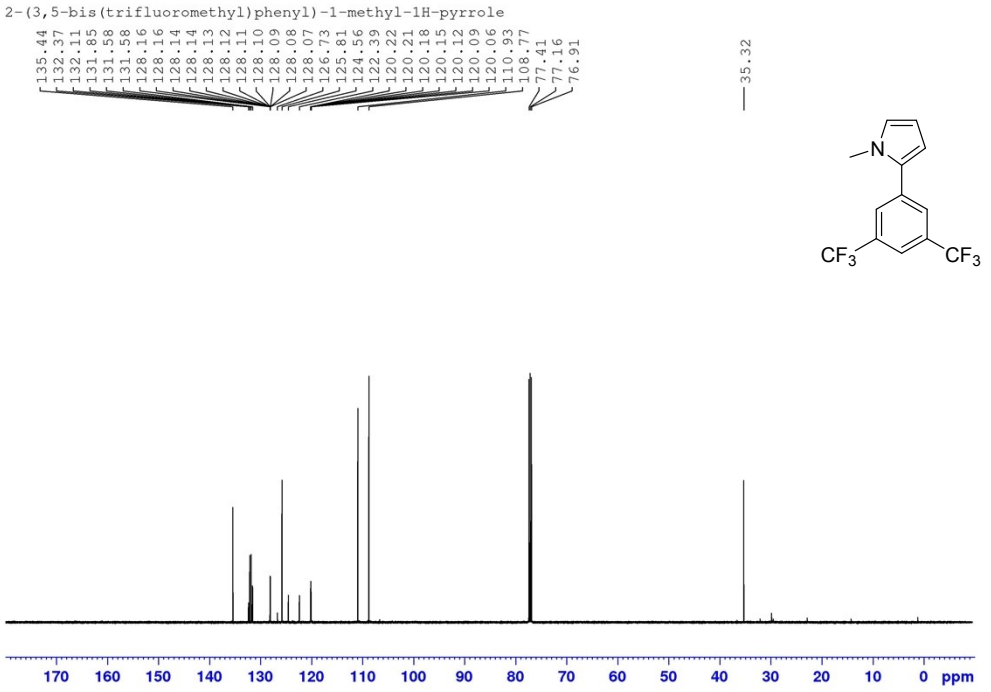

Figure S44. $^{13}C\{H\}$ NMR spectrum of 2-(3,5-bis(trifluoromethyl)phenyl)-1-methyl-1H-pyrrole ($CDCl_3$, 300 K).

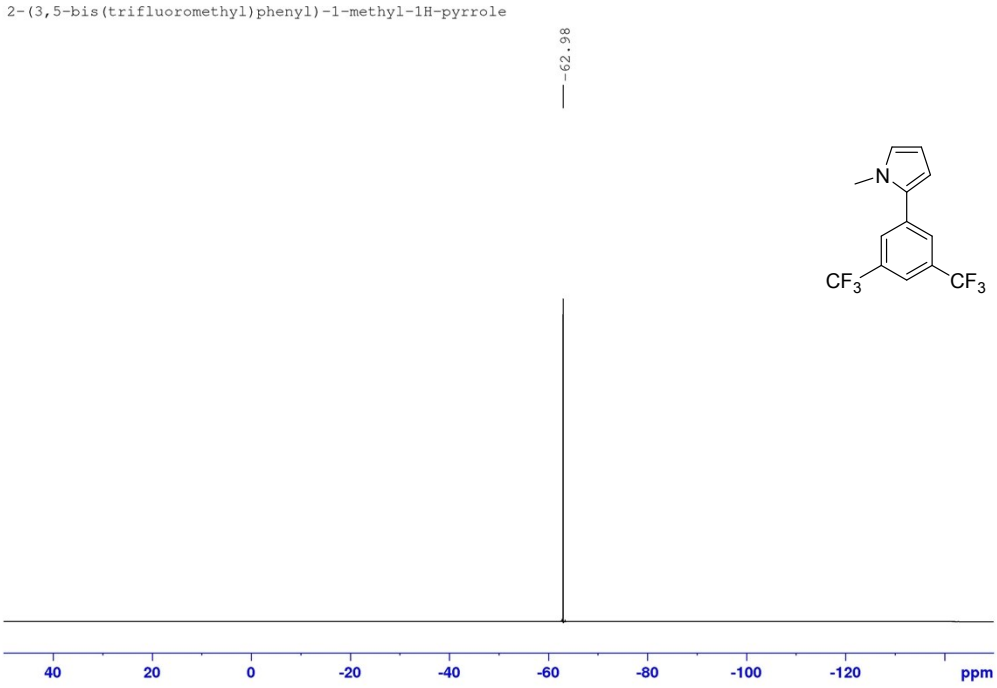

Figure S45. ^{19}F NMR spectrum of 2-(3,5-bis(trifluoromethyl)phenyl)-1-methyl-1H-pyrrole ($CDCl_3$, 300 K).

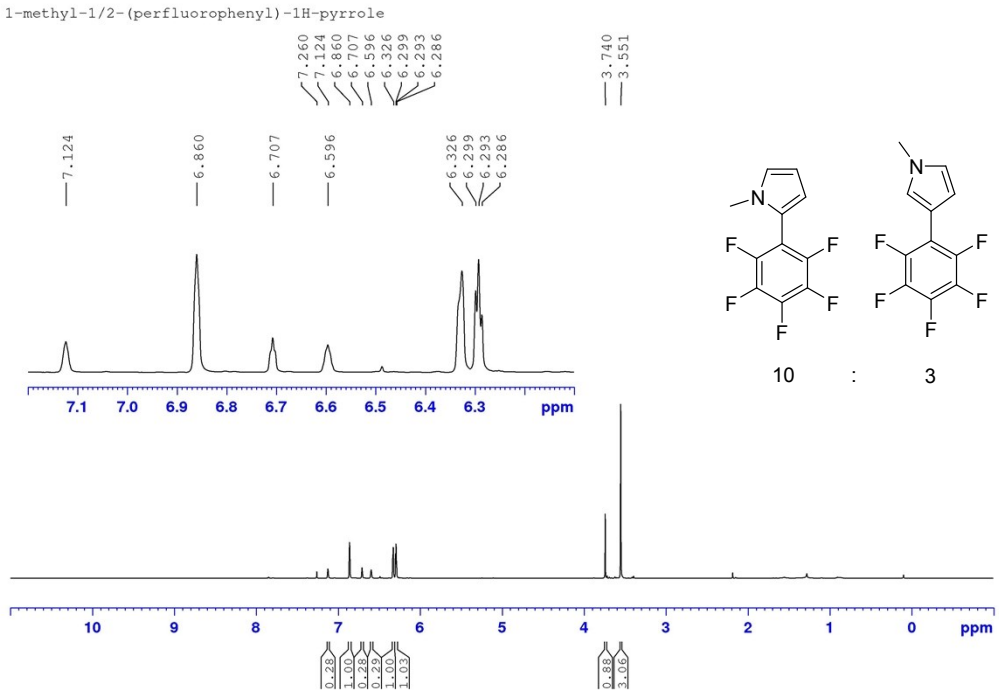

Figure S46. ^{1}H NMR spectrum of 1-methyl-2-(perfluorophenyl)-1H-pyrrole and 1-methyl-3-(perfluorophenyl)-1H-pyrrole ($CDCl_3$, 300 K).

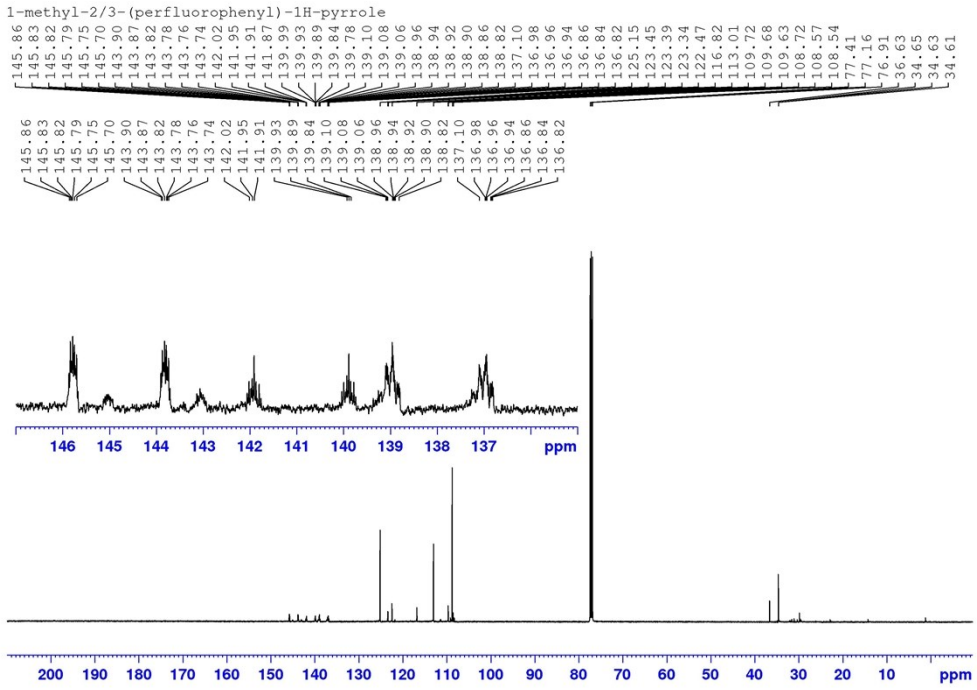

Figure S47. ^{13}C{H} NMR spectrum of 1-methyl-2-(perfluorophenyl)-1H-pyrrole and 1-methyl-3-(perfluorophenyl)-1H-pyrrole ($CDCl_3$, 300 K).

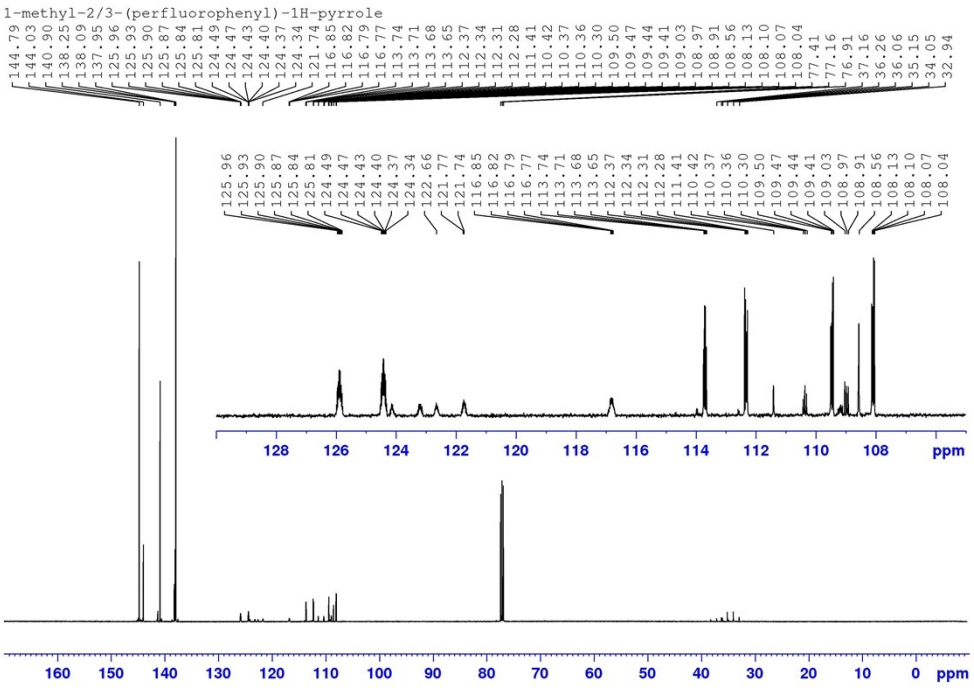

Figure S48. $^{13}C\{F\}$ NMR spectrum of 1-methyl-2-(perfluorophenyl)-1H-pyrrole and 1-methyl-3-(perfluorophenyl)-1H-pyrrole ($CDCl_3$, 300 K).

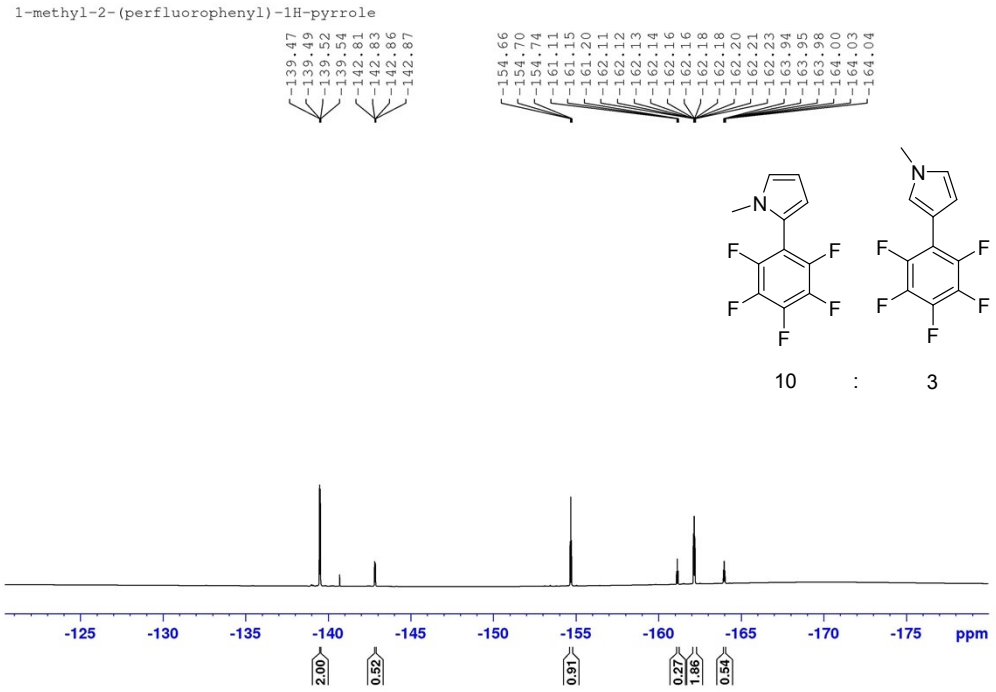

Figure S49. ^{19}F NMR spectrum of 1-methyl-2-(perfluorophenyl)-1H-pyrrole and 1-methyl-3-(perfluorophenyl)-1H-pyrrole ($CDCl_3$, 300 K).

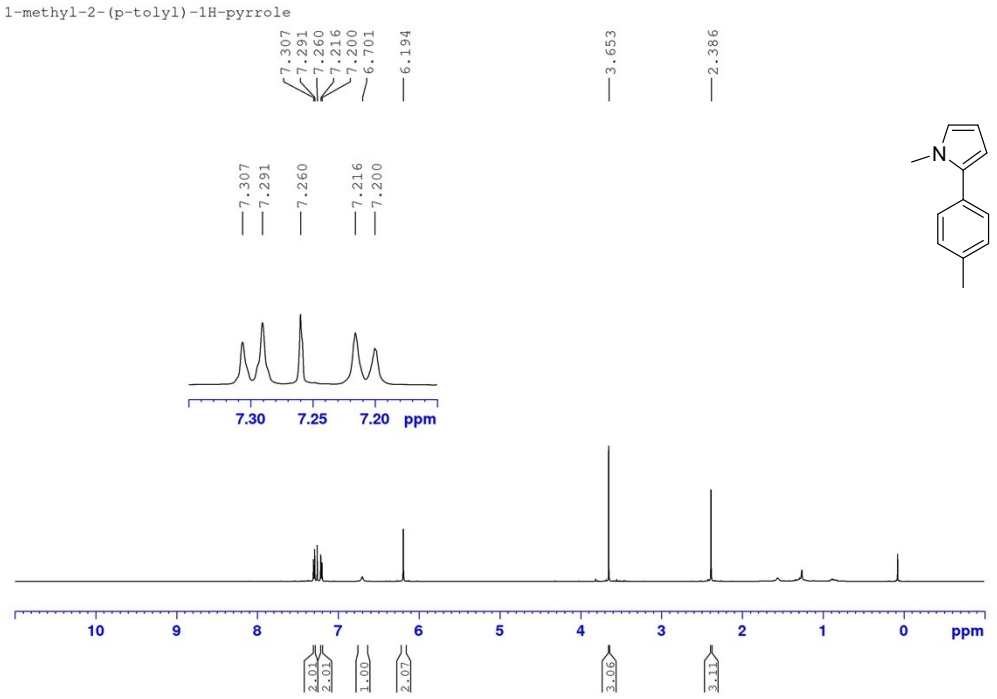

Figure S50. ^{1}H NMR spectrum of 1-methyl-2-(p-tolyl)-1H-pyrrole ($CDCl_3$, 300 K).

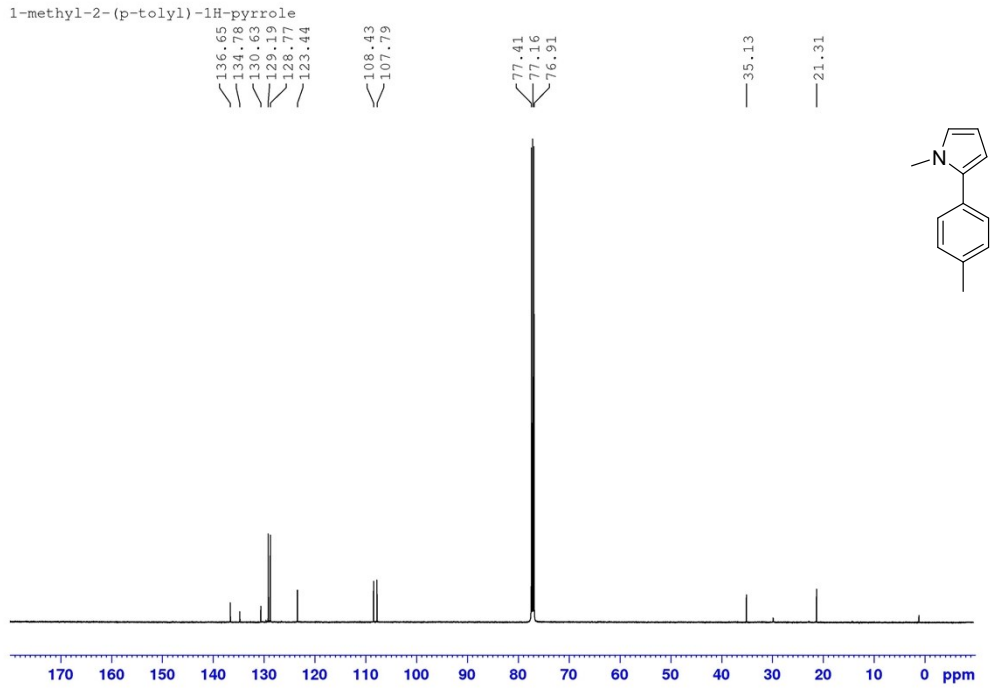

Figure S51. $^{13}C\{H\}$ NMR spectrum of 1-methyl-2-(p-tolyl)-1H-pyrrole ($CDCl_3$, 300 K).

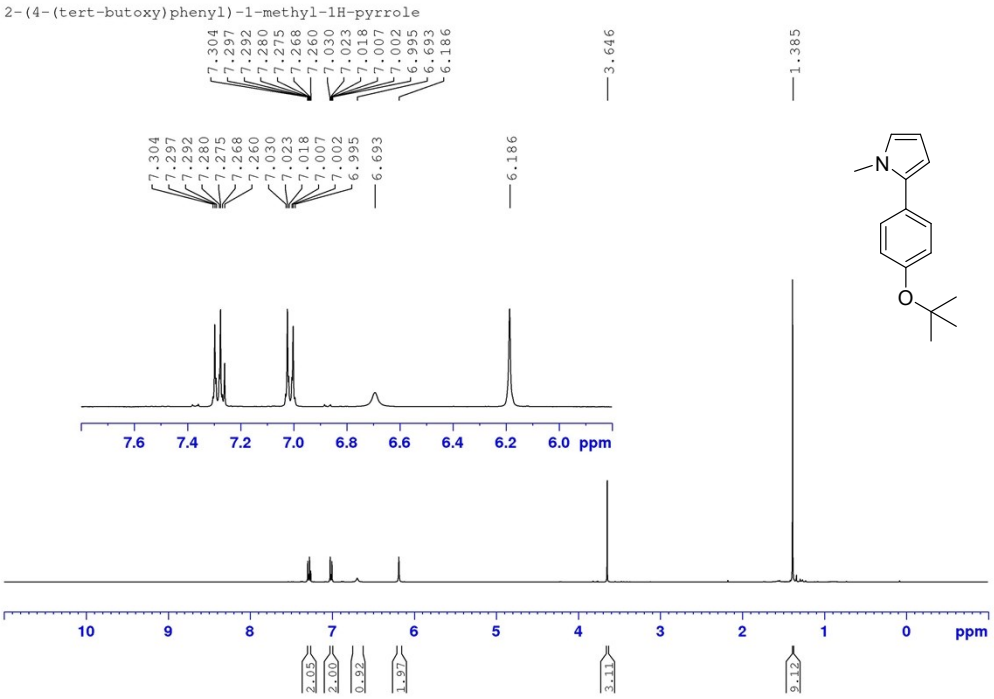

Figure S52. ^{1}H NMR spectrum of 2-(4-(tert-butoxy)phenyl)-1-methyl-1H-pyrrole ($CDCl_3$, 300 K).

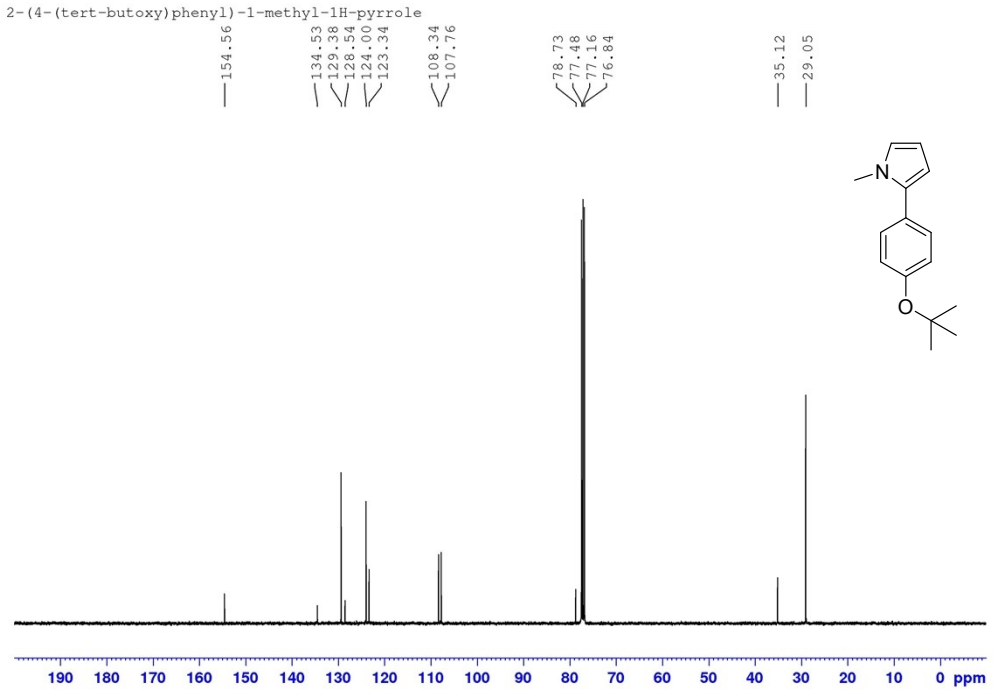

Figure S53. ^{13}C{H} NMR spectrum of 2-(4-(tert-butoxy)phenyl)-1-methyl-1H-pyrrole ($CDCl_3$, 300 K).

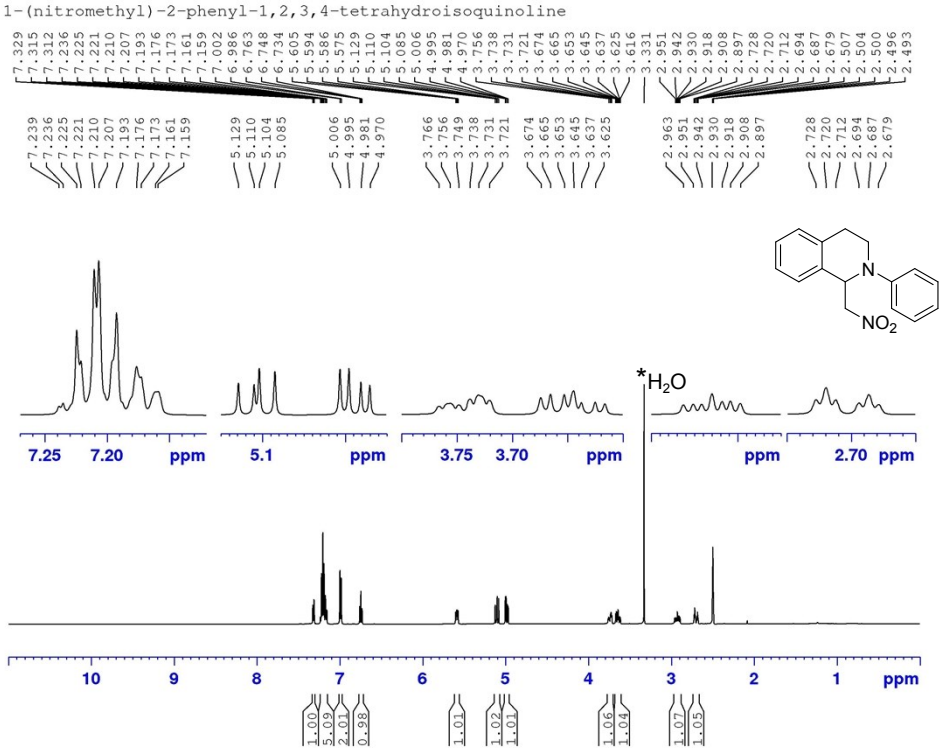

Figure S54. ^{1}H NMR spectrum of 1-(nitromethyl)-2-phenyl-1,2,3,4-tetrahydroisoquinoline (DMSO-d_6, 300 K).

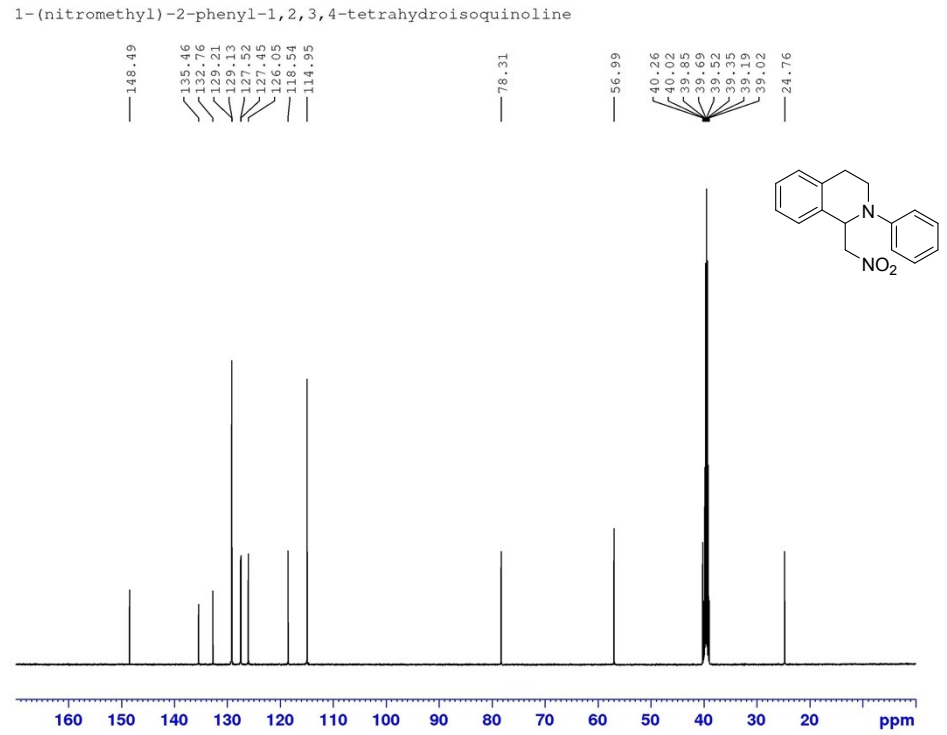

Figure S55. ^{13}C{H} NMR spectrum of 1-(nitromethyl)-2-phenyl-1,2,3,4-tetrahydroisoquinoline (DMSO-d_6, 300 K).

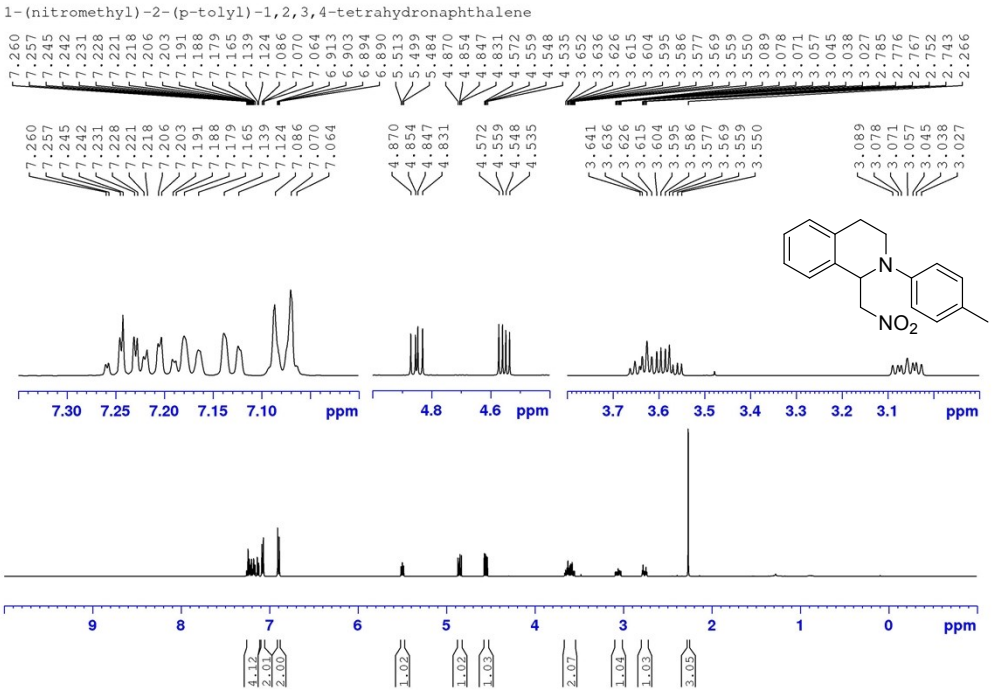

Figure S56. ^{1}H NMR spectrum of 1-(nitromethyl)-2-(p-tolyl)-1,2,3,4-tetrahydroisoquinoline ($CDCl_3$, 300 K).

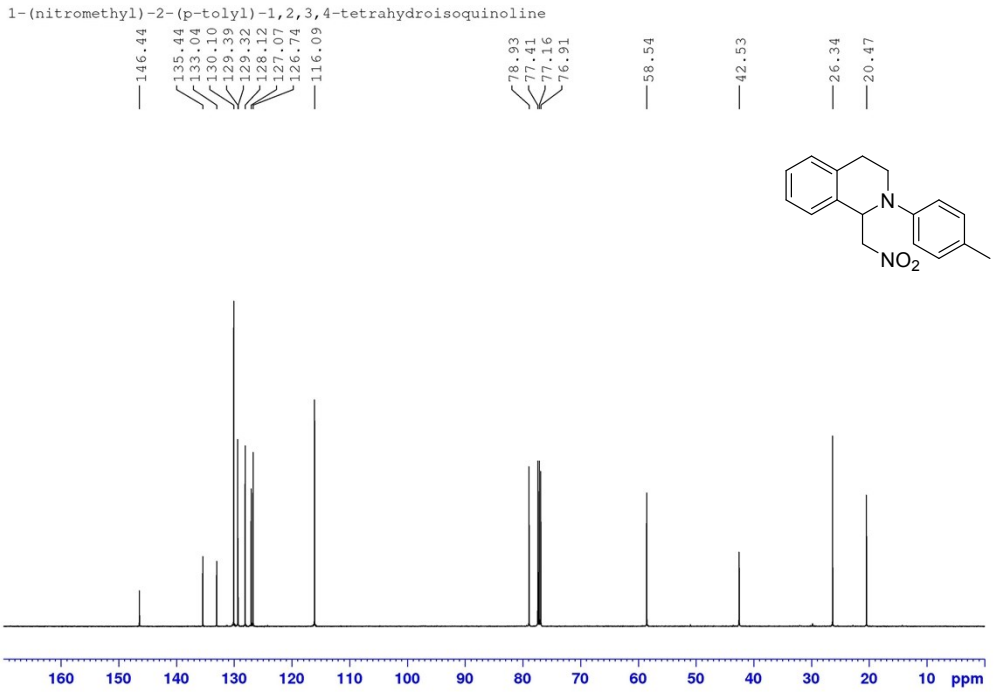

Figure S57. $^{13}C\{H\}$ NMR spectrum of 1-(nitromethyl)-2-(p-tolyl)-1,2,3,4-tetrahydroisoquinoline ($CDCl_3$, 300 K).

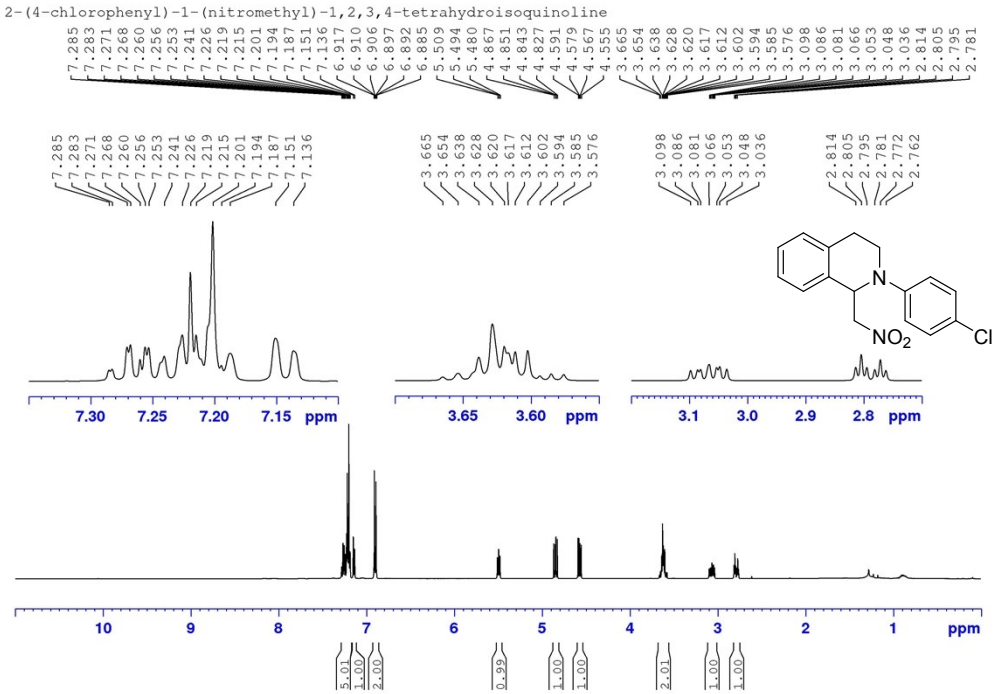

Figure S58. ^{1}H NMR spectrum of 2-(4-chlorophenyl)-1-(nitromethyl)-1,2,3,4-tetrahydroisoquinoline ($CDCl_3$, 300 K); trace amounts of impurities between 0.8 to 2.2 ppm were not removable by column chromatography.

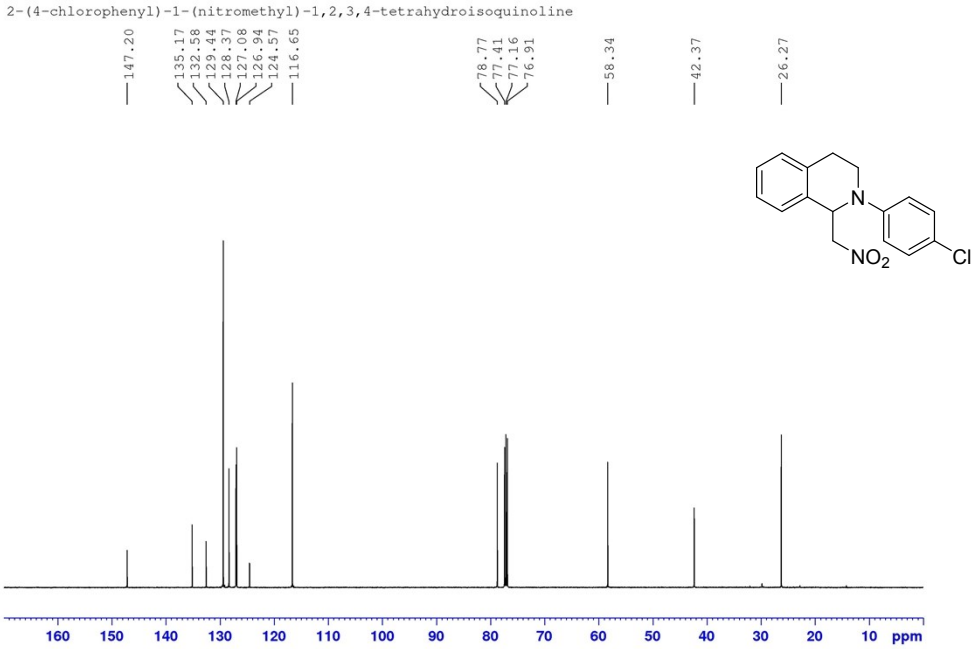

Figure S59. $^{13}C\{H\}$ NMR spectrum of 2-(4-chlorophenyl)-1-(nitromethyl)-1,2,3,4-tetrahydroisoquinoline ($CDCl_3$, 300 K).

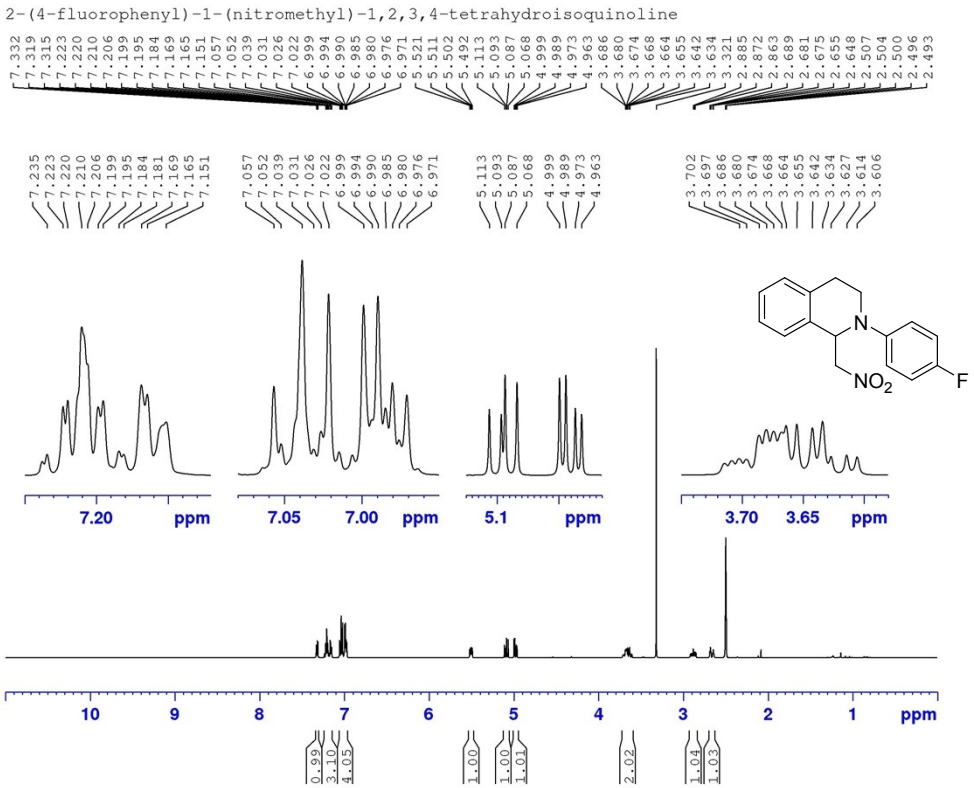

Figure S60. ^{1}H NMR spectrum of 2-(4-fluorophenyl)-1-(nitromethyl)-1,2,3,4-tetrahydroisoquinoline (DMSO-d_6, 300 K).

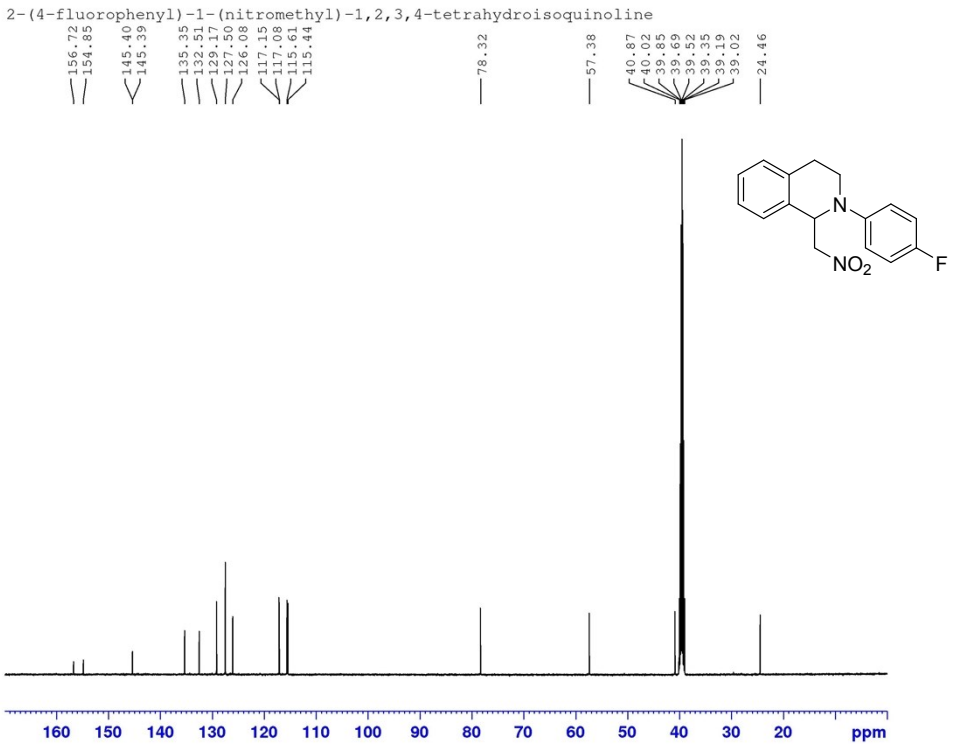

Figure S61. ^{13}C{H} NMR spectrum of 2-(4-fluorophenyl)-1-(nitromethyl)-1,2,3,4-tetrahydroisoquinoline (DMSO-d_6, 300 K).

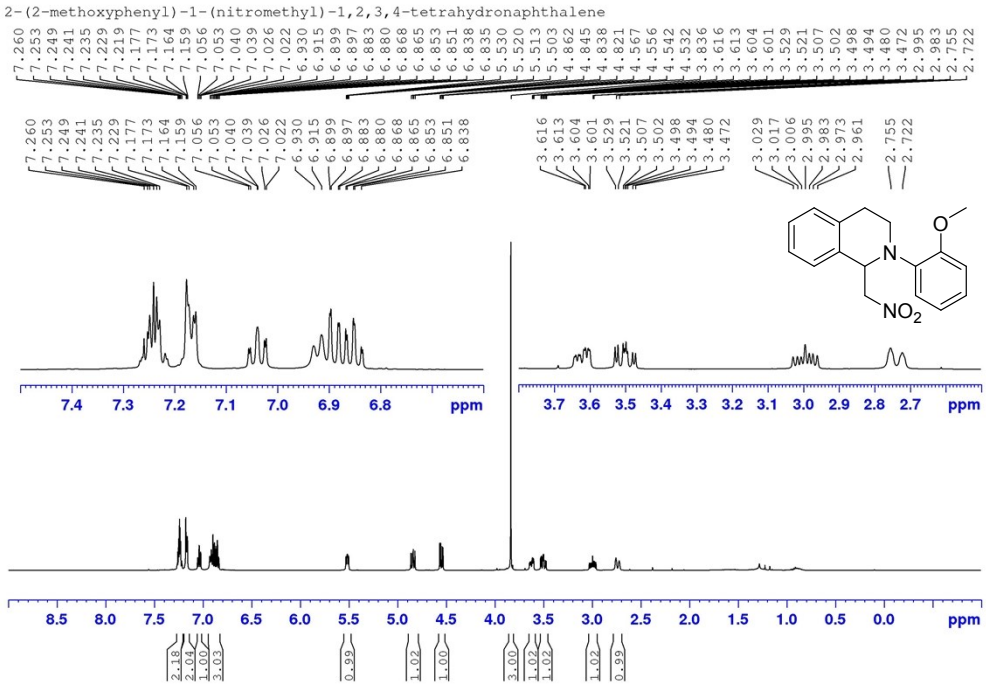

Figure S62. ^{1}H NMR spectrum of 2-(2-methoxyphenyl)-1-(nitromethyl)-1,2,3,4-tetrahydroisoquinoline ($CDCl_3$, 300 K).

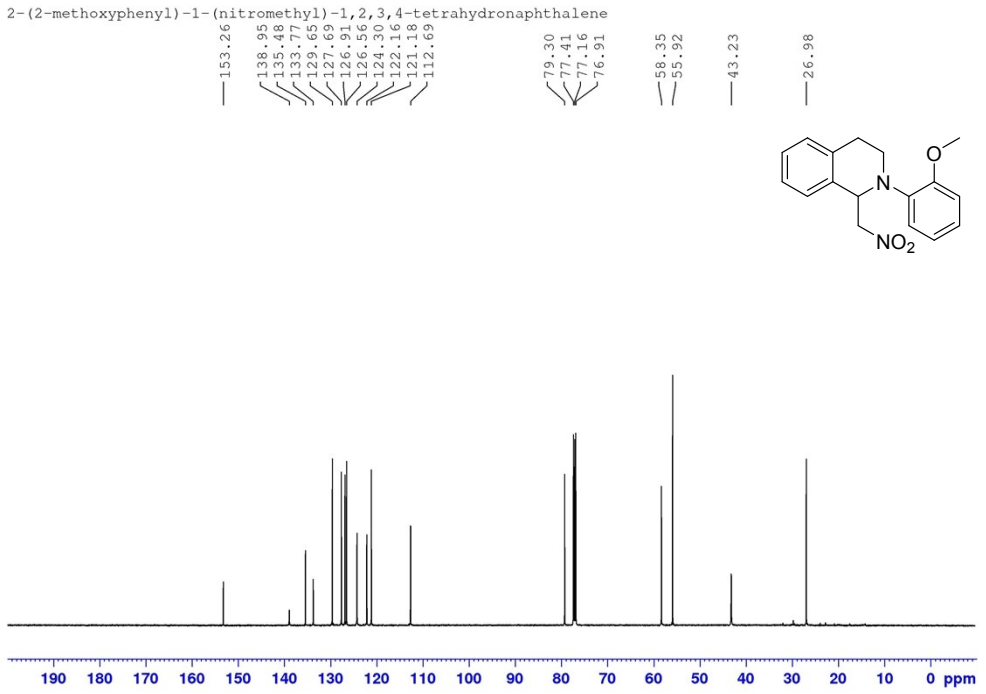

Figure S63. $^{13}C\{H\}$ NMR spectrum of 2-(2-methoxyphenyl)-1-(nitromethyl)-1,2,3,4-tetrahydroisoquinoline ($CDCl_3$, 300 K).

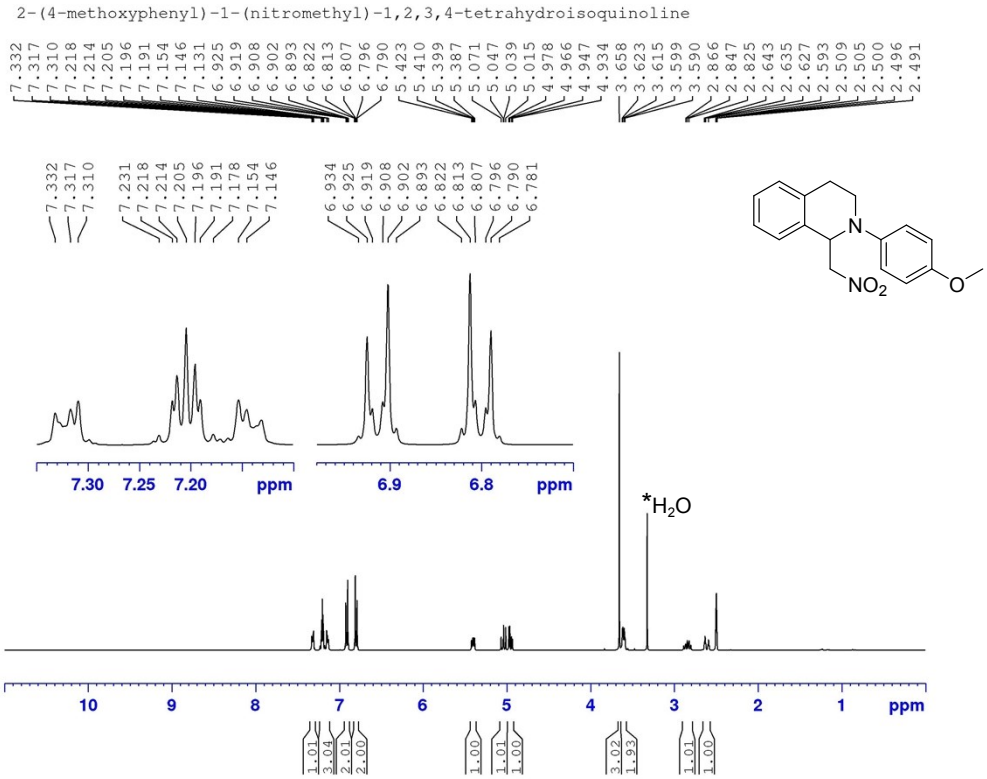

Figure S64. ^{1}H NMR spectrum of 2-(4-methoxyphenyl)-1-(nitromethyl)-1,2,3,4-tetrahydroisoquinoline (DMSO-d_6, 300 K).

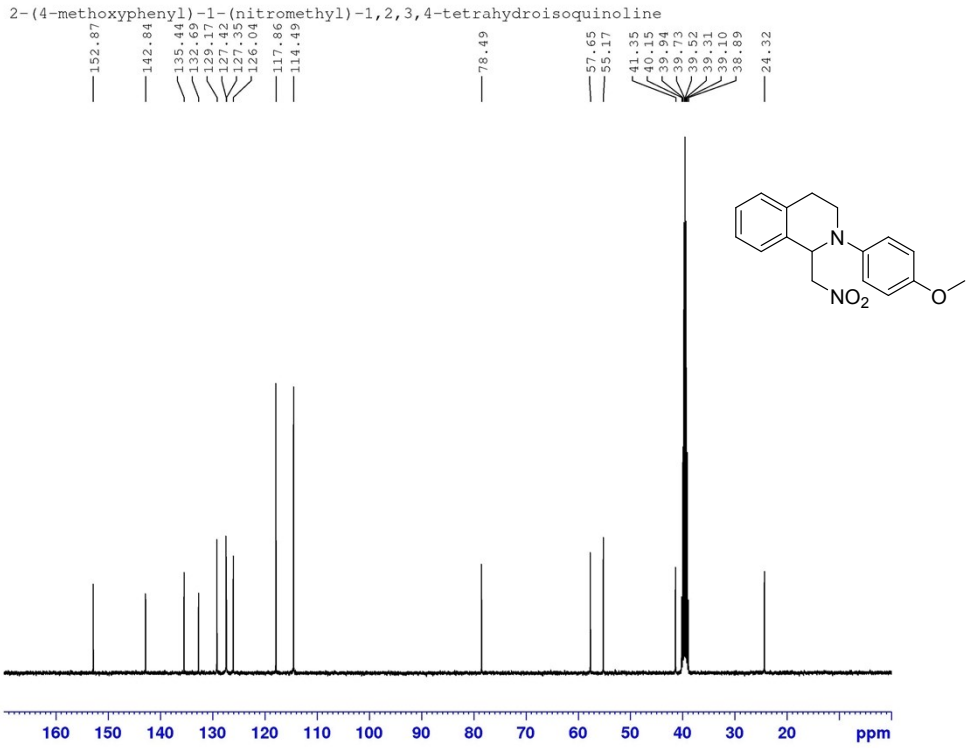

Figure S65. ^{13}C{H} NMR spectrum of 2-(4-methoxyphenyl)-1-(nitromethyl)-1,2,3,4-tetrahydroisoquinoline (DMSO-d_6, 300 K).

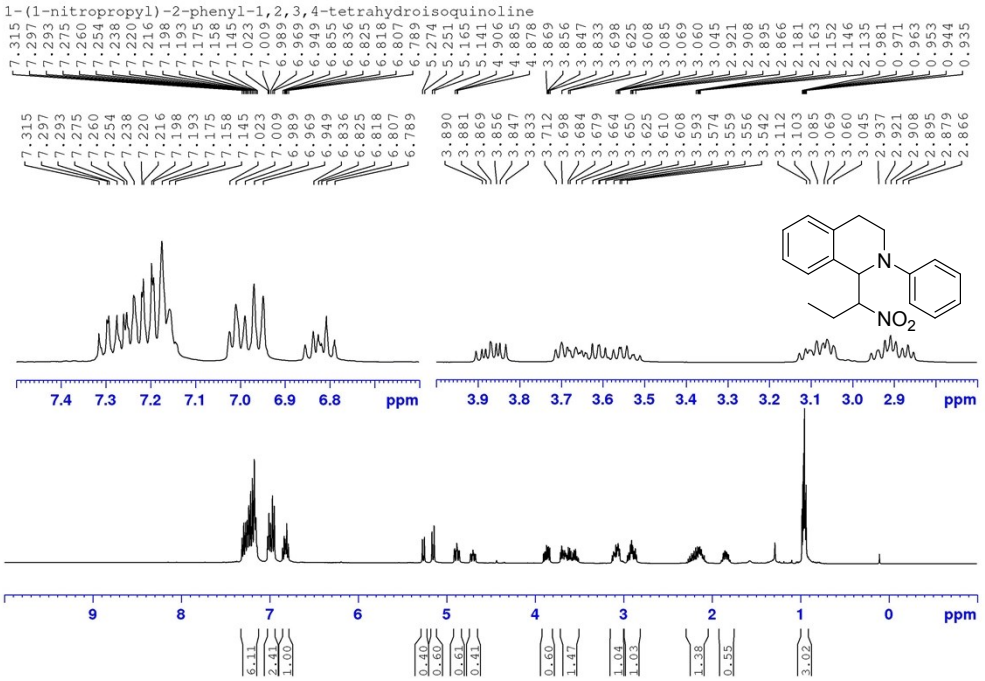

Figure S66. ^{1}H NMR spectrum of 1-(1-nitropropyl)-2-phenyl-1,2,3,4-tetrahydroisoquinoline ($CDCl_3$, 300 K).

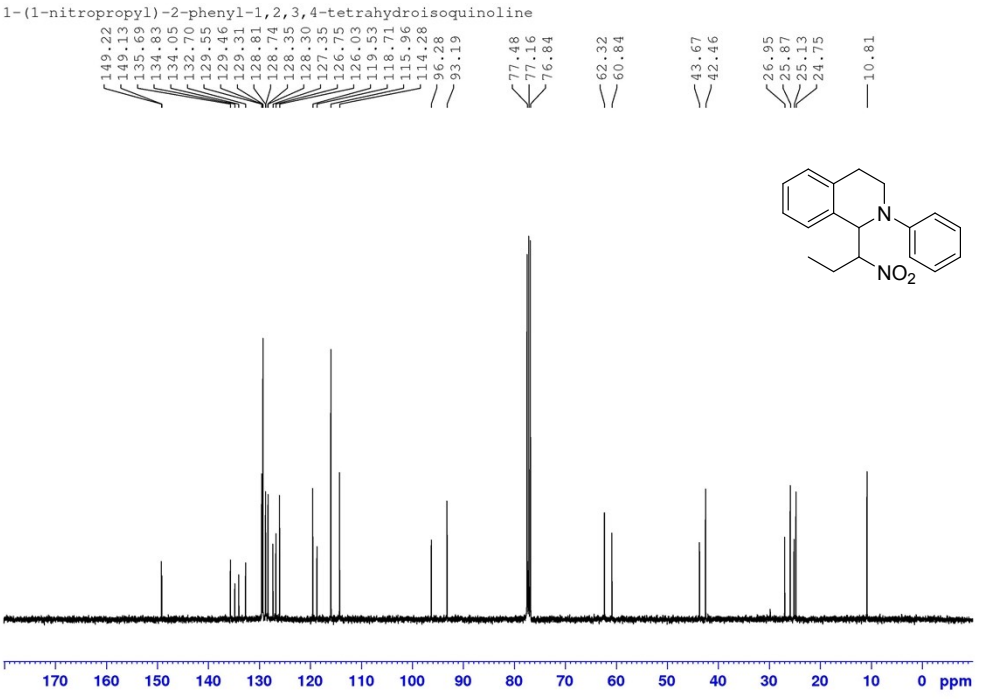

Figure S67. $^{13}C\{H\}$ NMR spectrum of 1-(1-nitropropyl)-2-phenyl-1,2,3,4-tetrahydroisoquinoline ($CDCl_3$, 300 K).

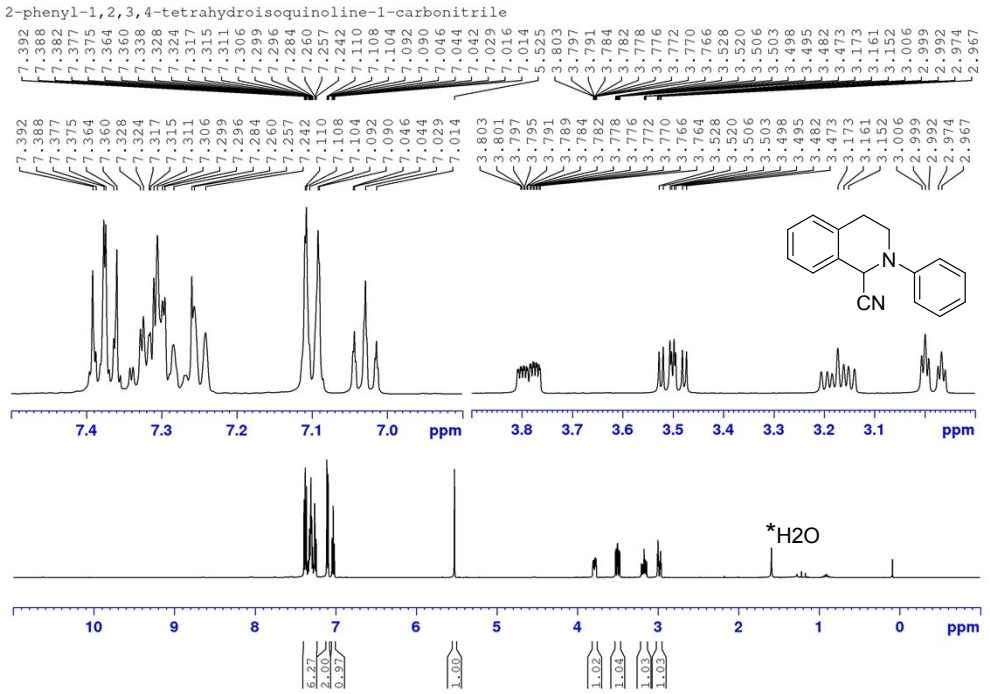

Figure S68. ^{1}H NMR spectrum of 2-phenyl-1,2,3,4-tetrahydroisoquinoline-1-carbonitrile ($CDCl_3$, 300 K).

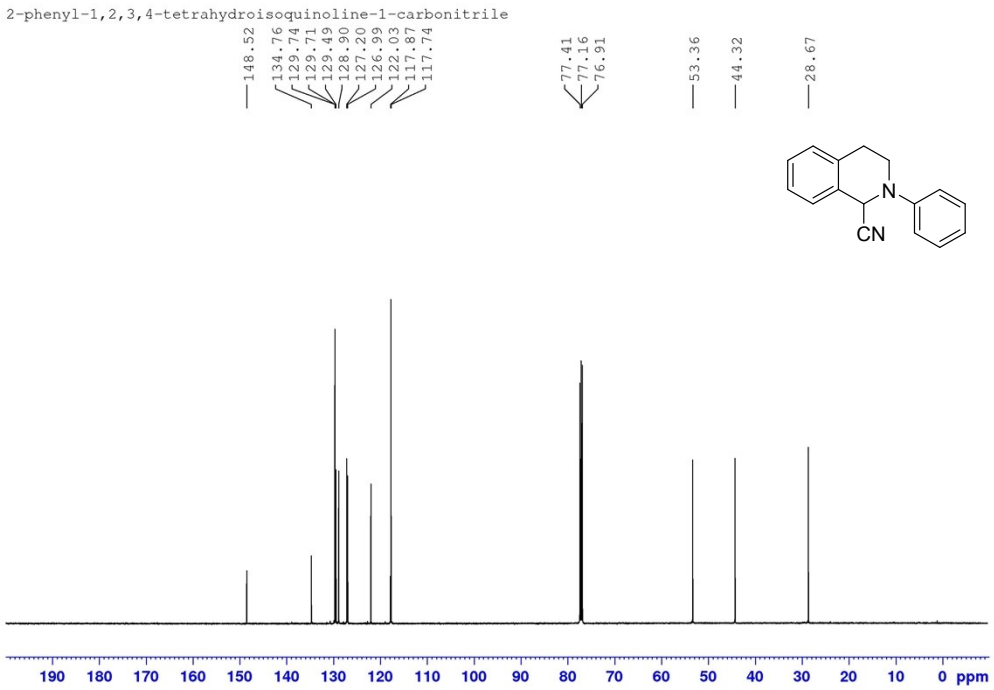

Figure S69. $^{13}C\{H\}$ NMR spectrum of 2-phenyl-1,2,3,4-tetrahydroisoquinoline-1-carbonitrile ($CDCl_3$, 300 K).

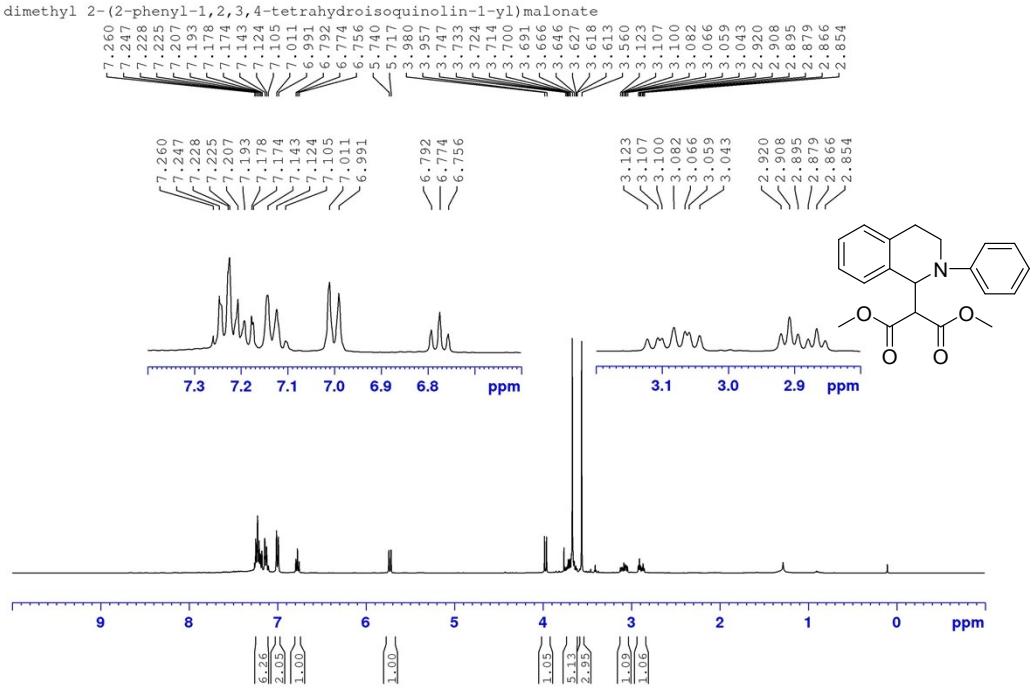

Figure S70. ^{1}H NMR spectrum of dimethyl 2-(2-phenyl-1,2,3,4-tetrahydroisoquinolin-1-yl)malonate ($CDCl_3$, 300 K).

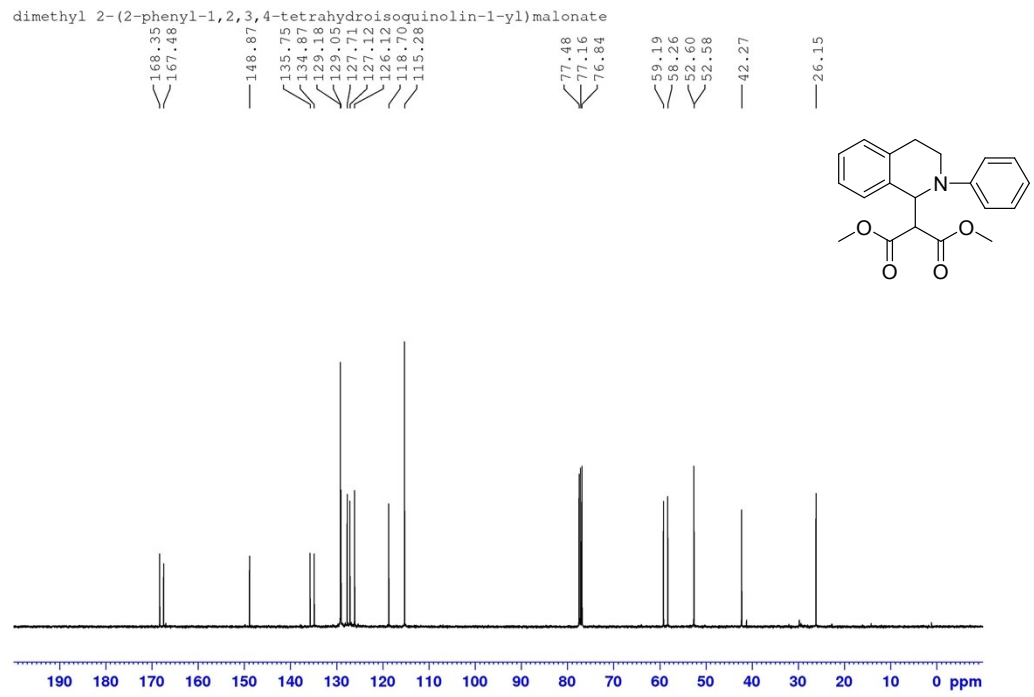

Figure S71. $^{13}C\{H\}$ NMR spectrum of dimethyl 2-(2-phenyl-1,2,3,4-tetrahydroisoquinolin-1-yl)malonate ($CDCl_3$, 300 K).

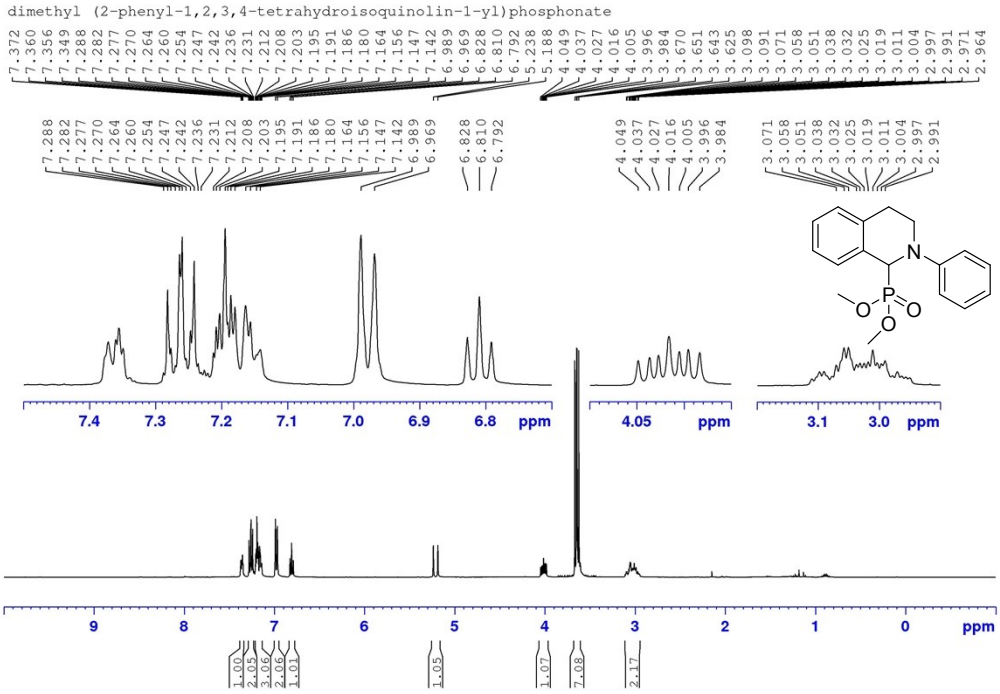

Figure S72. ^{1}H NMR spectrum of dimethyl (2-phenyl)-1,2,3,4-tetrahydroisoquinolin-1-yl)phosphonate ($CDCl_3$, 300 K).

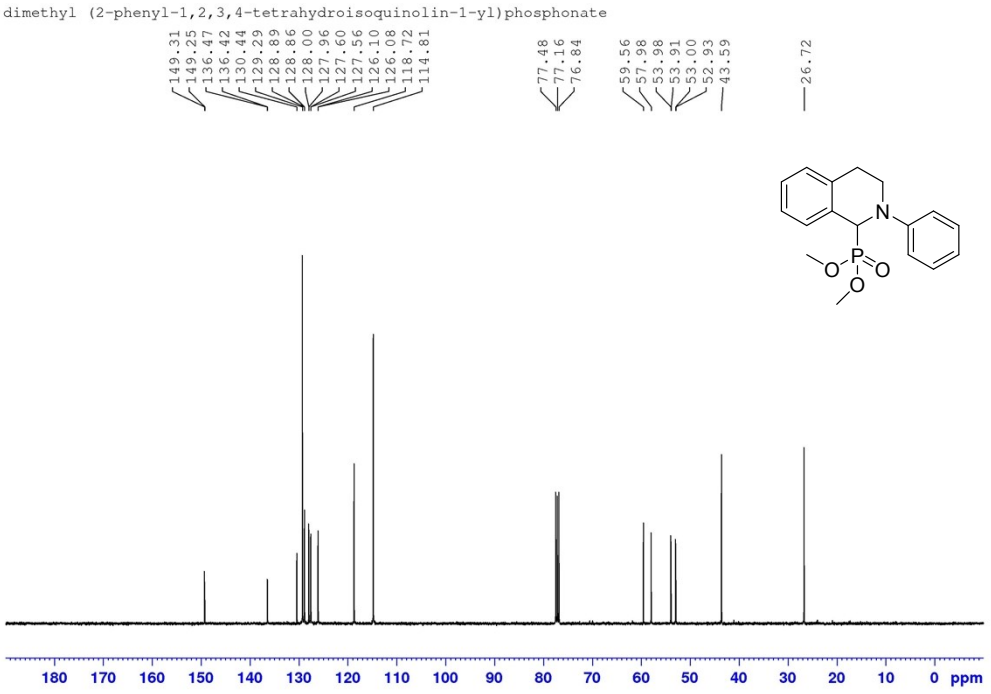

Figure S73. $^{13}C\{H\}$ NMR spectrum of dimethyl(2-phenyl)-1,2,3,4-tetrahydroisoquinolin-1-yl)phosphonate ($CDCl_3$, 300 K).

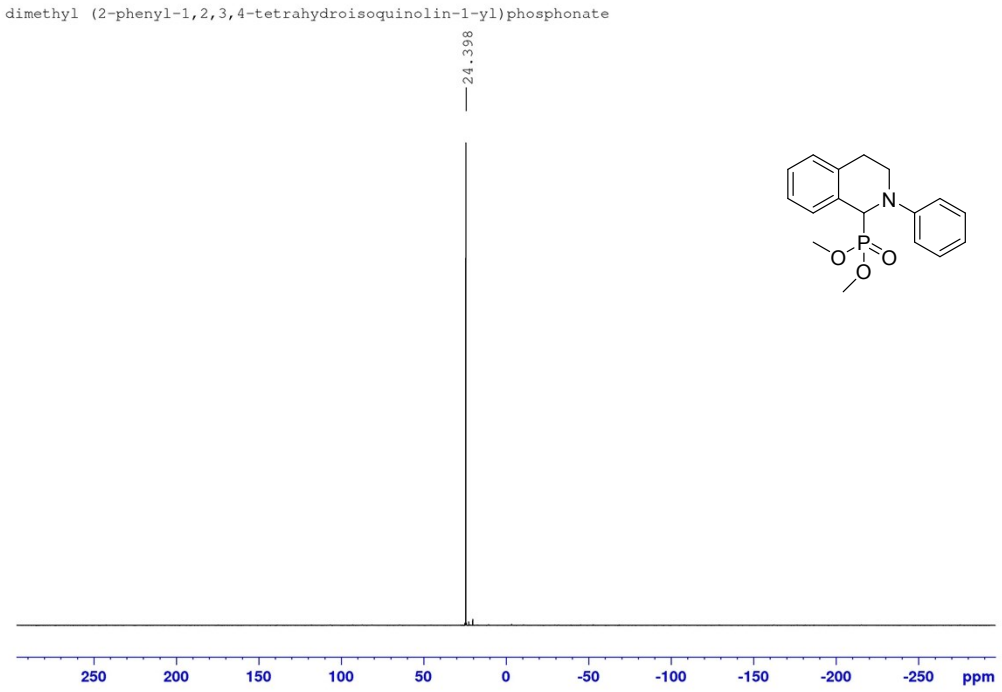

Figure S74. ^{31}P NMR spectrum of dimethyl(2-phenyl)-1,2,3,4-tetrahydroisoquinolin-1-yl)phosphonate ($CDCl_3$, 300 K).

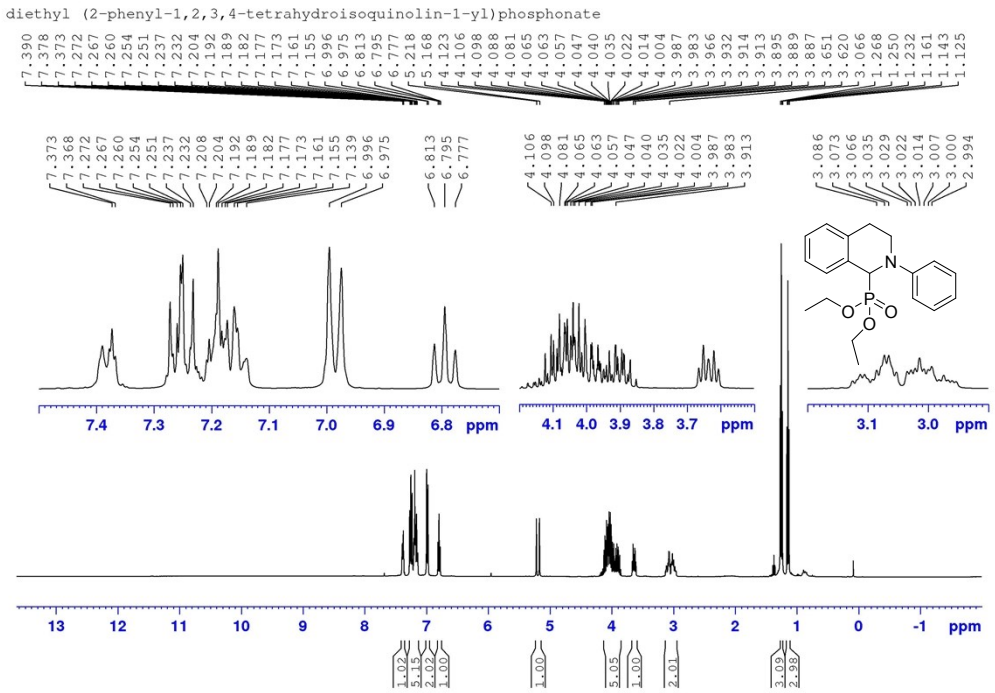

Figure S75. ^{1}H NMR spectrum of diethyl(2-phenyl)-1,2,3,4-tetrahydroisoquinolin-1-yl)phosphonate ($CDCl_3$, 300 K).

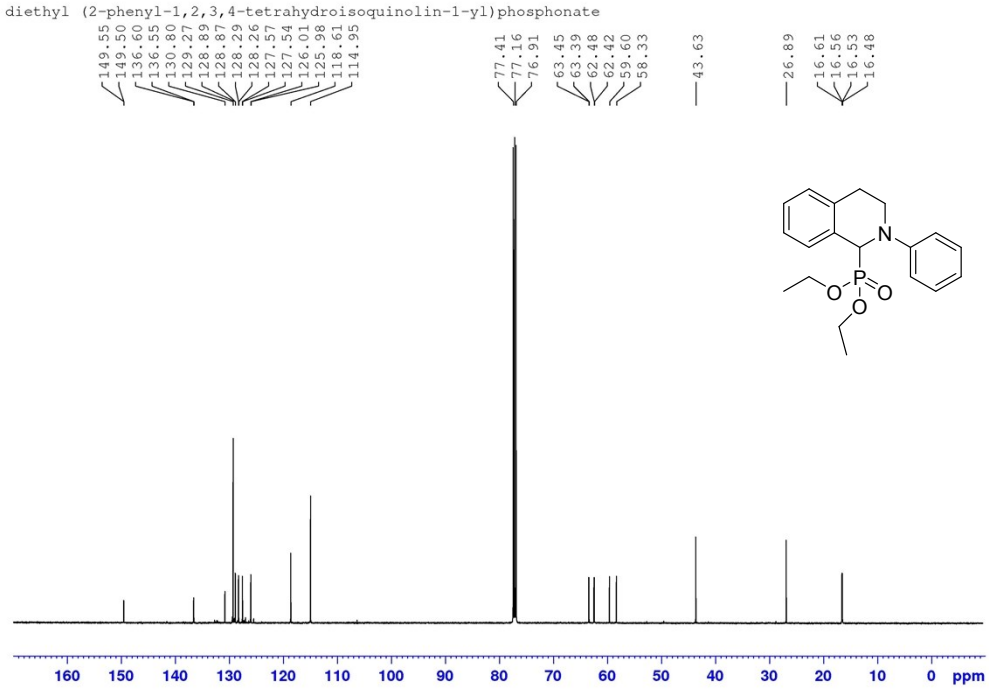

Figure S76. $^{13}C\{H\}$ NMR spectrum of diethyl(2-phenyl)-1,2,3,4-tetrahydroisoquinolin-1-yl)phosphonate ($CDCl_3$, 300 K).

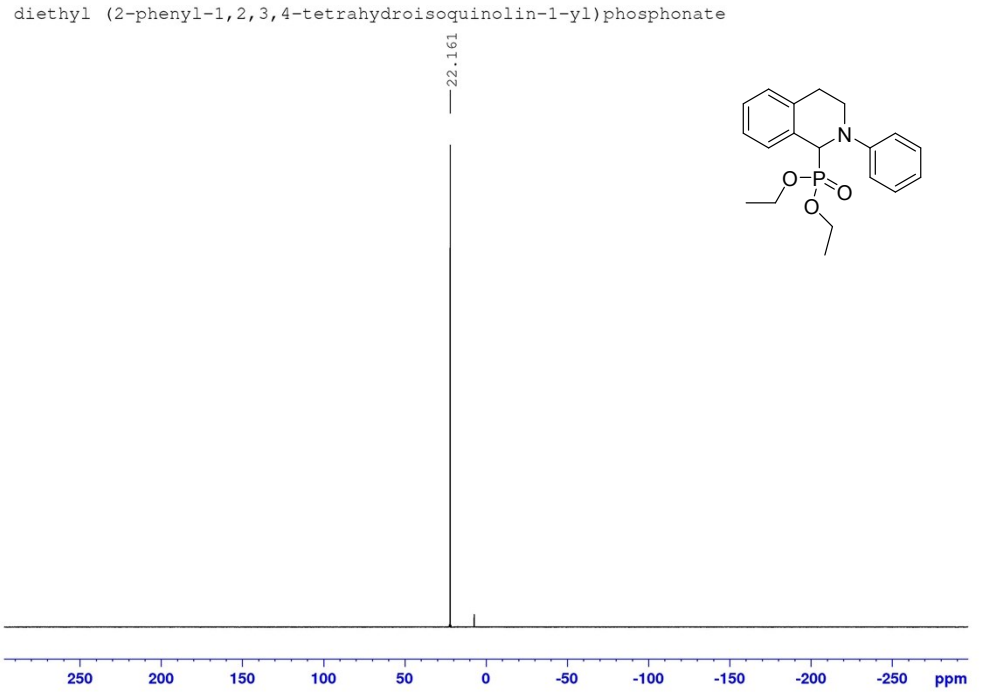

Figure S77. ^{31}P NMR spectrum of diethyl(2-phenyl)-1,2,3,4-tetrahydroisoquinolin-1-yl)phosphonate ($CDCl_3$, 300 K).